

FINAL REPORT

Optimized Enhanced Bioremediation Through 4D Geophysical
Monitoring and Autonomous Data Collection, Processing
and Analysis

ESTCP Project ER-200717

September 2014

William Major
NAVFAC EXWC

Roelof Versteeg
Subsurface Insights

Distribution Statement A

This document has been cleared for public release



REPORT DOCUMENTATION PAGE			<i>FORM APPROVED</i> <i>OMB NO. 0704-0188</i>		
Public reporting burden for this collection of information is estimated to average 1 hour per response, including the time for reviewing instructions, searching existing data sources, gathering and maintaining the data needed, and completing and reviewing this collection of information. Send comments regarding this burden estimate or any other aspect of this collection of information, including suggestions for reducing this burden to Department of Defense, Washington Headquarters Services, Directorate for Information Operations and Reports (0704-0188), 1215 Jefferson Davis Highway, Suite 1204, Arlington, VA 22202-4302. Respondents should be aware that notwithstanding any other provision of law, no person shall be subject to any penalty for failing to comply with a collection of information if it does not display a currently valid OMB control number. PLEASE DO NOT RETURN YOUR FORM TO THE ABOVE ADDRESS.					
1. REPORT DATE (DD-MM-YYYY) 09-12-2014		2. REPORT TYPE Final Report		3. DATES COVERED (From – To) 2008-2014	
4. TITLE AND SUBTITLE ER-0717: Optimized Enhanced Bioremediation through 4D Geophysical Monitoring and Autonomous Data Collection, Processing and Analysis			5a. CONTRACT NUMBER N/A		
			5b. GRANT NUMBER N/A		
			5c. PROGRAM ELEMENT NUMBER N/A		
6. AUTHOR(S) William Major, NAVFAC EXWC Roelof Versteeg, Subsurface Insights			5d. PROJECT NUMBER ER-200717		
			5e. TASK NUMBER N/A		
			5f. WORK UNIT NUMBER N/A		
7. PERFORMING ORGANIZATION NAME(S) AND ADDRESS(ES) Naval Facilities Engineering and Expeditionary Warfare Center 1000 23rd Avenue, Port Hueneme, CA 93043 & Subsurface Insights 62 Lebanon Street, Hanover, NH 03755-2510			8. PERFORMING ORGANIZATION REPORT NUMBER N/A		
9. SPONSORING / MONITORING AGENCY NAME(S) AND ADDRESS(ES) SERDP/ESTCP 4800 Mark Center Drive, Suite 17D08 Alexandria, VA 22350-3605			10. SPONSOR / MONITOR'S ACRONYM(S) SERDP/ESTCP		
			11. SPONSOR / MONITOR'S REPORT NUMBER(S) ER-200717		
12. DISTRIBUTION / AVAILABILITY STATEMENT Distribution Statement A: Approved for public release; distribution is unlimited					
13. SUPPLEMENTARY NOTES					
14. ABSTRACT One of the major limitations to the effectiveness of in situ bioremediation is that performance is dependent on effective amendment delivery. However, practitioners generally have little knowledge of the subsurface distribution of amendments and there is often substantial uncertainty about whether treatment design criteria have been met, or if (and where and when) additional injections are required. Such uncertainty is either addressed through dense sampling, or through overly conservative remedial efforts, both of which are costly. The performance objectives of the technology demonstration were to show that automated electrical geophysical monitoring can be used as an alternative to existing methods to provide timely, volumetric and cost effective information on spatiotemporal behavior of amendments used in enhanced bioremediation. These objectives included quantitative and qualitative measures. Quantitative measures were formulated in terms of spatial resolution, temporal resolution, and data-processing time/turnaround. Qualitative measures pertained to timely delivery of actionable to scientists/engineers in the field, and the ability of geophysical monitoring to map amendment behavior.					
15. SUBJECT TERMS					
16. SECURITY CLASSIFICATION OF:		17. LIMITATION OF ABSTRACT	18. NUMBER OF PAGES	19a. NAME OF RESPONSIBLE PERSON	
a. REPORT	b. ABSTRACT			c. THIS PAGE	Roelof Versteeg
Click here	Click here	Click here	U	96	19b. TELEPHONE NUMBER (include area code) 603-443-2202

Contents

1 Introduction	9
1.1 Background.....	9
1.2 Objective of the demonstration.....	10
1.3 Regulatory drivers	11
2 Technology	12
2.1 TECHNOLOGY DESCRIPTION	12
2.1.1 Time-lapse geophysics	13
2.1.2 The geophysical signatures of bioremediation.....	14
2.1.3 Electrical resistivity monitoring.....	17
2.1.4 Time-lapse radar geophysics.....	20
2.2 Hydrogeophysical Performance Monitoring System	21
2.2.1 Expected application of technology	21
2.3 TECHNOLOGY DEVELOPMENT PRIOR TO FIELD DEMONSTRATION	21
2.3.1 Timelapse resistivity inversion code.....	22
2.3.2 Web applications for data processing and result delivery.....	23
2.4 ADVANTAGES AND LIMITATIONS OF THE TECHNOLOGY	26
3 Performance objectives.....	29
3.1 Quantitative performance criteria.....	29
3.1.1 3D Spatial resolution of amendment maps	30
3.1.2 Relative concentration gradients of amendments in 3D.....	30
3.1.3 Processing and delivery time of HPMS server.....	30
3.1.4 Temporal resolution of amendment maps.....	31
3.2 Qualitative performance criteria.....	31
3.2.1 Effectiveness of HPMS system in delivering actionable information to RPMs .	31
3.2.2 Ability to map geochemical parameters of interest.....	31
4 SITE DESCRIPTION.....	32
4.1 Site selection criteria and site selection.....	32
4.2 Brandywine DRMO LOCATION AND HISTORY	34
4.3 SITE GEOLOGY/HYDROGEOLOGY	35
4.4 CONTAMINANT DISTRIBUTION	36
4.4.1 Cleanup Progress.....	38
5 TEST DESIGN	40
5.1 EXPERIMENTAL DESIGN	40
5.2 BASELINE CHARACTERIZATION	40
5.2.1 Background resistivity data.....	40
5.2.2 Background electrical logs	41
5.2.3 Background crosshole radar	43
5.2.4 Background sampling.....	44
5.3 TREATABILITY OR LABORATORY STUDY RESULTS	48
5.4 DESIGN AND LAYOUT OF TECHNOLOGY COMPONENTS.....	48
5.4.1 Injection points.....	52
5.4.2 Electrode wells	53
5.4.3 Sampling wells	54
5.4.4 Radar wells.....	55
5.4.5 Surface cables.....	56

5.5	FIELD TESTING	58
5.6	SAMPLING METHODS	58
5.7	Sampling Results	59
5.7.1	Initial sampling efforts: Investigation of correlation between geophysics and geochemistry.....	59
5.7.2	ABC amendment - long term monitoring results	63
5.7.3	Sampling for molasses injections.....	69
6	PERFORMANCE ASSESSMENT DISCUSSION.....	76
6.1	Quantitative performance criteria.....	77
6.1.1	3D Spatial resolution of amendment maps	77
6.1.2	Relative concentration gradients of amendments in 3D.....	77
6.1.3	Processing and delivery time of HPMS server.....	77
6.1.4	Temporal resolution of amendment maps.....	78
6.2	Qualitative performance criteria.....	78
6.2.1	Effectiveness of HPMS system in delivering actionable information to RPMs ..	78
6.2.2	Ability to map geochemical parameters of interest.....	78
7	COST ASSESSMENT.....	80
7.1	Deployment, operational and analysis costs.....	80
7.1.1	Cost model.....	81
7.2	COST DRIVERS	83
7.3	COST ANALYSIS	83
7.3.1	Cost analysis scenario 1: Single-injection monitoring.....	84
7.3.2	Cost analysis scenario 2: Site-scale monitoring at 10 locations.....	86
7.3.3	Cost analysis scenario 3: Site-scale, site-wide monitoring.....	88
8	IMPLEMENTATION ISSUES	91
8.1	Deployment	91
8.2	Operational Environment Issues.....	91
8.3	Regulatory Issues.....	92
9	APPENDICES.....	93
9.1	Appendix A: Points of Contact.....	93
10	References.....	94

List of Figures

Figure 2-1 Schematic of the HPMS. Data is collected in the field, and transmitted to a server for qa/qc and parsing in a relational database. Processing and inversion is done on a HPC cluster. Results (including time lapse tomograms) are accessible to endusers through a browser interface).

..... 12

Figure 2-2 Timelapse survey, which consists of multiple datasets. Each dataset is collected over a specific time period. For resistivity data, each dataset consists of thousands or tens of thousands of measurements

Figure 2-3 Changes in electrical properties resulting from amendment injection and resulting

biological activity.....	16
Figure 2-4 Electrical potential and current lines resulting from electrical resistivity measurement (from (EPA 2012)). In this figure the current electrodes are located at locations A and B. A voltage is applied over these electrodes. The resulting current lines create a potential distribution in the earth. The potential electrodes A and B measure this potential. For most surveys one would collect many such four electrode measurements with the electrodes placed at different locations.....	18
Figure 2-6 Schematic of the collection of crosshole radar data for (a) level-run and (b) tomography.....	21
Figure 2-7 Flowchart of 4D ERT Inversion.....	23
Figure 2-8 Flow chart of server based software for data ingestion and qa/qc	25
Figure 4-1 Site location of the Brandywine DRMO	36
Figure 4-2 Ground-water elevations and contaminant distribution in the vicinity of the Andrews AFB DRMO, Brandywine, MD. The fieldstudy described here focused on an area within the plume in the DRMO area.....	37
Figure 5-1 Resistivity background image, showing the pre-injection electrical structure of the subsurface.....	41
Figure 5-2 Background electrical-conductivity logs collected using the Geoprobe ® EC logging equipment during drilling for electrode wells E1, E2, E3, E5, E6, and E7	42
Figure 5-3 Borehole electromagnetic induction logs from wells G1-G4, displayed as resistivity.....	43
Figure 5-4 Background crosshole radar amplitude data collected in January 2008 prior to injections. Lower amplitude indicates greater attenuation, which is proportional to electrical conductivity.....	44
Figure 5-5 layout of monitoring system overlain on general area of injections (lower left). The system consists of 7 ERT boreholes and three surface cables. and 8 dedicated sampling wells. These were deployed around two of the sampling points (B6 and B7). Note that for the second injection in August 2010 additional surface cables were used. Each red dot on the lower left figure represents an amendment injection location	49
Figure 5-6 Site detail showing relationship between borehole wells and sample wells. Locations of two injections for long-term monitoring experiment are shown.....	50
Figure 5-7 Shed housing the instrumentation	51
Figure 5-8 Resistivity hardware: left single channel system. Right multi channel system. Both systems use the same electrodes. The multichannel system was used to monitor the second injection.....	51
Figure 5-9 March 2008 injection.....	52
Figure 5-10 Schematic overview of amendment injection procedure. From top right to bottom left: direct push rig pushes down injection rod and insert amendments over injection screen depth, starting at the deepest point.....	53
Figure 5-11 Schematic diagram showing construction of an electrode (E) well.....	54
Figure 5-12 Schematic diagram showing construction of a sampling ('S') well.....	55
Figure 5-13 Schematic diagram showing construction of a GPR ('G') well.....	56
Figure 5-14 Installation of trenches for surface electrodes for the first injection experiment.....	57
Figure 5-15 Surface array with temporarily installed electrodes for monitoring second injection experiment.....	57
Figure 5-16 Calibration dataset used to develop field-scale petrophysical relation to predict fluid	

conductivity from ERT-estimated bulk conductivity	60
Figure 5-17. Validation sampling results, for which fluid conductivity was predicted based on ERT results.....	61
Figure 5-18 Correlation between total organic acids and fluid conductivity.....	62
Figure 5-19 Predicted vs. observed TOA concentrations for August 2010 sampling event....	62
Figure 5-20 Comparison between correlation of fluid vs electrical geophysical conductivity in August 2008 (top) and July 2009 (bottom).....	65
Figure 5-21 Comparison of ERT estimated conductivity against fluid measured conductivity. Dots are ERT inversion results. Triangles represent measurement at well ports. Green - 10 ft bgs, yellow - 18 ft bgs, red - 25 ft bgs. See text for discussion of interpretation.....	66
Figure 5-22. 3D time-lapse ERT monitoring results up to 762 days after the March 2008 injection. Injection intervals are shown as black vertical lines. Bulk electrical conductivity differences are shown as isosurfaces. The left column shows the amendment sinking, spreading, and diluting over the lower confining unit during the first year. In the second year, a significant increase in bulk conductivity corresponds to the onset of biological activity as confirmed through sampling efforts. Increase in bulk conductivity during this period are likely caused by iron sulfide precipitation	67
Figure 5-23. Cross-hole ground-penetrating radar amplitudes for five well pairs at three times, January, April, and August 2008. Decreases in radar amplitude indicate increased fluid conductivity and thus amendment presence.	68
Figure 5-24. Conceptual model of amendment emplacement, expected biogeochemical changes and resulting geophysical signature	69
Figure 5-25 Molasses tanks. Three tanks with 3100 lbs of molasses each were used for the injection.....	70
Figure 5-26 Direct push rig used for 2nd injection	70
Figure 5-27 Surface array at site used in monitoring second injection.....	71
Figure 7-1 Cost-analysis comparison for HPMS and conventional sampling for Scenario 2, extended to a 30 year time frame (Table 7-4).....	88

List of tables

Table 1-1 Comparison of time lapse resistivity against sampling based approaches	10
Table 2-1 Geophysical method, primary physical property and inferred properties	13
Table 2-2 (from AFCEE, 2004). Different amendments and concentrations	15
Table 3-1 Performance objectives for effort	29
Table 4-1 Site Selection Criteria.....	33
Table 4-2 From (EPA 2006) Environmental investigations at the Brandywine site.....	35
Table 5-1. Baseline sampling results from gas chromatograph (GC) analysis.....	45
Table 5-2. Baseline sampling results from ion chromatograph (IC) analysis.....	45
Table 5-3. Baseline sampling results obtained from ICP-OES analysis.....	46
Table 5-4. Baseline sampling results for field parameters and field-kit analysis.	47
Table 5-5. Overview of sampling events performed by project team. The detailed results of the sampling events are provided in appendix 9.2.....	63
Table 5-6. Annotated results for the ERT monitoring of molasses amendment emplacement	72

Table 6-1 Performance objectives for effort	76
Table 7-1 Cost Savings mechanisms.....	80
Table 7-2 Cost model for a HPMS similar to the Brandywine dem/val	82
Table 7-3 Cost Analysis for HPMS - Scenario 1	84
Table 7-4 Cost analysis for a HPMS - Scenario 2– Scenario 2 (30-year costs).....	86
Table 7-5 Cost for site scale, site-wide monitoring	90
Table 9-1 Points of contact for ESTCP DEM/VAL effort.....	93

ACKNOWLEDGMENTS

ER-0717: *Optimized Enhanced Bioremediation through 4D Geophysical Monitoring and Autonomous Data Collection, Processing and Analysis* was funded by the Department of Defense's Environmental Security Technology Certification Program (ESTCP) and was executed in collaboration with the Andrews AFB Environmental Restoration Team. The support of the Andrews AFB staff for this project is gratefully acknowledged. Specifically, the authors like to thank Mike Rooney and Brian Dolan for continued support during the project.

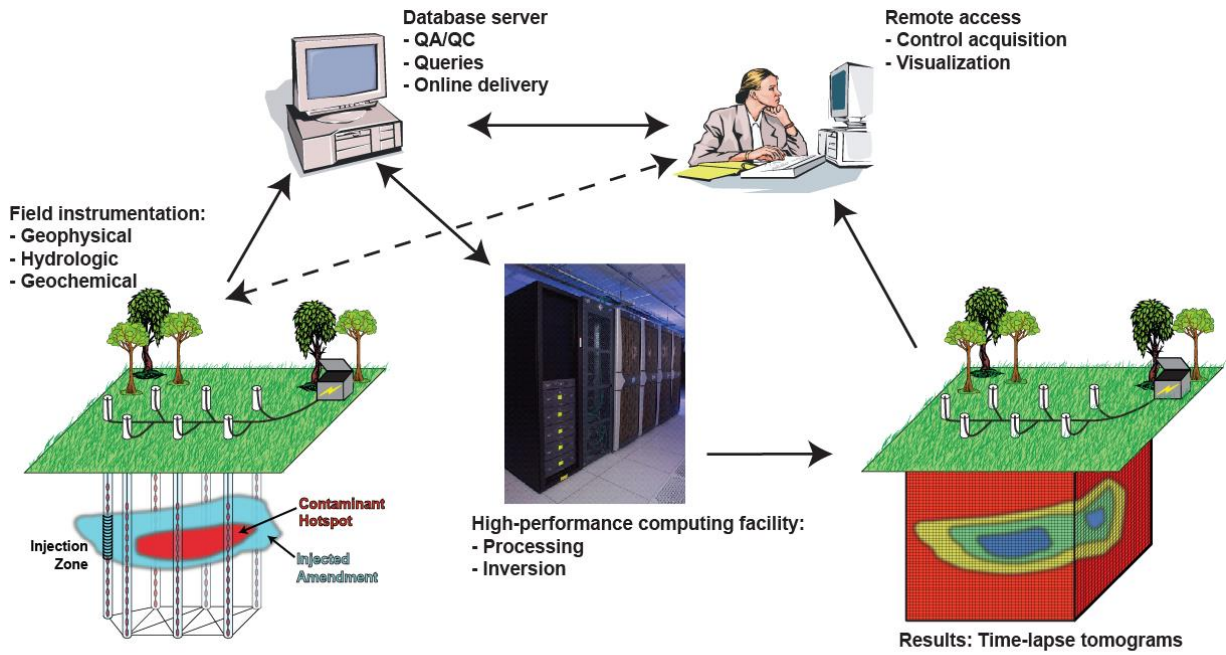
Executive Summary

Enhanced in situ bioremediation has become widely used, because it is relatively inexpensive and effective, as long as it is implemented appropriately. One of the major limitations to the effectiveness of in situ bioremediation is that performance is dependent on effective amendment delivery, and yet practitioners generally have little knowledge of the subsurface distribution of amendments. As a result, there is often substantial uncertainty about whether treatment design criteria have been met, or if (and where and when) additional injections are required. Such uncertainty is either addressed through dense sampling, or through overly conservative remedial efforts, both of which are costly.

This project demonstrated the use of geophysical techniques to provide near real-time information on the spatial and temporal distribution of amendments noninvasively and cost effectively. The technology uses electrical resistivity (ER) measurements from a series of wells to detect changes in electrical conductivity. ER monitoring is particularly useful for enhanced bioremediation because the amendment solutions used for bioremediation increase the bulk electrical conductivity significantly above the background conductivity. Time-lapse ER monitoring can delineate where amendments were initially delivered, as well as track their migration and depletion over time. Near real-time information is particularly valuable because it can allow modifications and/or additional injections while equipment is still present on site.

The system demonstrated in this project is referred to as the Hydrogeophysical Performance Monitoring System (HPMS). The HPMS consists of commercially available hardware and custom designed software for data collection, data transfer, data processing and web-based result visualization. Two demonstrations of the HPMS were performed at the Brandywine DRMO site in Brandywine, MD. The first demonstration, which lasted from March 2008 until the summer of 2010, involved injection of a proprietary lactate amendment (ABC[®]). The second demonstration, in August 2010, involved monitoring two injections of molasses, and showcased the delivery of near real-time results to project team members and program managers in the field.

Both demonstrations successfully demonstrated the ability of electrical geophysical monitoring to provide near real-time, actionable information on the spatial and temporal behavior of amendments, for considerably less cost than invasive sampling. The estimated cost of the HPMS system was roughly half the cost of invasive sampling, while providing more complete and timely information on the amendment distribution. The longer demonstration also showed that electrical geophysical monitoring can provide information on the biogeochemical changes associated with in situ bioremediation, while the shorter demonstration proved the system can provide stakeholders with actionable information on amendment behavior within 30 minutes after injection.



Elements of the Hydrogeophysical Performance Monitoring System

1 Introduction

1.1 Background

Thousands of Department of Defense (DoD) sites have contaminated soil and groundwater, resulting from a range of different operations related activities. As of 2005 the DoD had invested \$20 billion in the environmental restoration of contaminated sites, and the cleanup of contaminated groundwater remains one of the largest environmental liabilities of DoD (GAO 2005).

In-situ remedial efforts such as enhanced bioremediation (Cunningham, Rahme et al. 2001; Chen, Kao et al. 2010; Peale, Mueller et al. 2010; Park, Lamb et al. 2011) have shown to be successful in accelerating cleanup of recalcitrant compounds. Due to the potential for cost savings of in-situ techniques compared to ex-situ techniques such as pump-and-treat there is substantial interest from DoD in enhanced bioremediation (Parsons 2004) which is now being proposed as an integral part of remedial solutions at multiple Department of Defense sites.

Enhanced bioremediation involves the addition of microorganisms and/or nutrients to the subsurface environment to accelerate the natural biodegradation process. One of the most common bioremediation methods is the injection of organic liquid nutrients such as lactate, molasses, Hydrogen Release Compound (HRC)[®], and vegetable oils.

Multiple laboratory and field studies have resulted in a detailed understanding of the behavior of different liquid nutrient amendments and the expected microbial processes. These studies have led to regulatory acceptance of bioremediation as a remedial strategy, and as a result of this acceptance enhanced bioremediation services is now being offered by multiple commercial providers.

In the typical remedial scenario amendment is emplaced through injection throughout the contaminated zone. Such injections can be coupled with permeability or pH enhancements. Knowledge of amendment distribution is generally obtained from model based assumptions and sparse and expensive groundwater sampling efforts. Consequently, there is substantial uncertainty on whether injection design criteria have been met, or where additional injections may be required to achieve or maintain amendment concentrations required for optimal efficiency. Such uncertainty either is resolved through sampling, or is addressed through overly conservative remedial efforts, both of which negatively impact cost and efficiency of remedial effort.

This problem –how to reduce the uncertainty in amendment emplacement knowledge – is the problem addressed by our effort.

Time-lapse electrical resistivity measurements have been demonstrated to be capable of mapping spatial and temporal changes in subsurface electrical conductivity (Versteeg, Birken et al. 2000; Slater, Binley et al. 2002; Williams, Ntarlagiannis et al. 2005; Davis, Atekwana et al. 2006). Amendments used in bioremediation typically have an electrical conductivity that substantially differs from bulk background subsurface electrical conductivity. Amendments are typically injected in substantial volumes per injection point, and thus the injection of amendments will result in a substantial change in subsurface conductivities.

After injection the amendment will typically move (due to groundwater gradients). In addition,

changes in conductivities of both the liquid and solid phases will occur due to different geochemical processes. Thus, in theory both the initial injection and subsequent movement and changes in amendment properties can be mapped through time-lapse electrical measurements to provide spatial and volumetric information about amendment behavior.

The feasibility of doing this automatically and autonomously to provide near real time information on amendment behavior was demonstrated under this effort. This approach has multiple advantages compared to current approaches (Table 1-1). These are

- volumetric information versus point information: the approach demonstrated here provided information on amendment behavior in 3D, whereas traditional methods only provide information on amendment behavior at discrete sampling points
- dense versus sparse temporal information: our approach provides (dependent on configuration of the system) information on amendment behavior on an hourly or daily basis
- reduction in overall cost: while sampling and analysis costs are recurring costs, our system mainly requires an upfront installation cost, with components which largely can be reused between different sites; furthermore, geophysical data can be used to reduce the frequency of sampling or trigger more cost-effective sampling when subsurface changes are occurring..

	Sampling based approaches	Time lapse resistivity
Spatial density of information	Only point data	Volumetric information
Temporal information	Typically quarterly	Hourly to Daily
Cost	Sampling and analysis costs continue during project	Mainly up front installation cost

Table 1-1 Comparison of time lapse resistivity against sampling based approaches

With the technology described here, far fewer wells will be required for understanding amendment distributions, leading to significant cost savings (20 to 50% or greater per site) due to fewer monitoring requirements (e.g., wells, samples, lab analyses) and more optimized remedial applications based on rapid identification of missed target zones. This should lead to substantial cost savings over the life of the remedial effort.

1.2 Objective of the demonstration

The objective of the demonstration was to validate and demonstrate the use of autonomous time-lapse electrical resistivity as an effective amendment monitoring tool. This was done through a field based demonstration at the Brandywine DRMO. This demonstration had two parts: a one and a half year monitoring effort of the spatial and temporal evolution of a lactate based amendment which was injected as part of an ongoing bioremediation effort at the Brandywine DRMO, and two short term monitoring efforts of two molasses injections at the same site in August 2010. Real-time monitoring of the two latter injections (in tandem with the actual amendment emplacement) was demonstrated to DoD and DOE scientists both in person and through a live webcast.

1.3 Regulatory drivers

The United States Environmental Protection Agency (USEPA) Maximum Contaminant Levels (MCLs) in drinking water are 5 µg/l for PCE and TCE, and 70 µg/L for *cis*-DCE, and 2 µg/L for VC. Concentrations of PCE, TCE, *cis*-DCE and VC exceed these MCLs at a significant number of DoD sites. The use of amendment injection for enhanced bioremediation of chlorinated solvents is one of the primary methods used by DoD to bring these sites into compliance with federal, state, and local regulations. Use of 4D geophysical methods to verify amendment distribution and the remedial process within specific contamination zones provides site stakeholders with quantitative data which support the assessment of remedial progress and functioning.

This project also addressed several high priority needs from the Navy Environmental Quality, Research, Development, Testing/Evaluation Requirements including:

- 1.I.01.g Improved Remediation of Groundwater Contaminated with Halogenated Hydrocarbons and Other Organics;*
- 1.III.02.a Remote Sensing for Site Characterization and Monitoring;*

Additionally, the following DoD needs from the Air Force Assessment Survey (NAS) are also addressed:

- 100-130 Effective DNAPL Characterization, Monitoring and Detection Technology;*
- 100-131 Improved Remediation Monitoring Technologies;*
- 500-570 Improve Understanding of DNAPL Groundwater Transport to Accurately Predict Fate of Contaminants*

2 Technology

The system used in this demonstration goes by the acronym HPMS (Hydrogeophysical Performance Monitoring System). It couples automatic and autonomous electrical geophysical monitoring with automated data processing and result delivery. The elements of this system are shown in Figure 2-1 and discussed in the following section. It should be noted that electrical resistivity monitoring (and the use of resistivity monitoring for long term process studies) is done by numerous other groups. The system described here bears resemblance to different systems, including most recently the system developed and demonstrated by the British Geological Survey (BGS) (Ogilvy, Meldrum et al. 2009). However, while the concept of resistivity monitoring is well established and many groups have demonstrated aspects of our systems (most commonly remote data retrieval from field systems), apart from the BGS system we are aware of no other field demonstrations of **fully automated** systems.

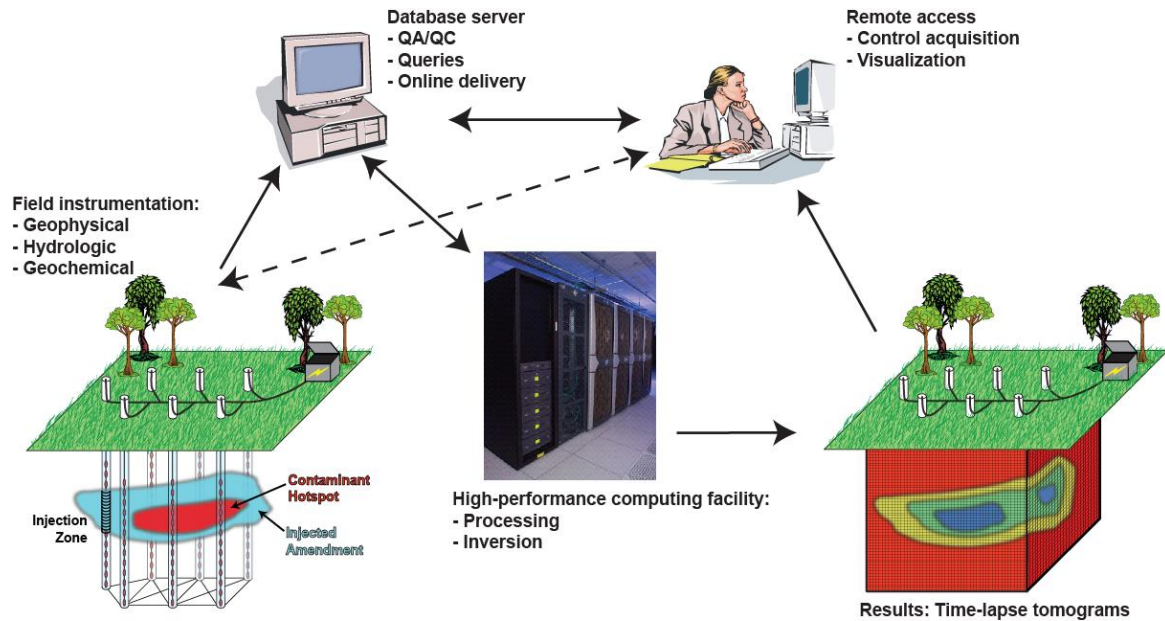


Figure 2-1 Schematic of the HPMS. Data is collected in the field, and transmitted to a server for qa/qc and parsing in a relational database. Processing and inversion is done on a HPC cluster. Results (including time lapse tomograms) are accessible to endusers through a browser interface).

2.1 TECHNOLOGY DESCRIPTION

Our demonstration/evaluation project capitalized on previous developments documented in the geophysical literature. We rely heavily on existing hardware for acquisition of time-lapse electrical data, as well as on research and development by the project team members and others on time-lapse monitoring of natural and engineered hydrologic processes. In this section (Section 2.1) we review the state of geophysical monitoring methods and discuss the relevance of various methods to monitoring bioremediation. In subsequent sections, we focus on developments made under this ESTCP project.

2.1.1 Time-lapse geophysics

Geophysical methods are a standard tool for obtaining information on volumetric distributions of subsurface physical properties of rocks and fluids. One can distinguish primary physical properties (those which appear in the equations describing the physics of each method) and the inferred properties. The inferred properties are typically obtained through a petrophysical relationship, such as Archie's law (Archie 1942) which relates the electrical conductivity of a sedimentary rock to its porosity and brine saturation. Such petrophysical relationships are generally obtained experimentally through laboratory or field measurements. However, efforts are underway to develop such relationships from fundamental material properties. A range of geophysical methods exist (Table 2-1) each of which can provide information on different primary physical and inferred properties.

Method	Primary Physical property	Inferred properties
Gravity	Density	Lithology, porosity
Seismic	Wave velocity, elastic moduli and density	Pressure, fluid saturation, porosity, stress field
Electrical	Electrical conductivity	Fluid type and saturation, chemistry
Electromagnetic	Magnetic permeability and electric permittivity	Fluid type and saturation, chemistry

Table 2-1 Geophysical method, primary physical property and inferred properties

If one collects multiple geophysical datasets with the same parameters at the same location at different times, changes in the geophysical data between each collection can be associated with dynamic subsurface processes that are occurring over the period spanned by the acquisition efforts. This approach is known as time-lapse or 4D geophysics, and has been demonstrated to work for all geophysical methods listed in table 1 for a wide range of applications (Burkhart, Hoover et al. 2000; Fanchi 2001; Day-Lewis, Harris et al. 2002; Li 2003; Gasperikova, Hoversten et al. 2004; Dodds 2005; Arts, Chadwick et al. 2007; Orange, Constable et al. 2007; Versteeg and Johnson 2008; Zach, Frenkel et al. 2009).

The resulting dataset is typically referred to as a time-lapse survey. A time-lapse survey is made up of numerous individual time-lapse datasets, each of which can have many individual geophysical measurements. In order to facilitate the interpretation of time-lapse surveys (and driven by the need to avoid spatial aliasing) each individual dataset is typically collected at fixed time intervals (Figure 2-2). This interval is typically dictated by the need to avoid spatial aliasing of the processes being imaged. In the case of time-lapse datasets which need to be collected manually cost considerations provide a constraint on the number of datasets collected, however, in many current cases where acquisition is fully automated geophysical monitoring systems collect data continuously.

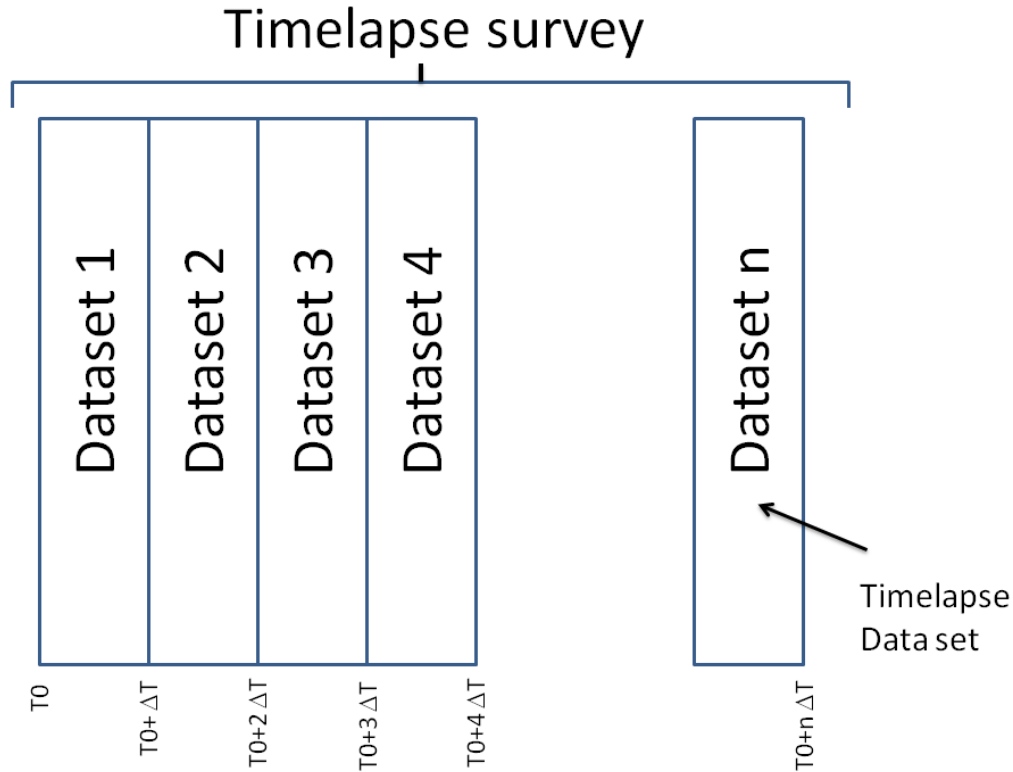


Figure 2-2 Timelapse survey, which consists of multiple datasets. Each dataset is collected over a specific time period. For resistivity data, each dataset consists of thousands or tens of thousands of measurements

It should be noted that while time-lapse geophysics is well established and has been demonstrated numerous times, the process of interpreting changes in geophysical data in terms of changes in subsurface properties is complex. The interpretation of subsurface changes and processes can be assisted by certain constraints: for instance, in the case of anthropogenically caused changes we typically know the "when". Similarly, laboratory and theoretical studies can tell us the "what", and the relationship between rock properties and geophysical properties can help address the "how".

2.1.2 The geophysical signatures of bioremediation

As noted in the introduction, enhanced bioremediation through injecting amendments is increasingly used to accelerate cleanup. A range of different amendments exists, all of which serve as nutrients for the microbial communities (Table 2-2). Amendments include both water soluble amendments (such as lactate, ethanol and molasses) as well as slow release compounds (such as vegetable oil, Hydrogen Release Compound®, a proprietary mixture, and mulch). In general, it is not uncommon to inject thousands of gallons of amendment mixture per injection point.

In general, the amendment mixture will have an electrical conductivity which will differ from the background electrical conductivity, and thus the injection of large amounts of amendment will change the subsurface bulk conductivity (which is a combination of the conductivity of the solid phase and liquid phase components).

	Substrate	Injected form and concentration	Targeted concentration in treatment zone
Water Soluble	Sodium Lactate	Diluted 3 to 60 percent by weight	50 to 300 mg/l
	Butyrate	Diluted 3 to 60 percent by weight	50 to 300 mg/l
	Methanol	Diluted 3 to 60 percent by weight	50 to 300 mg/l
	Ethanol	Diluted 3 to 60 percent by weight	50 to 300 mg/l
	Molasses	Diluted 1 to 10 percent by weight	50 to 500 mg/l
	High Fructose Corn Syrup	Diluted 1 to 10 percent by weight	50 to 500 mg/l
Slow Release	Whey (fresh/powdered)	Dissolved (powdered form) or injected as slurry (fresh)	50 to 500 mg/l
	Hydrogen Release Compound (HRC ®)	injection of pure product (4/12 lbs per vertical foot of injection)	100 to 500 mg/l
	Vegetable Oil (e.g. food grade soybean oil)	Oil in water emulsions with 5 to 15 percent oil by volume	100 to 500 mg/l
	Mulch and compost (cellulose)	Mixed with sand at 20 to 60 percent mulch by volume	100 to 1000 mg/L TOC within biowall reaction zone

Table 2-2 (from AFCEE, 2004). **Different amendments and concentrations**

In addition to the change in bulk conductivity resulting from changes in the fluid conductivity we can also see a change in the bulk conductivity resulting from biological activity (Figure 2-3). A change in bulk electrical property can thus result from changes in pore fluid specific conductance, changes in redox potential, and/or changes in grain size boundaries.

These changes in electrical properties can be detected by a number of geophysical methods such as electrical resistivity methods (including both Self potential, standard resistivity and induced polarization), Time and Frequency Domain Electromagnetics (TDEM) and Ground Penetrating Radar (GPR).

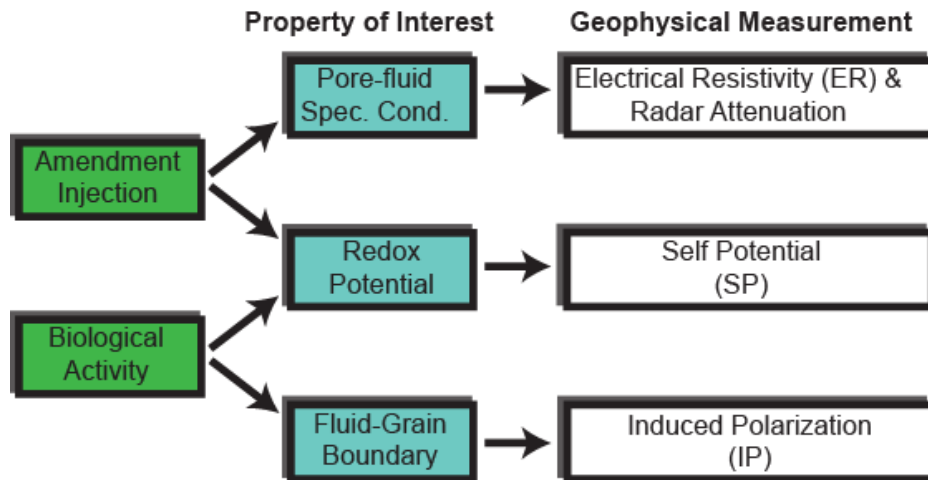


Figure 2-3 Changes in electrical properties resulting from amendment injection and resulting biological activity

Multiple laboratory and field studies have validated the relations shown in Figure 2-3. A non-exhaustive list of papers describing such studies for different methods includes:

- *Electrical Resistivity*: Electrical resistivity methods have been used to map biological activity (Sauck, Atekwana et al. 1998; Aal, Atekwana et al. 2004; Atekwana, Atekwana et al. 2004; Atekwana, Werkema et al. 2004), which manifests as a macroscopic increase in pore-fluid electrical conductivity arising from an increase in organic acids. ER has also been used to verify installation of permeable reactive barriers (Slater and Binley 2003).
- *Induced Polarization*: Different studies have shown the sensitivity of IP to mineral precipitation and changes occurring at pore-grain interfaces, where biological reactions occur (Lesmes and Frye 2001; Slater and Lesmes 2002; Slater and Glaser 2003). Whereas electrical resistivity is sensitive to pore fluid resistivity (and thus total dissolved solids or ionic strength), the IP method measures the capacitive behavior of the subsurface, which depends strongly on the properties of the mineral surface. IP data may provide useful information to help answer outstanding questions regarding how amendments, biofilms, and bioclogging alter porosity and permeability.
- *Self Potential*: The SP method has long been used in mineral resources exploration for ore bodies, which represent electrically conductive bodies between oxidizing and reducing areas. In near-surface environmental/water-resource geophysics, the SP method is used increasingly to study redox conditions (Naudet, Revil et al. 2003; Naudet, Revil et al. 2004; Revil and Naudet 2004; Versteeg, Blackwelder et al. 2004). Given the importance of redox condition to understanding the efficiency of bioremediation, SP is a promising approach for performance monitoring.
- *Ground Penetrating Radar*: GPR (predominantly in a cross borehole mode) has been used extensively in pilot-scale projects to monitor (1) bioremediation (Lane, Day-Lewis et al. 2004; Lane, Day-Lewis et al. 2006; Lane, Day-Lewis et al. 2007) (2) installation of reactive barriers

(Lane, Day-Lewis et al. 2007) and (3) tracer tests (Day-Lewis, Lane et al. 2003; Day-Lewis, Lane et al. 2004)

Although geophysical monitoring can be done using various electrical and electromagnetic geophysical sensing modalities (such as GPR and TDEM) which can provide information on changing electrical properties in the subsurface, direct-current electrical resistivity is very amenable to a monitoring approach as it does not require moving sensors, and can be done using a semi permanently emplaced sensor array. This is shown by numerous publications on timelapse electrical geophysical monitoring applied to both hydrological and geochemical investigations, including (Daily 1984; Laine 1987; Parra 1988; Parra and Owen 1988; Bevc and Morrison 1991; Daily and Owen 1991; Van, Park et al. 1991; Daily, Ramirez et al. 1992; Shima 1992; White 1994; Ramirez, Daily et al. 1995; Zhang, Mackie et al. 1995; Ramirez, Daily et al. 1996; Frangos 1997; Rodriguez and Rodriguez 1999; Slater and Sandberg 2000; Suzuki and Higashi 2001).

Although such studies demonstrated the ability of electrical geophysics to provide information on subsurface processes, both the practical applicability of geophysical monitoring for amendment monitoring purposes, as well as the specific costs/benefits had not been clearly demonstrated previous to the demonstration discussed in this report.

2.1.3 Electrical resistivity monitoring

While an exhaustive discussion of the theory, instrumentation, acquisition and processing of electrical resistivity falls outside the scope of this report, it is beneficial for the readers of this report to have at the minimum a basic understanding of what an electrical resistivity instrument measures and how these measurements are made. For a more in depth discussion the reader is referred to e.g. the website maintained by the EPA on electrical resistivity (EPA 2012) or textbooks such as Reynolds (1997) or Kearey, Brooks et al. (2002).

Electrical resistivity instrumentation measures potential differences between pairs of electrodes, where the potentials either (1) result from an current applied by the instrumentation (the method generally referred to by the term "electrical resistivity"), or (2) are associated with naturally occurring potential differences, for instance those resulting from fluid movement or redox conditions (the method referred to as Self or Spontaneous Potential (SP)). Electrical resistivity instrumentation typically both measures the potentials during the transmit on time, as well as the decay of potential with time after shutoff of an applied current (so called Induced Polarization (IP) measurements).

In a typical electrical resistivity (also known as Direct Current (DC) resistivity) measurement four electrodes are used. Two of these serve as current electrodes, and two of these as potential (or measurement) electrodes. These electrodes are typically made of metal (in most cases stainless steel electrodes are used, even though graphite electrodes are fairly common). A voltage (typically 10-200 V) is applied to the current electrodes and as a result of this voltage a potential exists in the ground (Figure 2-4). The value of this potential is measured by the potential electrodes.

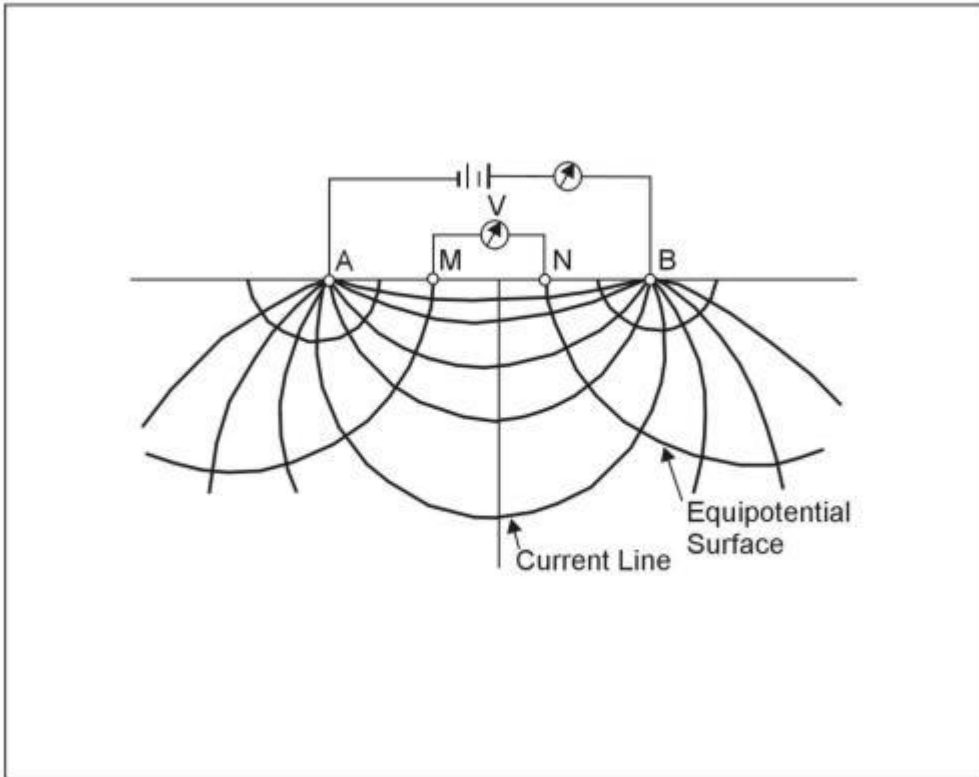


Figure 2-4 Electrical potential and current lines resulting from electrical resistivity measurement (from (EPA 2012)). In this figure the current electrodes are located at locations A and B. A voltage is applied over these electrodes. The resulting current lines create a potential distribution in the earth. The potential electrodes A and B measure this potential. For most surveys one would collect many such four electrode measurements with the electrodes placed at different locations.

By making measurements with current and potential electrodes at many different locations one can collect sufficient data with which to construct an electrical geophysical section (a 2D slice or a 3D volume of the earth for which we have discrete values of electrical conductivity). This is done through so called inverse modeling (discussed in more detail later in this report) in which the field data (combinations of electrode locations, applied voltage, observed current and observed potential difference) are used as the input to a software package which creates an electrical section.

Up to about the 1980s the only type of resistivity instruments were so called four electrode instruments. In these instruments each electrode was connected by a long spool of wire to the measurement instrument. Acquisition of data for these systems required field staff to move each electrode manually to the specific measurement location, after which the acquisition lead would manually engage the instrument. Collecting surveys with many measurement locations using this approach was fairly cumbersome. Collecting time-lapse surveys over long time periods was essentially impossible using this hardware.

2.1.3.1 Multichannel resistivity instrumentation

Over the last fifteen years electrical resistivity systems have become increasingly automated. Current systems can be controlled through software which runs either on board of the instrument or on a separate PC connected to the instrument. In addition, systems have evolved which have multiple electrodes (which can be switched through so called multiplexers) and multiple channels.

A multi-electrode resistivity instrument consists of a switchbox (typically known as a multiplexer or mux) to which many electrodes can be connected. Generally speaking each switchbox has about 20-60 electrodes, and switchboxes can be connected together. Relays in these switchboxes can be controlled electronically to select any combination of four electrodes as the potential and current electrodes. These electrodes are placed along the ground surface (generally in either 2D or 3D regular grids) or in vertical arrays in the subsurface. This configuration now allows a computer to control the data acquisition without any manual intervention. A sequence of measurements (typically hundreds to thousands of measurements) can be defined, and the acquisition software will collect the associated data. Each measurement typically takes several (1-4 seconds, depending on a number of settings), and a sequence typically takes anywhere between 10 minutes and one day.

More recently (since about 2005) a number of systems have come on the market which are so called multichannel systems. In a multichannel system there is the possibility of measuring the potential over multiple combinations of potential electrodes at the same time. In such a measurement there is still only one pair of current electrodes, but multiple (typical four - ten) pairs of potential electrodes. This allows for a substantial decrease of acquisition length, and thus allows for an increased temporal resolution in monitoring applications.

Different commercial manufacturers sell multichannel resistivity instruments in the United States and abroad. For the field demonstration at Brandywine, we used both a single channel, 180 electrode system by MPT (for the first injection) and an 8 channel, 128 electrode system by MPT¹ (for the second injection). The MPT systems consist of a control unit and one or more multiplexers. The control unit of both systems was connected to a dedicated computer which controls data acquisition. We used a USGS-owned Multiphase Technologies MPT-EIT2003 system for the first injection. The system was configured with an external, 2400W DC power supply, allowing for injection of up to 4A. We used an INL owned MPT DAS 1 system for the second injection monitoring. This system uses externally supplied 12 V power to internally generate the required voltage and currents for injection.

2.1.3.2 Electrical resistivity instrumentation - software

Resistivity hardware is typically provided with vendor and instrument specific control software. While the details of these software packages differ, software provided with the current generation of hardware all provide similar capabilities in terms of survey scheduling and repeat data acquisition. A user generated sequence of measurements can be loaded and scheduled to be collected at user controllable intervals. Once data acquisition is completed data needs to be processed (inverted) to yield a 2D profile of electrical resistivity. The theory behind numerical modeling of resistivity (Dey and Morrison 1979) and the associated implementation of resistivity inversion (LaBrecque, Miletto et al. 1996; Loke and Barker 1996) is well established.

Multiple codes exist for inversion of electrical geophysical data. Such codes include both

¹ The use of and reference to specific instrumentation does not constitute an endorsement of this instrumentation by any member or member organization of the project team.

research codes, open source codes (Pidlisecky, Haber et al. 2007) and codes manufactured and sold by and through instrument vendors. In our demonstration we used an electrical geophysical inversion code initially developed at the Idaho National Laboratory and currently being maintained and enhanced at the Pacific Northwest National Laboratory by Dr. Tim Johnson. This code was developed specifically for time-lapse monitoring of large electrical geophysical datasets. This code is discussed in more detail in Section 2.3.

2.1.3.3 Resistivity cables and electrodes

Electrical resistivity instrumentation needs to be connected through cables to electrodes (which are placed either on or near the ground surface or in vertical boreholes). Resistivity cables typically use 20 or 22 gage multi-conductor wire which is terminated on one side with a connector which attaches to the resistivity hardware (the multiplexers). Typically the cable has a lead in part followed by a part along which electrodes (in the case of borehole cables) or electrode connectors (in the case of surface cables) are placed. Borehole electrodes are typically molded around the cable. Electrode connectors for surface electrodes are typically metal connectors of 3-4 inches which are recessed in the cable. An alligator clip can be connected to this connector which in turn attaches to a metal electrode (typically a metal rod of 1-2 feet) which is hammered in the ground. Such cables can be readily purchased from a number of vendors. The cost of such cables fluctuates with the price of copper, but can be substantial. In our project both borehole and surface cables were used. Details on the cost of the cables used in this effort are given in section 4.

2.1.4 Time-lapse radar geophysics

As stated previously, time-lapse electrical methods are more amenable to autonomous monitoring than are time-lapse radar methods, which require labor-intensive fieldwork and data processing. Although radar methods have proven effective for monitoring biostimulation in previous work (Lane et al., 2004, 2006), they are not integrated into the HPMS. Radar methods were used here instead to provide a second line of information to help validate our electrical results, which are the focus of our demonstration project.

Cross-hole ground-penetrating (XHGPR) radar data may be collected using full tomographic and (or) zero-offset (or ‘level-run’) geometries (Figure 2-5). As with ERT, XHGPR can image changes in subsurface properties associated with biostimulation (Lane et al., 2004, 2006, 2007) or tracer experiments (Day-Lewis et al., 2003, 2004). The velocity of electromagnetic waves is a function of pore-fluid (e.g., vegetable oil emulsion vs. water), and the attenuation of electromagnetic waves is a function of electrical conductivity, and thus total dissolved solids. Level-run data collected between the four ground-penetrating radar wells installed at our well cluster.

Cross-hole radar data were collected using a borehole radar system and electric-dipole antennas with a center frequency of 100 MHz. XHGPR provides a second line of evidence to support interpretation of the ERT results, providing validation to the extent possible using a second type of geophysical imaging. Radar amplitudes for horizontal raypaths between well pairs were collected in January 2008, April 2008, and August 2008 XHGPR events. The first data collection period was prior to ABC injections, and the second and third events subsequent to those injections.

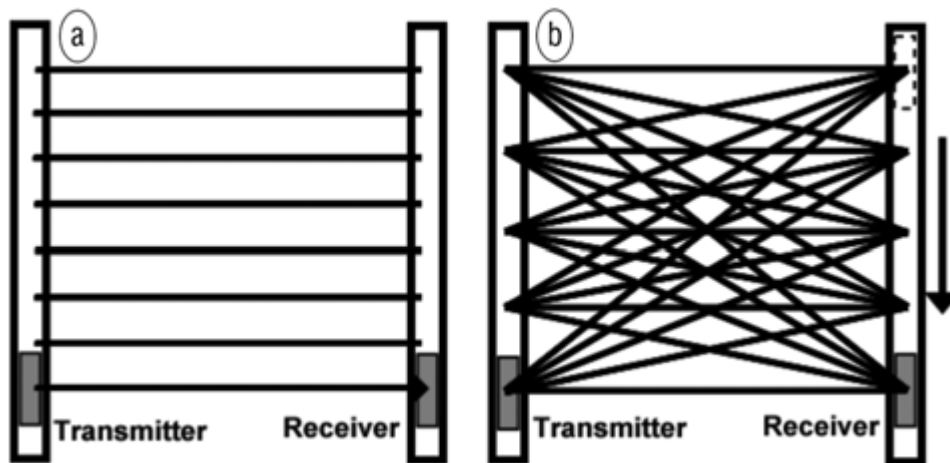


Figure 2-5 Schematic of the collection of crosshole radar data for (a) level-run and (b) tomography.

2.2 Hydrogeophysical Performance Monitoring System

2.2.1 Expected application of technology

This technology can be applied to monitoring of both environmentally and energy related processes. This technology is currently being applied by report authors Versteeg and Johnson to autonomously monitor rain infiltration at the Hanford 300 Area, and has been applied to monitor river-groundwater exchange, and is being further developed. USGS PI's have adapted and extended the direct-push installation of electrodes for use at other sites, including the DOE Naturita and Hanford 300 Area sites; this work has greatly reduced installation cost and capital costs associated with instrumentation, as compared to the setup at Brandywine. As correct application and deployment of this technology does not require end users to manage or process geophysical data (they directly get access to changes in subsurface conductivity) it is well suited to monitor bioremediation efforts, and follow progress of remedial activities in general.

2.3 TECHNOLOGY DEVELOPMENT PRIOR TO FIELD DEMONSTRATION

The general concept and components of the HPMS system were developed in prior efforts by the project team (LaBrecque, Heath et al. 2004; Lane, Day-Lewis et al. 2004; Lane, Day-Lewis et al. 2004; Versteeg 2004; Versteeg, Ankeny et al. 2004; Versteeg, Richardson et al. 2005; Versteeg, Wangerud et al. 2005; Versteeg, Richardson et al. 2006). The components include:

- multi-electrode electrical resistivity instruments and software to collect data
- multi-electrode cables and electrodes
- software middleware and hardware for data transfer
- server based software for data ingestion, qa/qc and management

- inversion codes for the inversion of electrical geophysical data
- web interfaces allowing for result access by end users

The commercially available components developed previously and by others, were discussed in Section 2.1. The resistivity cables, acquisition unit, and electrodes used in our demonstration all are commercial off the shelf components. While in our demonstration we used hardware from one vendor, multi-channel, multi-electrode systems from multiple vendors could be used within a HPMS implementation.

In this section, we detail those components for which substantial advances or extensions were made under the ESTCP project ER-0717 (1) the time-elapse inversion resistivity code used in this project and (2) the web based component for data processing and result delivery. Both of these components have seen substantial enhancements after the completion of the technical part of ER-0717 in August of 2010.

2.3.1 Time-lapse resistivity inversion code

An essential part of electrical geophysical monitoring is data processing. This data processing translates the field measurements into a subsurface bulk electrical conductivity distribution through process called inversion. While this can be done analytically for simple models and small datasets, for all modern day datasets this is done through a numerical code. There are several commercially available ERT inversion codes, but each of these has limitations making them less than optimal for autonomous ERT monitoring.

Specifically, commercially available codes are typically designed to run on standard laptops and desktop personal computers, and use either a single cpu, or in some cases several cpu's that share the same memory (shared memory processors). Shared memory ERT codes are limited in their ability to invert large data sets such as those produced in 3D applications (such as the application discussed here). In order to accommodate larger data sets, compromises must be made that reduce the accuracy of the solution and degrade the ability of the code to resolve changes in subsurface bulk conductivity that ultimately describe the process of interest (e.g. amendment transport and bio-activity in this application). In addition to the computational limitations noted above, commercially available codes cannot be easily integrated in an automated data processing flow because they are controlled through GUI's (Graphical User Interfaces) that require user input at runtime. There are generally no mechanisms built in to such codes that facilitate autonomous control within a larger monitoring system.

To address these limitations, a new parallel 3D time-lapse (i.e., 4D) ERT inversion code was developed under funding support from the Department of Energy (Johnson, Versteeg et al., 2010). This code was validated and tested against the data from the Brandywine site as described in (Versteeg and Johnson 2008; Versteeg and Johnson 2009; Johnson, Versteeg et al. 2010; Johnson, Versteeg et al. 2010), and has since been used in numerous characterization and monitoring applications at the Hanford Site. This same code is currently being optimized for remedial applications in fractured rock under ESTCP project ER-201118. The code is built around the message passing interface standard (Gropp, Lusk et al. 1996) allowing scalability on large distributed memory high-performance computing systems. For instance, as of March 2012 the code has been successfully executed on 2 cpu's for an inversion problem estimating several thousand bulk conductivity values, to over 3500 cpu's for a problem estimating over 1 million

bulk conductivity. For the Brandywine project, inversions were executed using 106 cpu's on a parallel computing system housed at the Idaho National Laboratory.

The computational requirements of ERT inversion can be particularly demanding for time-lapse monitoring where one inversion must be completed to produce each 'snapshot'. Given the capabilities of modern multichannel ERT instrumentation to quickly collect large amounts of data, time-resolution provided by an ERT monitoring system will be approximately equivalent to the time required to produce a single snapshot. Therefore, faster inversion times will improve temporal resolution, and even enable real-time 3D monitoring such as demonstrated in this project.

Each time-lapse dataset results in an image of the subsurface electrical conductivity. The change in electrical conductivity from pre-injection conditions is determined by subtracting the pre-injection baseline image from the time-lapse image (Figure 2-6). These changes are then interpreted in terms of amendment migration and/or biogeochemical processes.

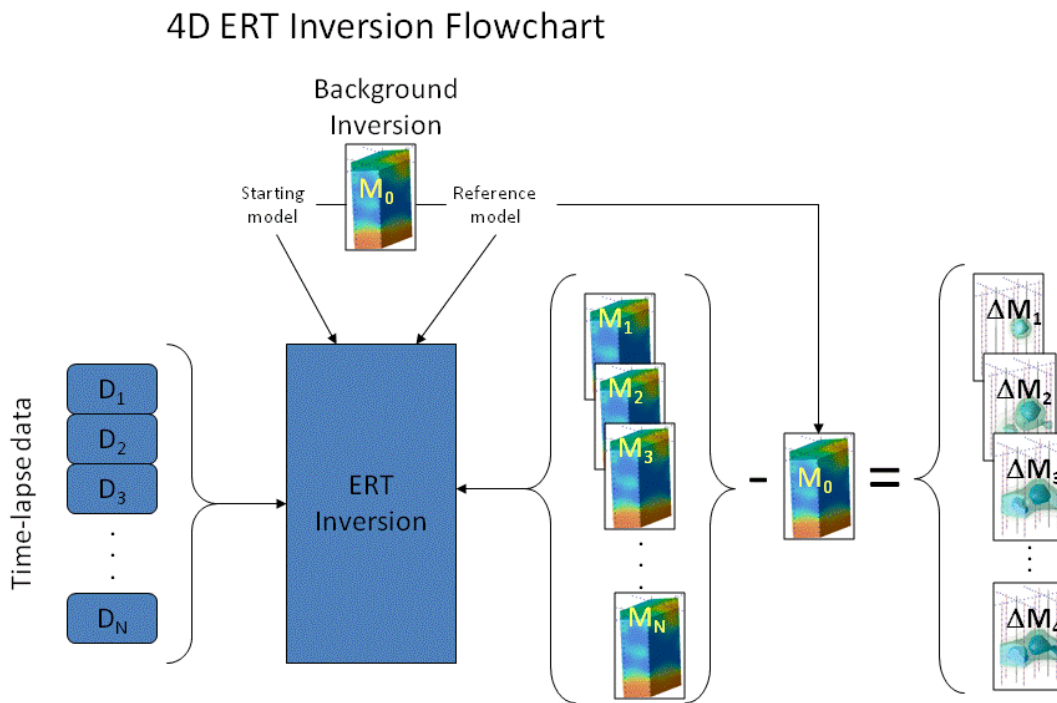


Figure 2-6 Flowchart of 4D ERT Inversion

2.3.2 Web applications for data processing and result delivery

The project team has been using web applications for automated data processing and result delivery since about 2001 (Versteeg and Birken 2001). These web applications were initially fairly

simple. Over the last ten years the capabilities of these web applications (both in terms of back end data processing and end user ability to access data) have increased substantially and the underlying code which performs data processing and result delivery has been refactored (rewritten) multiple times. Such changes typically add functionality and add increased robustness, and are transparent to the end user (as the user interacts with the system to a web browser, there is no need to upgrade software). In general, the trend in this rewriting has been an increased use of an object-oriented approach, and the use of frameworks. The code used under this effort was implemented as a Zend Framework web application (Pope 2009).

During the demonstration project incremental versions of the code were used to provide monitoring capabilities, and in the fall of 2010 the capability of the code at that time to provide real time monitoring was demonstrated live to DoD and DOE staff. The description below provides a high level description of code functionality.

The HPMS system can be thought of as having three elements

- Middleware software
- Server based software for data ingestion, qa/qc and management
- Software which provides client side functionality

2.3.2.1 Middleware software

Middleware software and hardware includes those components of the HPMS system which allow for the transfer of data collected in the field to a server. There are many relatively equivalent solutions for this. In general, data transfer happens using wired or wireless ethernet (which is commercially available from multiple providers), enabled by either commercial or custom written software (e.g. scripts written using the open source package putty and stfp). Over the duration of the project several data transfer solutions were used, all of which were easy to implement. Towards the end we used a small C# code which kept track of new files, and once new files arrived transferred these files using the sftp protocol to a secure server. A commercial wireless data subscription and a USB wireless ethernet card were used for data transfer. The main function of the middleware software is to watch for survey files which are completed by the data acquisition system. Once acquisition is completed data is transferred to the server. Note that the middleware software does not control actual data acquisition: this is controlled by vendor provided software, which is typically configured to repeat the same set of surveys continuously.

The data files which are generated by resistivity systems, have a well-defined format and structure, and in general have names which are automatically assigned by the acquisition software or can be selected by the user. Note that a file can have multiple parts (for instance, header and raw data as well as data containing information on errors encountered during acquisition).

The format and organization of such data is generally different between vendors, and some vendors store their data in flat ascii files, whereas other vendors use a binary format. In this project each survey results in a single ascii file with an unique name.

2.3.2.2 Server based software for data ingestion, qa/qc and management

A server is a central component of the HPMS system. This server receives data from the field,

provides data management and processing, and runs the web server software. Note that the term “server” here refers to the actual physical computer; the term “web server software” refers to the software, which allows the computer to host a website (and to serve web pages).

The server houses several pieces of software which take care of data ingestion, qa/qc and management. From a functional perspective **what** these packages are supposed to do has remained more or less the same over the duration of the project. However, the underlying code and detailed capabilities has changed over the duration of the project, and has kept on changing after project completion.

We describe here the software flow at the end of the project (Figure 2-7 shows a flowchart of the software)

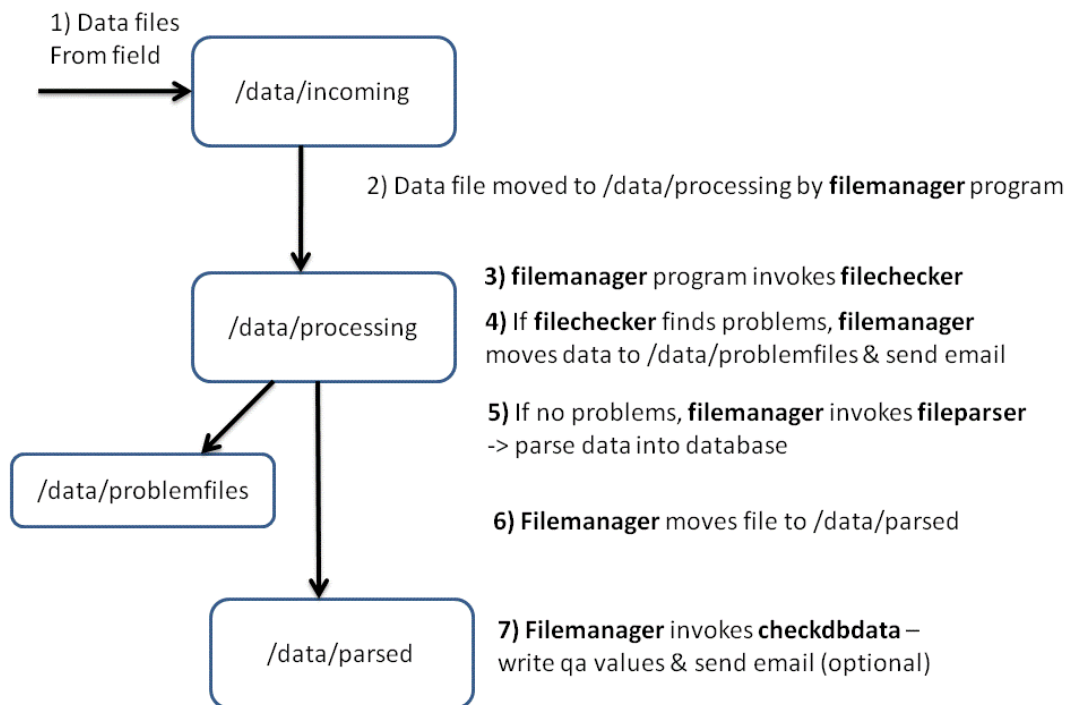


Figure 2-7 Flow chart of server based software for data ingestion and qa/qc

The data arrive on the server (transferred there by the field middleware) in a specific directory (the "incoming" directory).

A master control program called **filemanager** controls what happens with this file when it arrives. The file manager periodically examines the incoming directory for new files. If a file exists, it is moved to a "processing" directory, and a **filecheck** program is invoked by the file manager. This program reads the file, and performs checks to make sure that the file has no issues. Typical issues encountered are

- corrupted file (e.g. in transfer)
- file which was not completed normally
- file which does not have a recognized name or extension

If the file does not pass the initial tests, it is moved to a /data/problemfiles directory, and an email is sent to alert the cognizant staff that an issue exists.

If the filecheck program finds no issues, another program is invoked. This is a fileparser program. This program parses the metadata and data into a relational database. Subsequent to this the data file is moved into the /data/parsed directory.

Once this is done, a third program (**checkdbdata**) is run on the data. This program examines the new data, and calculates qa/qc values on different aspects of the data. These attributes typically include average, min/max and median reciprocity, current and voltage. These attributes are compared to previous similar data, and when the values have changed substantially an email is sent. This allows one to detect when issues have arisen. For example, if the power supply which provides the voltage for the current injection has gone bad one would expect to see an abrupt change in average voltage.

It should be noted that problems with resistivity data can both be global and local. For instance, in time-lapse surface resistivity measurements it is very common that one electrode gets disconnected (for instance through someone dislodging a clip or by animal activity). Another common occurrence would be that someone who was working on a site switched two connectors after system maintenance. Testing for such occurrences is an ideal task for automation, and can provide a much clearer view of whether something happened with a system than manual data examination.

2.3.2.3 Software which provides client side functionality

The third part of the HPMS system is the web interface which allows users to get access to data and results. As with the other parts of our system, this web interface has gone through several incarnations. As the lead for this project has changed institutions the original server site for the project is no longer available. However, a web site which provides access to the data and results is available to the readers of this report.

This site is implemented using Zend Framework (Pope 2009), a PHP web application framework. The site makes extensive use of javascript to provide a rich web interface, and allows users to visualize data and results on demand.

2.4 ADVANTAGES AND LIMITATIONS OF THE TECHNOLOGY

The primary alternative technology to our method is periodic direct sampling and analysis of groundwater chemistry. There are two main advantages of our approach compared to direct sampling (see also Table 1-1). These are

- volumetric, temporally dense information on amendment behavior
- lower recurring costs than direct sampling method

Volumetric, temporally dense information on amendment behavior: The primary advantage of the technology demonstrated here is the ability to provide volumetric, temporally dense, information on amendment behavior to the site operator in near real time. Essentially, operators can track amendment movement in near real time, and are able to link amendment injection histories to resulting amendment distributions. Alternative technologies rely on direct measurements in soil and groundwater. Because of the associated analysis time and cost, these methods do not provide a viable alternative to obtain similar information.

Lower recurring costs than direct sampling method: Our approach has substantially lower recurring cost than direct sampling methods. In addition, while our system requires some upfront costs in terms of resistivity system, infrastructure and electrode installation the most expensive components of the HPMS system are reusable. A detailed cost analysis is given in the subsequent section of this report which lists both initial and recurring costs. The system discussed here is substantially cheaper than the alternative of sampling and analysis.

There are four limitations of our method. These are

- applicability in complex environments
- installation cost for resistivity wells
- spatial resolution
- need for a sufficient contrast in electrical properties between amendment and initial bulk conductivity

Applicability in complex environments: In extremely complex geologic and highly heterogeneous environments our approach will be challenging to implement. For instance, even though our approach can, in principle, be used in bedrock aquifers, there is an important limitation in that the geophysical signal is a function of changes to pore-fluids or at fluid-grain boundaries; hence it varies with porosity, and if the changing pore fluid occupies only a small fraction of the bulk (e.g., 2% porosity), the signal will be relatively weak. Another constraint is that electrical methods require good contact between electrodes and the soil, and if this is not possible (for instance if the soil is very dry) electrical methods will not provide good data.

Installation cost for resistivity wells: For the site discussed here we used electrodes placed along boreholes using direct push technology (Geoprobe®) in the first test. For the second test we used surface electrodes in addition to the borehole electrodes. Our analysis includes a cost and performance comparison of surface against borehole electrodes. For extensive but shallow sites, or for fractured rock sites installation costs of borehole electrodes will be substantial and may make this technology non-cost competitive unless cheap ways to install vertical resistivity strings are developed. Several groups are working on such installation methods, which may include improved direct-push installation which could deploy many strings per day (rather than the ~3 wells/day rate done under this effort). Notably, our team has, since 2007, streamlined the hardware and installation approach to greatly reduce costs. For example, the USGS PI's have installed 9 direct-push wells instrumented with electrodes, thermistors, and sampling points (similar in capability to the Brandywine wells) at a DOE site in Naturita, Colorado, for a small fraction (~10%) of the cost of the Brandywine installation. This is discussed further in the cost analysis section;

Spatial resolution: The resolution of our inversion results degrades with the horizontal offset between wells relative to the vertical distance over which the imaging is performed. Thus, if high resolution is required this method may not provide it;

Need for a sufficient contrast in electrical properties between amendment and initial bulk conductivity: as discussed previously, our method depends for its efficiency on a sufficient contrast in electrical properties between the amendment and the ambient groundwater. Thus, for cases where such a contrast does not exist the amendment would need to be “doped” with a

substance that provides contrast; this could create complications or additional cost.

3 Performance objectives

The performance objectives for our method as provided to the ESTCP office in the demonstration plan are listed in the demonstration plan, as well as whether these objectives were met. These objectives and a discussion of the results are provided in Table 3-1 .

Type of Objective	Primary Performance Criteria	Expected Performance (Metric)	Actual Performance Objective Met?
Quantitative	3D Spatial resolution of amendment maps	Better than 1.5 m	Yes
	Relative concentration gradients of amendments in 3D	Resolution in 15 % brackets	Yes
	Processing and delivery time of HPMS server	< 2 minutes	< 10 minutes ²
	Temporal resolution of amendment maps	Better than 2 hours	Yes
Qualitative	Effectiveness of HPMS system in delivering actionable information to RPMs	Utilization of system by RPMs demonstrating use and application	Yes
	Ability to map geochemical parameters of interest	Demonstrated correlation and between geochemistry and HPMS results	Yes

Table 3-1 Performance objectives for effort

3.1 Quantitative performance criteria

² In our initial proposal we specified 2 minutes, but this period did not differentiate explicitly between the time when the raw data would be available (which is around 1 minute) and the time when the processed data are available (which depends on the size of the problem and the available computational resources, and was about 10 minutes in our case). Here, we make this distinction. We successfully collected and made data available in under the original 2-minute window, but we choose to report the time including processing, i.e., 10 minutes.

3.1.1 3D Spatial resolution of amendment maps

The spatial resolution of amendment maps is given in meters. It is defined as the extent to which our method can resolve the exact spatial position of the amendment. This resolution can be calculated from independent knowledge of the position of the amendment. This information can be obtained both from knowledge on the injection location (as was done for both amendment injection efforts) or from sampling efforts (as was done for the first amendment injection). The 3D ERT inversions performed produced meshes of conductivity in between wells. Mesh element sizes varied in volume from $2.0e-4 \text{ m}^3$ near electrodes to 1 m^3 within the imaging zone. Element size is not equivalent to resolution (Day-Lewis, Singha et al. 2005), but is an upper bound. Geophysical tools (e.g., the resolution matrix) exist to evaluate resolution more quantitatively, but these are computationally intractable for large 3D problems. Based on modeling, we estimate our resolution is on the order of 1 m, thus meeting our performance criteria.

3.1.2 Relative concentration gradients of amendments in 3D

The relative concentration gradient of amendment injections is given in %, where 100 % is the highest concentration, and 0 % is the background value. It can be calculated from the inverted resistivity datasets. This concentration gradient can be calculated independently from the sampling efforts.

3.1.3 Processing and delivery time of HPMS server

The processing and delivery time of the HPMS server is defined as the wall clock time expired between the arrival of data on the server and the associated posting of results on the web interface. During this time, the following steps happen automatically

1. Data arrival at the server triggers start of processing flow
2. Data is filtered using data qa/qc and common survey filters
3. Data is passed onto the inversion program
4. Parallel inverse code is executed
5. Result of inversion is included in output file for visualization
6. Results are visualized
7. Update is posted to website

The majority of the time in these steps (> 99 %) is spent in step 4, the execution of the parallel inverse code. Most of the other steps take 1-5 seconds to execute. The inversion step wall-clock time depends both on the number of nodes available to the inverse code, the size of the grid, and the number of data points to invert, as well as on the initial model. The fastest execution time is achieved if the number of nodes is the same as the number of electrodes, and if the starting model is relatively close to the final model. Note that there are several approaches used in time-lapse inversion. These range from (a) starting with a uniform half space every step (b) starting from the model obtained in the previous step, (c) starting with the model resulting from the inversion of the first dataset or (d) starting with some model which is an average of many models. Approaches (b-d) will require fewer iterations than approach (a).

In our inversion implementation we started with a model which is the result of the inversion of the first (background) dataset. In this case a typical inversion can be performed for the data described here in about 10 minutes thus meeting our performance criteria.

3.1.4 Temporal resolution of amendment maps

The temporal resolution is given as the time between each resistivity dataset. This temporal resolution is exactly the time it takes to collect each dataset. This time depends on the type of instrument use (single vs multi-channel), the total number of electrodes in the system, and the measurement schedule. The temporal resolution was on the order of 2 days for the ABC injection which was monitored for 1.5 years starting in March 2008 and on the order of 25 minutes for the molasses injection.

3.2 Qualitative performance criteria

3.2.1 Effectiveness of HPMS system in delivering actionable information to RPMs

The effectiveness of the HPMS in delivering actionable information to RPMs can be judged by (1) the form in which the HPMS provided information on amendment behavior, (2) on the ease of getting access to this information, and (3) on the time elapsed between when the amendment injection and when the information was available.

Form: Our system provides information through an animation of spatial and temporal behavior of amendment behavior. This form makes it intuitively obvious to see where amendment is going

Ease of access: Our system provides information through a standard web browser. No special software needs to be installed, and the information is available to any authorized user on demand.

Time elapsed: the time elapsed between data collection and information being available is in the range of tens of minutes to tens of hours (depending on several factors discussed previously). This is substantially faster than sampling based analysis results (which typically take weeks to months to become available).

During the August 2010 molasses injection, our field team and guests to the site from DOE, DoD and industry, saw near-real time maps of amendment behavior as a molasses amendment was being injected. Actionable information was being delivered to operators and decision makers in near real time.

3.2.2 Ability to map geochemical parameters of interest

The ability to map geochemical parameters of interest is based on relationships between the bulk electrical properties and those geochemical parameters. The derivation and validation of this relationship was demonstrated by providing a pre sampling estimate of anticipated sample results for our Fall 2008 sampling effort to the DoD program manager. We also demonstrated (as discussed in sections 5 and 6) that our results are highly correlated with known geochemical processes on site, thus meeting our performance criteria.

4 SITE DESCRIPTION

4.1 Site selection criteria and site selection

As discussed previously the overall objective of this field-scale demonstration was the validation of autonomous electrical geophysical monitoring to track amendment injection and behavior. This objective encompassed four sub-objectives:

- map time-lapse geophysical data into the spatial distribution of injected amendments,
- estimate changes in relevant geochemical parameters, especially redox, associated with bioremediation,
- calibrate and ground truth the geophysical results using direct sampling, and
- develop a guidance document, which will allow for the implementation of this system at DoD sites.

In order for this demonstration to be relevant, the field-scale demonstration needed to be done at a DoD site where bioremediation was ongoing. After selection of the project for award a site solicitation letter was drafted and distributed. This letter was sent to RPM's both by the project's PI's and the ESTCP program office. The site selection criteria outlined in our solicitation letter are listed and elaborated upon in Table 4-1.

These criteria were driven by the cost-effectiveness of our demonstration/evaluation and are not limitations inherent to our approach. For example, our technology is applicable in fractured rock and outside the northeastern US, but our project budget was based on important fiscal assumptions, such as (1) viability of direct-push installation of wells; (2) shallow contamination, enabling rapid and cost-effective installation of direct-push wells; (3) low-cost travel for USGS field crews; (4) ability to "piggyback" on planned amendment injections; and (4) existing site infrastructure for data transfer and instrument housing.

Parameter	Preferred Value	Relative Importance (1-5, 1 highest)	Brandywine DRMO, Andrews AFB, Brandywine MD
Chlorinated HC	DNAPL, Above MCL	1	TCE
Subsurface geology	Unconsolidated sediments	1	Unconsolidated sediments
Depth to groundwater contamination	20 – 30 ft	1	~2 to ~30 ft
Estimated cost of DP well installation	\$2K – \$3K per well	1	\$3K per well
Site planned remedial action	Amendment injection Fall of 2007	1	Amendment Injection Fall 2007
Utility access	Electrical access available	2	Electrical access available

Telecommunication access	Wireless, Ethernet or phone landline	2	Wireless, cable, Ethernet and phone
Regulatory Interface	Established relations – no permit problems anticipated	3	Established Relations – no permit problems anticipated
Field logistics/site location	Northeastern U.S.	3	Maryland; existing site infrastructure; site is secure
Prior Site Characterization	Well characterized site (geology and contamination)	4	Very well characterized site
Post amendment injection sampling	Extensive sampling for contaminant and amendment planned	4	Extensive sampling of contaminant and amendment planned
Second phase of injections	Opportunity to benefit follow-on injections	4	Second phase planned
Existing monitoring well availability	Comprehensive network of monitoring wells	4	Comprehensive network of monitoring wells
Contamination Extent	Large contaminant plume for potential follow-on technology implementation	4	Large plume and remedial efforts planned (over 1000 injection points and different amendments)

Table 4-1 Site Selection Criteria

Over a dozen site nominations were received in response to the site solicitation letter, and top sites were visited by one of the project PIs. Subsequent to receiving these responses discussions with the site program managers and with the ESTCP program office resulted in the selection of the Andrews Air Force Base (AFB) Brandywine DRMO in Brandywine MD for our test site as this provided the best match to our site-selection criteria.

The Andrews AFB DRMO remedial plan included planned amendment injections involving multiple amendment types (e.g., ABC, as well as sodium-bicarbonate pH adjustment), over 1000 injection points, and two-phases of injections. The site was well characterized, has shallow contamination consisting of chlorinated solvents, and direct-push technology is viable; as noted, these factors contribute to a cost-effective demonstration of the HPMS, but are not requirements of our technology. The spatial density of injections (every 20 feet) would allow us to monitor multiple injections with the limited footprint of our demonstration system.

In addition, the multi-stage injection plan would allow our results to directly benefit future work at the site; hence our demonstration project could provide information for site managers that may be useful in verifying the efficacy of the first phase of injections and in designing the second phase

Finally, the DRMO site is fenced-off and secure, but visitors did not need to go through base security to reach the site, thus facilitating field trips and access for visitors. The proximity to Washington and Baltimore area airports allowed for cost efficient site visits by the project staff (as well as field demonstrations).

4.2 Brandywine DRMO LOCATION AND HISTORY

The Brandywine DRMO (EPA 2006) is an inactive U.S. Department of Defense (DOD) facility that occupies approximately eight acres of land. The U.S. Navy operated the site as a storage yard and marketing office from an unknown date until 1955, when it was transferred to the U.S. Air Force. In 1973, the Defense Supply Agency (DSA) assumed control of the site, and the Defense Property Disposal Organization (DPDO) received a permit from Andrews AFB to use the property. The Brandywine DRMO site is located in southern Prince George's County, Maryland, about 8 miles south-southeast of the AFB. The site lies within the Potomac River Basin. A remedial investigation was completed in 2005 (URS 2005), and thus the site is well characterized.

From approximately 1953 until 1988, the DRMO site was used principally as a storage area for surplus electrical equipment, other materials, and for storage of hazardous wastes. The site accepted materials, including hazardous wastes, from several installations, including Andrews AFB, Bolling Air Force Base, the Washington Naval Yard, the Navy Research Laboratory, the Naval Surface Warfare Center (NSWC)-Indian Head Ordnance Station, and White Oak Laboratory (now known as NSWC-White Oak). Drums of waste solvents, capacitors and transformers containing polychlorinated biphenyls (PCBs) were stored at the DRMO. Records indicate there were two burn pits used for disposal and burn of waste and several above and below ground tanks. The Air Force (AF) removed the burn pits and tanks in 1989.

This site was proposed to the National Priorities List of the most serious uncontrolled or abandoned hazardous waste sites requiring long-term cleanup action on July 28, 1999. The site was formally added to the list May 10, 1999, making it eligible for federal cleanup funds. Numerous environmental investigations have occurred at the Brandywine site (Table 4-2)

Year	Investigation
1985	Phase I IRP Records Search (ES, 1985)
1988 to 1990	USGS Groundwater and Soil Investigation (USGS, 1991)
1991	HAZWRAP TCE Plume Delineation Study (Dames & Moore, 1992a)
1992	Pumping Test (Dames & Moore, 1992b)
1993 to 1994	Soil and Tank Removal Action (HNUS, 1995)
1996	HAZWRAP EE/CA (for groundwater treatment) (Dames & Moore, 1996)
1999	Groundwater Treatment System Operations and Emissions Test (IT, 1999)
2002 to 2003	Remedial Investigation (URS, 2005)
2006	EE/CA (for surface soil contamination) (URS, 2006a)
2006	Focused Feasibility Study (for groundwater contamination) (URS, 2006b)
2006	Groundwater Treatability Studies (URS, 2006c)

Table 4-2 From (EPA 2006) Environmental investigations at the Brandywine site

4.3 SITE GEOLOGY/HYDROGEOLOGY

The site surficial materials consist of silt, silty-sand, and sand. Two formations are identified on the site: the Brandywine formation (about 0-30 feet) and the Calvert formation (directly below the Brandywine formation) which behaves as an aquitard. Contamination is shallow, extending to about 30 ft below ground surface (bgs) in the Brandywine Formation. The target zone for remediation is bounded below by the Calvert Formation. The water table is at about 5ft bgs. Groundwater flow is toward the north, with a measured groundwater velocity of about 50 ft/year.

4.4 CONTAMINANT DISTRIBUTION

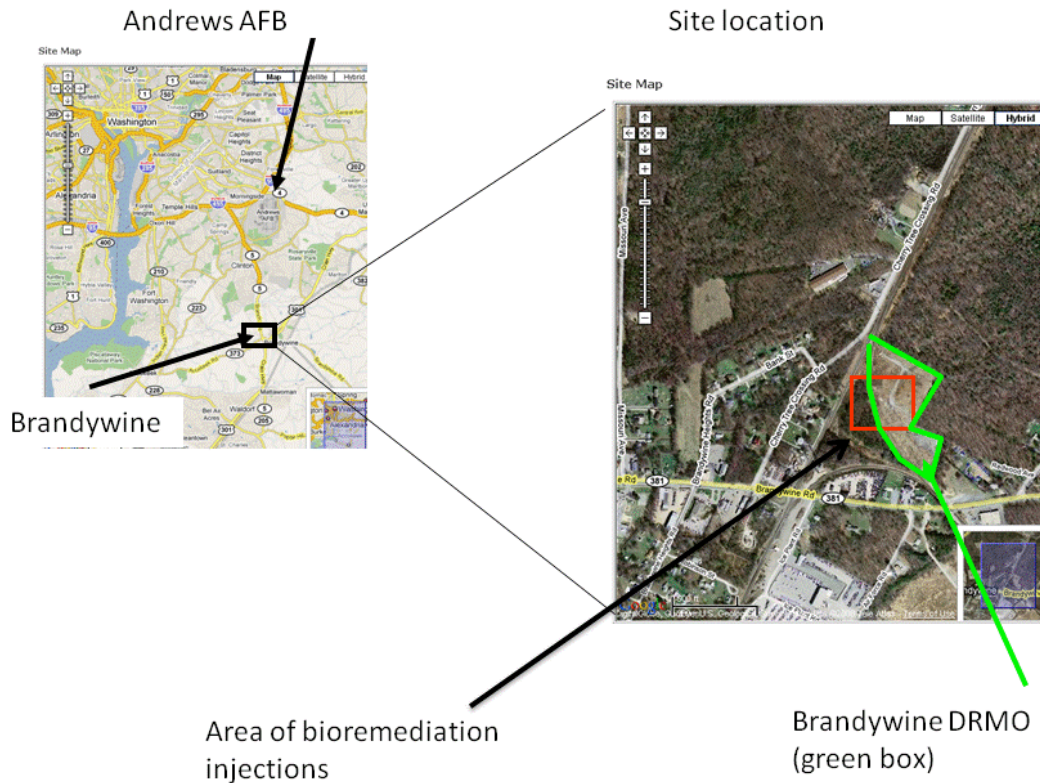


Figure 4-1 Site location of the Brandywine DRMO

The extent of groundwater contamination at the Brandywine site is discussed in depth in the Brandywine Remedial Investigation (RI) report (URS 2005). The material presented in this section is verbatim from section 2.5.3 the ROD (EPA 2006).

Based on historical evidence and the groundwater and soil data presented and discussed in the Brandywine RI, the releases of CERCLA-regulated hazardous substances at the Brandywine DRMO resulted in three distinct plumes of dissolved chlorinated solvents in the groundwater. The area of highest contaminant concentrations occurs west and northwest of the DRMO yard. The release or releases responsible for generating this plume most likely occurred near the northwest corner of the DRMO yard. A smaller, disconnected plume is located within the DRMO yard. There also is a smaller plume located to the northeast of the DRMO yard. The spill or spills responsible for groundwater contamination within the DRMO yard were events separate from the spills responsible for groundwater contamination northwest of the yard; the plumes are spatially disconnected. The plume within the DRMO yard is smaller and has lower concentrations of contaminants as is the smaller plume to the northeast.

The most significant groundwater contaminants at the site, as defined by areal extent and concentrations above the maximum contaminant levels (MCLs) for federal drinking water

standards, are trichloroethene (TCE), tetrachloroethene (PCE), and cis-1,2-dichloroethene (DCE). The maximum concentrations of TCE and PCE measured at the site are 224.2 milligrams per liter (mg/L) and 0.349 mg/L, respectively. The MCL for TCE and PCE is 0.005 mg/L. The maximum cis-1, 2- DCE concentration measured at the site was 13.4 mg/L. The MCL for cis-1, 2-DCE is 0.070 mg/L. The results of the site investigations indicate that the VOCs in groundwater at the Brandywine site are present both as dissolved contaminants and as droplets or pools of dense non-aqueous phase liquid (DNAPL) that contain primarily TCE.

A Focused Feasibility Study (FFS) was undertaken in 2005 to evaluate remedial action alternatives that would address contamination associated with groundwater at the Brandywine site (URS 2006). The FFS concluded that the Contaminants of Potential Concern (COPCs) in groundwater at the site are TCE, PCE, cis-1, 2-DCE, vinyl chloride, naphthalene, 2-methylnaphthalene, iron, and manganese. The TCE and PCE were likely released into the groundwater due to site activities.

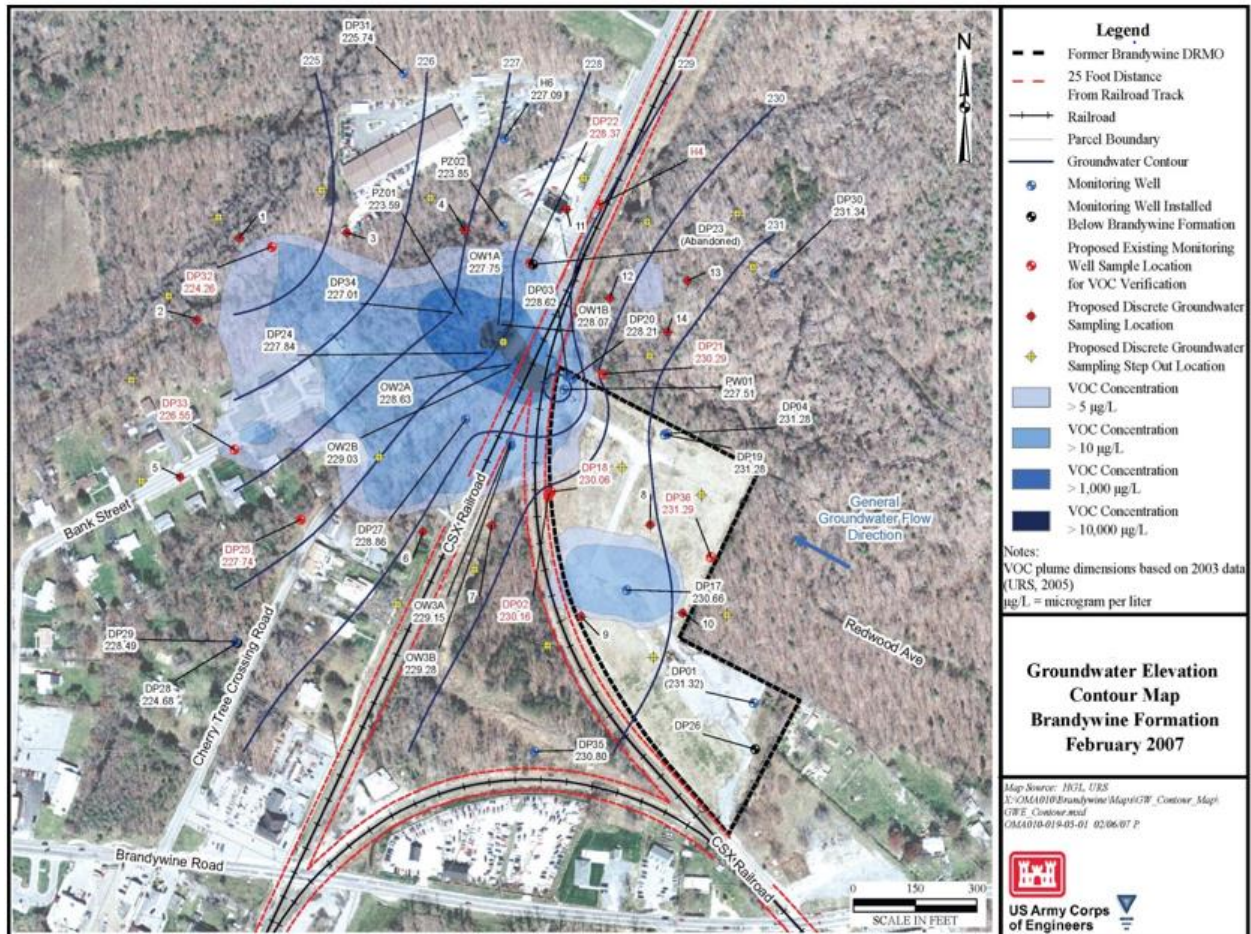


Figure 4-2 Ground-water elevations and contaminant distribution in the vicinity of the Andrews AFB DRMO, Brandywine, MD. The fieldstudy described here focused on an area within the plume in the DRMO area.

4.4.1 Cleanup Progress

In 1989, the AF initiated and removed polychlorinated biphenyl (PCB) contaminated soil on site. In September 1996, the AF issued a Decision Document for the installation of horizontal extraction wells and a treatment system to treat the contaminated groundwater. According to the information provided by Andrews AFB and Maryland Department of the Environment (MDE), at the last minute Andrews AFB changed the design from horizontal wells to an on-site interceptor trench with a treatment system. Andrews AFB explained that the design change was because they did not receive access to offsite areas and that private parties wanted compensation. Following the construction of the interceptor trench, Andrews AFB and MDE disputed the issue of permit requirements for the treatment system for almost four years. The treatment system was subsequently turned on. Because the majority of the contamination is off site, the treatment is unable to capture and treat the entire groundwater contaminant plumes.

The remedial investigation and feasibility study (RI/FS) began in October 2001. Sampling activities began in December 2001. There was a Phase 1, a Phase 2, and Phase 2b due to the complex geology and hydrogeological conditions. The Phase 2b effort tried to detect dense non-aqueous phase liquid (DNAPL) in groundwater. The investigation was complete in 2007. It did identify DNAPL of trichloroethylene (TCE). Trichloroethylene (TCE) was detected at 224 parts per million (ppm) or 224,000 parts per billion (ppb) in groundwater. Based upon the detection of DNAPL, an interim ROD was issued to remediate the contaminated groundwater. The selected remedy to treat the contaminated groundwater is Bioaugmentation with Gradient Control, Institutional Controls and Groundwater Monitoring.

An Engineering Evaluation/Cost Analysis (EE/CA) was finalized in September 2006 for PCB-contaminated soil and sediment removal in the adjacent wetland. The Action Memorandum to fund the EE/CA was signed in 2007. Removal of the PCB-contaminated soil and sediment began in July 2007. The removal is complete as of November 2007. The team received the final report documenting that the PCB removal is complete in January 2009.

In addition, a pre-design investigation to further characterize the extent of the DNAPL was completed in 2007. EPA, MDE and PGCHD received the final remedial design/remedial action (RD/RA) work plan for the groundwater treatment in January 2008. The field work for the groundwater treatment began in July 2007 by installing the groundwater interceptor trench on the property purchased by Andrews AFB, 2007. All of the in situ injections to treat the groundwater are complete as of August 2008. The electric hookup was delayed until an easement could be agreed to between the AF and Southern Maryland Electric Co, (SMECo). The utilities including electric are connected and testing of the extraction trench and treatment system began in October 2008. Full scale treatment and monitoring begin in December 2008. A second set of in-situ groundwater injections was completed in November 2010. Monitoring of the injections and extraction and treatment system continues.

Performance monitoring of the treatment system continues. Quarterly reports on the groundwater data to evaluate the efficiency of the in situ injections continue to be received and reviewed. The extraction trench and treatment system continues to extract and treat the contaminated groundwater in the vicinity of the trench. In addition, the extraction trench is drawing

the in-situ injections toward the trench. The permeable reactive in-situ zones (barriers according to the remedial design) have not been installed.

EPA and the Air Force signed the federal facility agreement (FFA) to address the subsequent work to be conducted at the Brandywine DRMO NPL site in December 2009. A Draft Site Management Plan (SMP) was reviewed in March 2010. The final SMP contains a two year schedule that was finalized in May 2011. The 5-Year Review Report was accepted by EPA on May 17, 2011.

5 TEST DESIGN

5.1 EXPERIMENTAL DESIGN

The experimental design used to evaluate the performance objectives was driven by the constraints provided by the remedial effort described in the previous section (a bioremediation injection which was scheduled to occur in early spring of 2008). It was also driven by the site-specific remedial action at Brandywine, available infrastructure and the performance objectives. At the selected site, hundreds of amendment injections were scheduled to take place. Our experimental design was formulated to take advantage of this by monitoring two of these injections. For this, we needed to deploy electrodes and cables as well as our resistivity system. This required a semi-permanent housing for our hardware, access to line power, minimal sources of cultural noise (pipes, power lines, etc.). As our HPMS installation and associated infrastructure (e.g., shed, wells) should not interfere with the amendment emplacement efforts we selected a location for our layout at the edge of the treatment area. In addition to the site-design requirements associated with our geophysical data acquisition system, our experimental design also needed to consider collection of geochemical confirmatory data throughout our experimental plot. This required the emplacement of a sufficient number of sampling wells in our site. As a second line of geophysical evidence, our experimental plan included collection of crosshole radar data; thus our experimental design included installation of larger diameter (3-inch) wells to facilitate collection of radar data and borehole electromagnetic logs.

Our initial experiment involved the monitoring of the injections of the propriety amendment ABC performed as part of the site remedial effort. Based on feedback received from the ESTCP panel during an interim progress report in which the question arose to what extent our method would be applicable to other amendments a second experiment was added which focused on the injection and short term monitoring of a second amendment. This experiment was performed in August of 2010, and used molasses. The primary objective of the second experiment was to demonstrate (1) the applicability of our approach for a variety of amendments, including injections without pH adjustments, and (2) the ability of our system to provide near real-time monitoring information.

5.2 BASELINE CHARACTERIZATION

Baseline geophysical characterization consisted of collecting of background datasets prior to the injections. The background data collection included (1) electrical resistivity datasets for tomographic inversion, (2) borehole electrical logs collected during direct push installation, (3) cross-hole ground-penetrating radar data; and (4) chemical sampling data. These various background datasets are discussed in the following sub sections.

5.2.1 Background resistivity data

Background electrical resistivity data was collected prior to the amendment injection, and inverted using the resistivity inversion code discussed in Section 4 to provide a distribution of electrical properties. The background, i.e., pre-injection, electrical resistivity image is presented in

Figure 5-1; this is the pre-injection conductivity distribution against which subsequent tomograms are differenced for time-lapse imaging. This image is in agreement with the known geology. It indicates 2-3 meters of fill material above the less conductive Brandywine Formation, extending to a depth of about 10 meters, below which the more conductive Calvert Formation is present. As stated previously, the Calvert Formation acts as an aquitard limiting the downward migration of contaminants. The target zone for treatment thus extends from land surface to the top of the Calvert Formation.

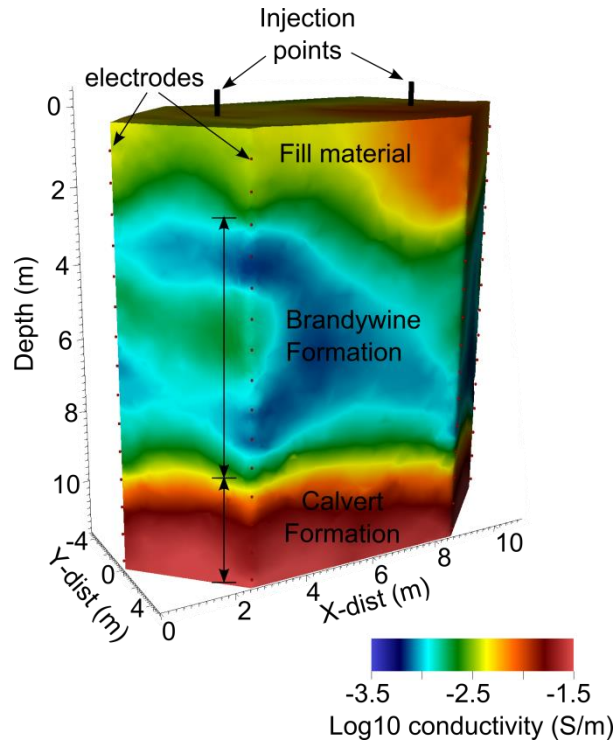


Figure 5-1 Resistivity background image, showing the pre-injection electrical structure of the subsurface.

5.2.2 Background electrical logs

Electrical conductivity (EC) logs were collected using the Geoprobe® rig's EC log capability during well installation. Because these logs slowed the drilling process, logs were not collected for all wells, but rather only for the locations to be instrumented with electrodes for acquisition of ERT data (E1-E7) (Figure 5-2). Borehole electromagnetic (EM) logs were collected post-installation in the four GPR wells (G1-G4) using a Mt. Sopris 2PIA-1000 conductivity/magnetic-susceptibility probe based on the Geonics EM-39 (Figure 5-3). The EC and EM logs are qualitatively consistent with the ERT results shown in Figure 5-1, i.e., they show the high conductivity fill overlying the lower conductivity Brandywine Formation, overlying the high conductivity Calvert Formation.

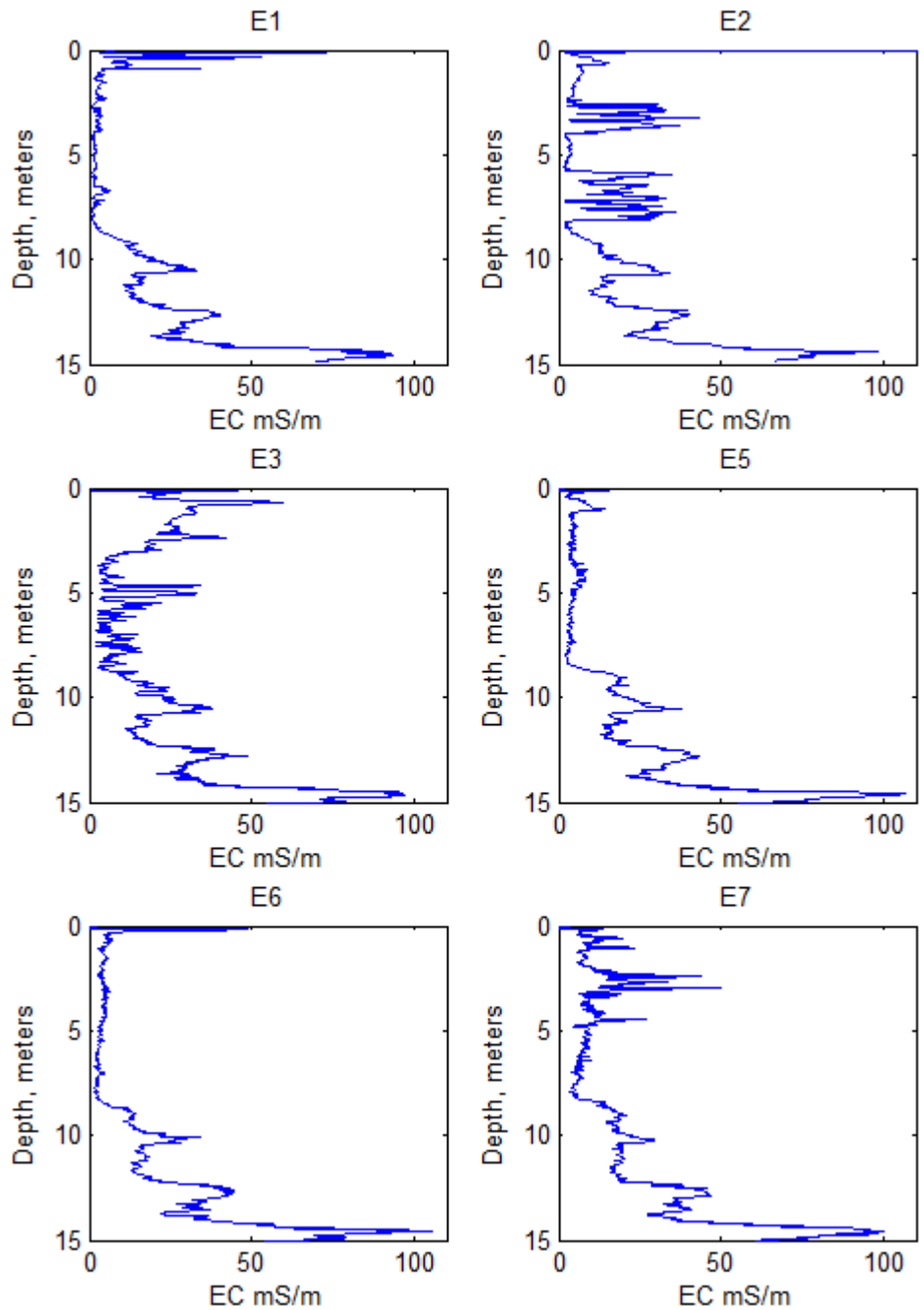


Figure 5-2 Background electrical-conductivity logs collected using the Geoprobe® EC logging equipment during drilling for electrode wells E1, E2, E3, E5, E6, and E7

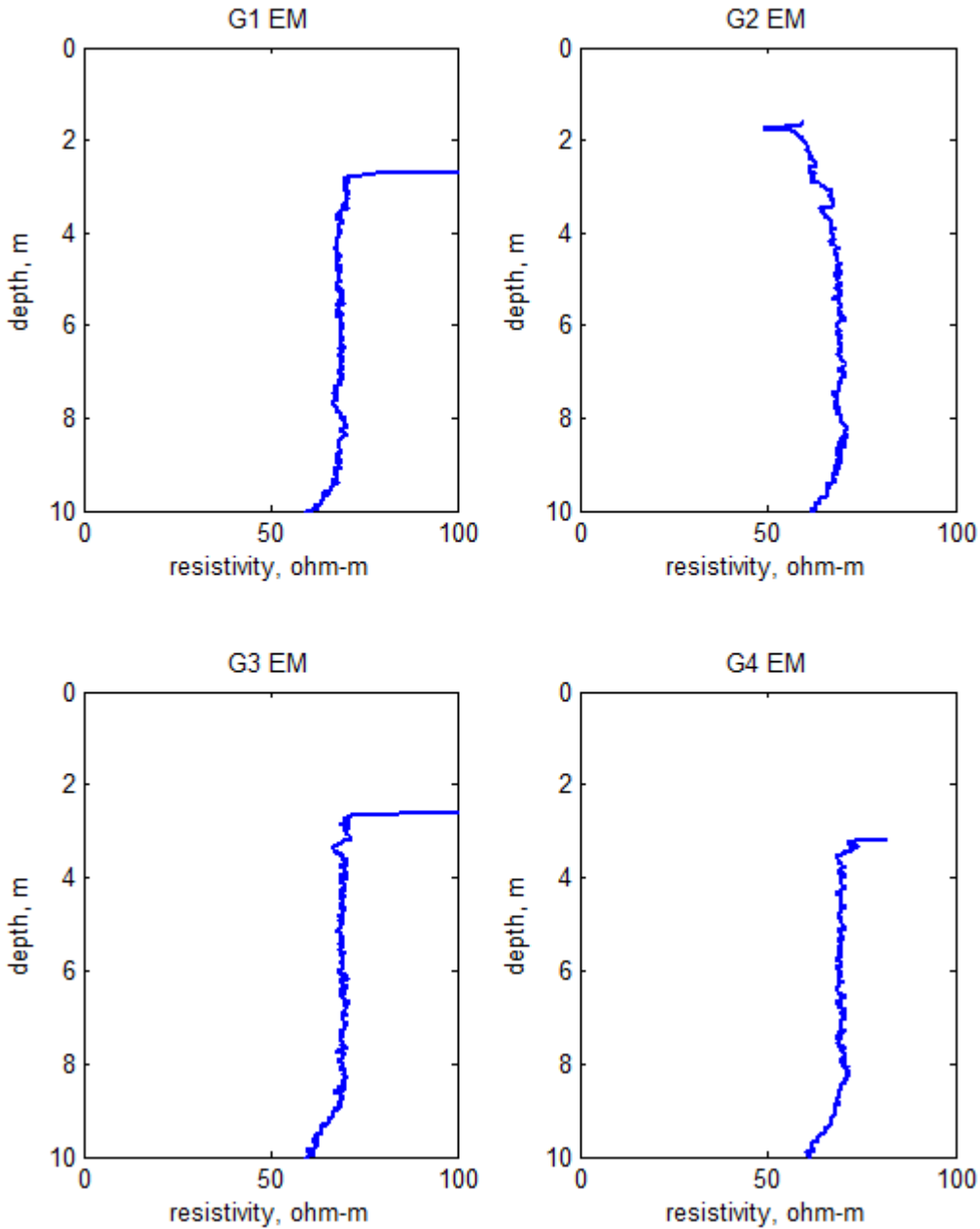


Figure 5-3 Borehole electromagnetic induction logs from wells G1-G4, displayed as resistivity.

5.2.3 Background crosshole radar

Crosshole radar data were collected in five planes between the four ground-penetrating radar wells G1-G4. Radar results (Figure 5-3) are qualitatively consistent with the EC and background ERT results, showing higher amplitude signal (and thus lower attenuation and lower electrical conductivity) in the Brandywine Formation than in the overlying fill or underlying Calvert Formation.

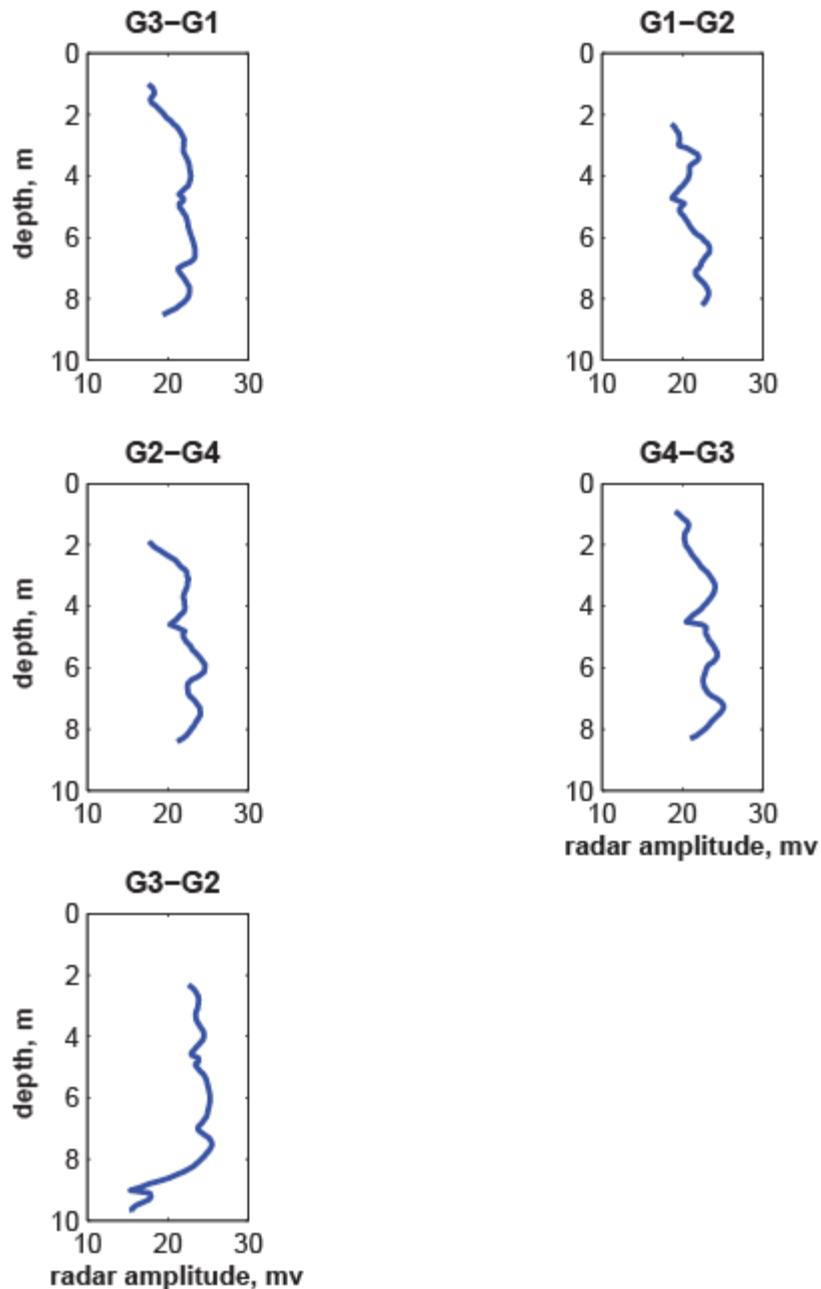


Figure 5-4 Background crosshole radar amplitude data collected in January 2008 prior to injections. Lower amplitude indicates greater attenuation, which is proportional to electrical conductivity.

5.2.4 Background sampling

A pre-injection round of chemical sampling was done for various constituents (Tables 5-1 to 5-4) in January 2008 to provide insight into site geochemical conditions, the electrical conductivity of native groundwater, and background, pre-treatment contaminant levels. No contaminants were detected in samplings from our wells. As these wells are located on the edge of the treatment area this lack of contaminants is not surprising.

Table 5-1. Baseline sampling results from gas chromatograph (GC) analysis.

Port	1,2-trans		1,2-cis		TCE	PCE	Formate	Lactose	Acetate	Propionate	Isobutyrate	Butyrate	Isovalerate	Valerate	Hexanoate
	VC	1,1-DCE	DCE	DCE											
E3T	ND	ND	ND	ND	ND	ND	ND	ND	ND	ND	ND	ND	ND	ND	ND
E3M	ND	ND	ND	ND	ND	ND	ND	ND	ND	ND	ND	ND	ND	ND	ND
E3B	ND	ND	ND	ND	ND	ND	ND	ND	ND	ND	ND	ND	ND	ND	ND
E4T	ND	ND	ND	ND	ND	ND	ND	ND	ND	ND	ND	ND	ND	ND	ND
E4M	ND	ND	ND	ND	ND	ND	ND	ND	ND	ND	ND	ND	ND	ND	ND
E4B	ND	ND	ND	ND	ND	ND	ND	ND	ND	ND	ND	ND	ND	ND	ND
E6T	ND	ND	ND	ND	ND	ND	ND	ND	ND	ND	ND	ND	ND	ND	ND
E6M	ND	ND	ND	ND	ND	ND	ND	ND	ND	ND	ND	ND	ND	ND	ND
E6B	ND	ND	ND	ND	ND	ND	ND	ND	ND	ND	ND	ND	ND	ND	ND
S1M	ND	ND	ND	ND	ND	ND	ND	ND	ND	ND	ND	ND	ND	ND	ND
S6M	ND	ND	ND	ND	ND	ND	ND	ND	ND	ND	ND	ND	ND	ND	ND
S8M	ND	ND	ND	ND	ND	ND	ND	ND	ND	ND	ND	ND	ND	ND	ND

Table 5-2. Baseline sampling results from ion chromatograph (IC) analysis.

sample	$\mu\text{g Cl} \backslash \text{mL}$	$\mu\text{g NO}_2 \backslash \text{mL}$	$\mu\text{g NO}_3 \backslash \text{mL}$	$\mu\text{g PO}_4 \backslash \text{mL}$	$\mu\text{g SO}_4 \backslash \text{mL}$
mean % error	-0.4 ± 4.5	-2.9 ± 4.1	2.5 ± 3.9	-4.6 ± 4.0	3.0 ± 3.2
E6M Spike		0.415	0.665		
% Recovery		97.0	111.1		
S8M Spike	14.405				7.906
% Recovery	93.7				108.1
E3B	6.138		0.245		1.477
E4B	6.367			0.180	1.164
E6B	5.532				0.529
E3M	6.123				0.520
E4M	7.578			0.700	0.558
E6M	7.459		0.153	0.107	0.781
E3T	12.340				1030.115
E4T	11.990		0.488		205.444
E6T	7.324		0.363		6.440
S1M	7.908		0.022		33.832
S6M	7.575		0.219		0.383
S8M	7.513				3.780

Table 5-3. Baseline sampling results obtained from ICP-OES analysis.

sample	µg Ca/ mL	µg Mg/ mL	µg Na/ mL	µg K/ mL	µg Fe/ mL
E3B	3.355	0.701	4.151	1.002	3.246
E4B	1.590	0.205	4.334	0.325	0.865
E6B	1.383	0.196	4.008	0.436	0.649
E3M	2.338	0.558	6.700	0.954	1.079
E4M	1.623	0.393	6.576	0.154	4.114
E6M	1.087	0.422	5.512	0.311	1.914
E3T	250.600	38.870	15.550	4.291	24.24
E4T	56.670	12.510	16.100	1.444	
E6T	14.350	4.279	3.896	5.607	0.300
S1M	3.695	2.783	7.211	1.263	4.244
S6M	0.946	0.245	6.344	< 0.065	2.467
S8M	3.764	1.007	4.658	1.773	1.747

Table 5-4. Baseline sampling results for field parameters and field-kit analysis.

Well No.	Location	Time	Date	Event	Conductivity	pH	DO	Iron (total)	Iron 2+	Sulfide	Nitrite
E3	T	12:20	24-Jan	1 Begin	1586	4.64	0.129	OR*	OR	0.105	0.03
		13:15	24-Jan	1 End	1407	4.47					
	M	10:17	23-Jan	1 Begin	72	5.27	0.307	1.418	1.387	0.047	0.019
		11:35	23-Jan	1 End	56.4	5.41					
	B	11:48	23-Jan	1 Begin	65.1	5.99	0.219	3.484	3.503	0.05	0.017
		12:38	23-Jan	1 End	56.3	5.9					
E4	T	14:30	24-Jan	1 Begin	569	5.02	1.071	OR	OR	0.036	0.033
		15:20	24-Jan	End	463	5.02					
	M	12:52	23-Jan	1 Begin	62.5	5.85	0.25	4.034	3.886	0.056	0.021
		14:47	23-Jan	1 End	57.9	5.52					
	B	14:54	23-Jan	1 Begin	40.3	5.54	0.19	0.937	0.935	0	0.02
		15:45	23-Jan	1 End	40.7	5.5					
E6	T	10:10	24-Jan	1 Begin	152.3	6.59	1.071	0.314	0.403	0.085	0.032
		11:40	24-Jan	1 End	119.4	5.95					
	M	16:03	23-Jan	1 Begin	45	5.54	0.307	1.998	1.939	0.064	0.023
		17:25	23-Jan	1 End	51	5.41					
	B	8:55	24-Jan	1 Begin	49.9	5.48	0.415	0.767	0.812	0.08	0.027
		9:58	24-Jan	1 End	37.2	5.44					
S6	M	15:40	24-Jan	1 Begin	53.1	5.66	0.28	2.267	2.269	0.105	0.031
		16:45	24-Jan	1 End	48.7	5.5					
S1	M	9:10	25-Jan	1 Begin	125.4	5.12	2.053	3.889	3.979	0.06	0.035
		10:15	25-Jan	1 End	119.8	4.92					
S8	T		25-Jan		132.9	6.14					
	M	10:45	25-Jan	1 Begin	75.2	5.74	0.203	1.91	1.829	0.059	0.019
		11:46	25-Jan	1 End	58.8	5.66					
SCR*		26-Jan		40.2	5.51						
E5	T		26-Jan		81.6	4.95					
	M		26-Jan		61	5.63					
	B		26-Jan		43.5	5.69					
E7	T		26-Jan		91.2	5.62					
	M		26-Jan		44	5.38					
	B		26-Jan		37.1	5.35					
S7	T		26-Jan		266	6.47					
	M		26-Jan		118	6.05					
	SCR		26-Jan		40.2	5.63					
S6	T		26-Jan		779	4.51					
	M		26-Jan		53	5.7					
	SCR		26-Jan		52.6	5.75					
S5	T		26-Jan		274	5.16					
	SCR		26-Jan		43.7	5.73					

Note: All unit is mg/L, except pH (unitless) and Conductivity ($\mu\text{s}/\text{cm}$)
 * OR= over range (>6ppm)
 *SCR=screen

5.3 TREATABILITY OR LABORATORY STUDY RESULTS

This project did not have a formal treatability study. However, prior to monitoring each of the different amendment injections (both the ABC and the molasses injection), we performed laboratory measurements to assess whether the injections of the amendment would sufficiently increase the ambient electrical conductivity. Such measurements can be done easily. First, one can measure the electrical conductivity of the injectate (which is typically a mixture of water and the actual active amendment in the range between 10 and 40 % volume amendment). Second, one can run soil column experiments, taking electrical resistivity monitoring measurements during injection of the amendment into porous media. Note that such measurements typically provide qualitative insight into the expected changes in electrical properties (increase/decrease and approximate percentage), but that such laboratory data cannot be used for quantitative interpretation of field-scale results; rather, the field-scale relation between bulk and fluid conductivity is described by Archie's Law (Archie, 1942), the parameters of which vary from site to site or even spatially across a given site. The laboratory study results confirmed for both amendments that a substantial increase in electrical conductivity was to be expected.

5.4 DESIGN AND LAYOUT OF TECHNOLOGY COMPONENTS

Based on our demonstration objectives, site layout, and remedial design, we emplaced sampling and resistivity wells surrounding injection points B6 and B7 (Figure 5-5, Figure 5-6). The cables from the resistivity system were buried and run through conduit into a small control shed (Figure 5-7). This shed also housed the resistivity system and the control comp. Note that we used two different resistivity systems (Figure 5-8): for the initial amendment injection we used a MPT single channel, 120 electrode system, and for the injections in August 2010 we used a MPT multi-channel, 128 electrode system. The main difference between these systems is that the multi-channel system can collect data faster, thereby increasing the temporal resolution of our monitoring.

The spacing of the resistivity wells was driven by two factors. These are the expected behavior of the amendment in terms of movement, and the required spatial resolution of the electrical imaging. From previous work at the site we knew that the groundwater velocity at the site was approximately 60 feet per year (roughly from East to West). Initial plans called for monitoring the injection for about 1 - 1.5 year, and with this speed the assumption was that we should be able to track at least the easternmost amendment without it leaving the area of the monitoring system.

The spatial resolution of the array can be calculated numerically, and as part of the design effort we did perform a modeling effort. While such a modeling effort should ideally be done for all resistivity efforts an useful rule of thumb is that for cross-hole imaging (i.e. imaging in which data from two boreholes equipped with electrodes is being used), the horizontal offset between the two electrode strings should not exceed the vertical length of each electrode string (measured as the distance between the top and the bottom electrode), and ideally should be 1/2 or less the vertical length of an electrode string. Thus, for 10 m electrode strings, a good distance to use as distance between electrodes is 5 m spacing. Our layout (Figures 5-5, 5-6) gives inter well offsets of 2-4 meters for electrode wells about 10 m deep, thus providing a good expected resolution. For surface resistivity data collection, with electrodes installed at ground surface, the appropriate rule of thumb is that imaging can be done to a depth $\sim 1/5^{\text{th}}$ the horizontal spread of electrodes, with resolution

degrading with depth and controlled in part by electrode spacing. For the molasses monitoring two additional surface lines with 30 electrodes each were installed. These lines are centered on our existing array (Figure 5-5). The first of these lines (surface line 1) is roughly EW, and passes over wells E1 and E6. This line is centered over the line E and is 135 long. A second line (surface line 2) is 328 long, and runs perpendicular to line 1. These lines all cross at the center of our array.

As noted, the objective of the sampling wells is to allow for the acquisition of confirmatory geochemical data. This drove the distribution and design of these wells.

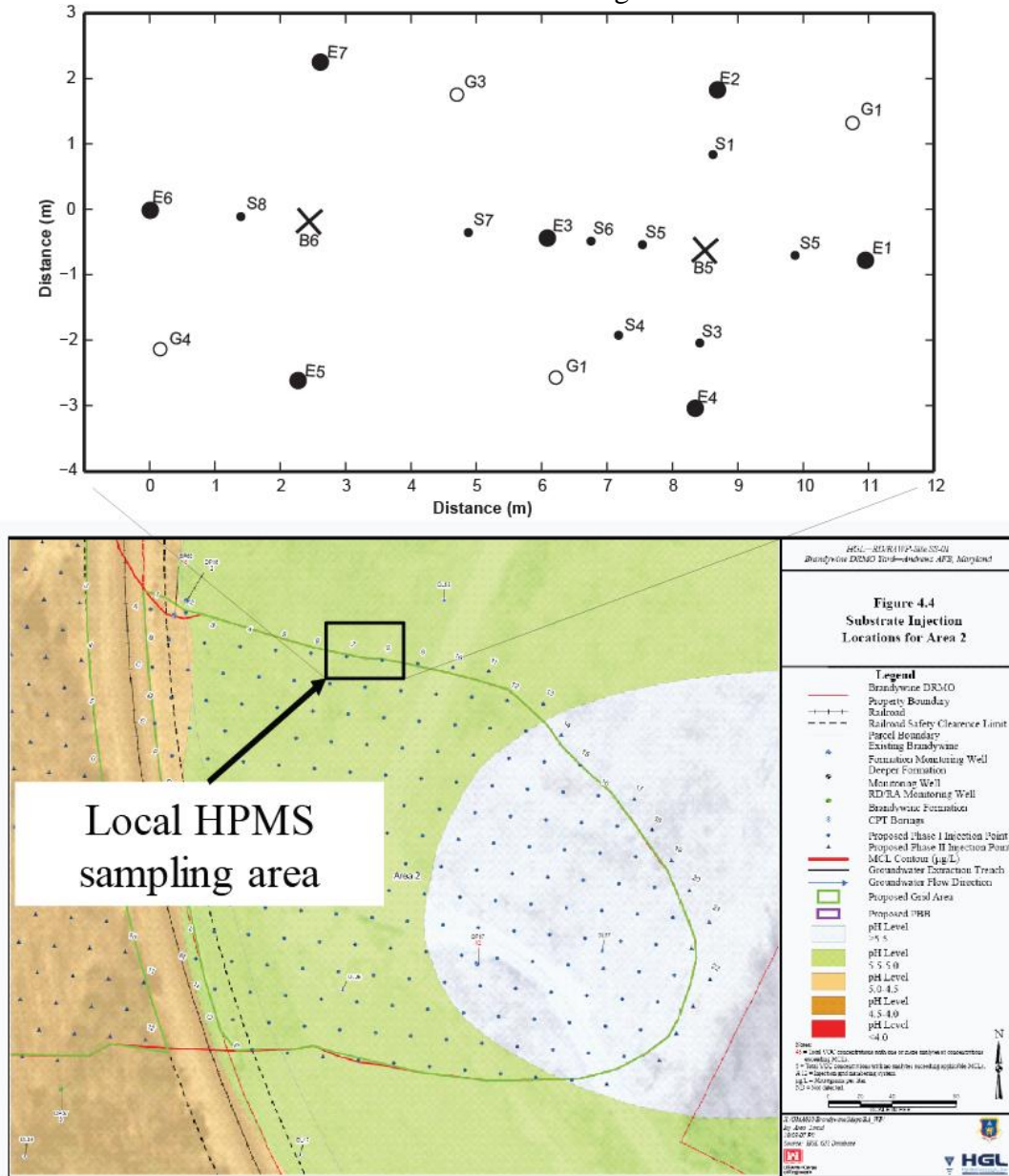


Figure 5-5 layout of monitoring system overlain on general area of injections (lower left). The system consists of 7 ERT boreholes and three surface cables, and 8 dedicated sampling wells. These were deployed around two of the sampling points (B6 and B7). Note that for the second injection in August 2010 additional surface cables were used. Each red dot on the lower left figure represents an amendment injection location

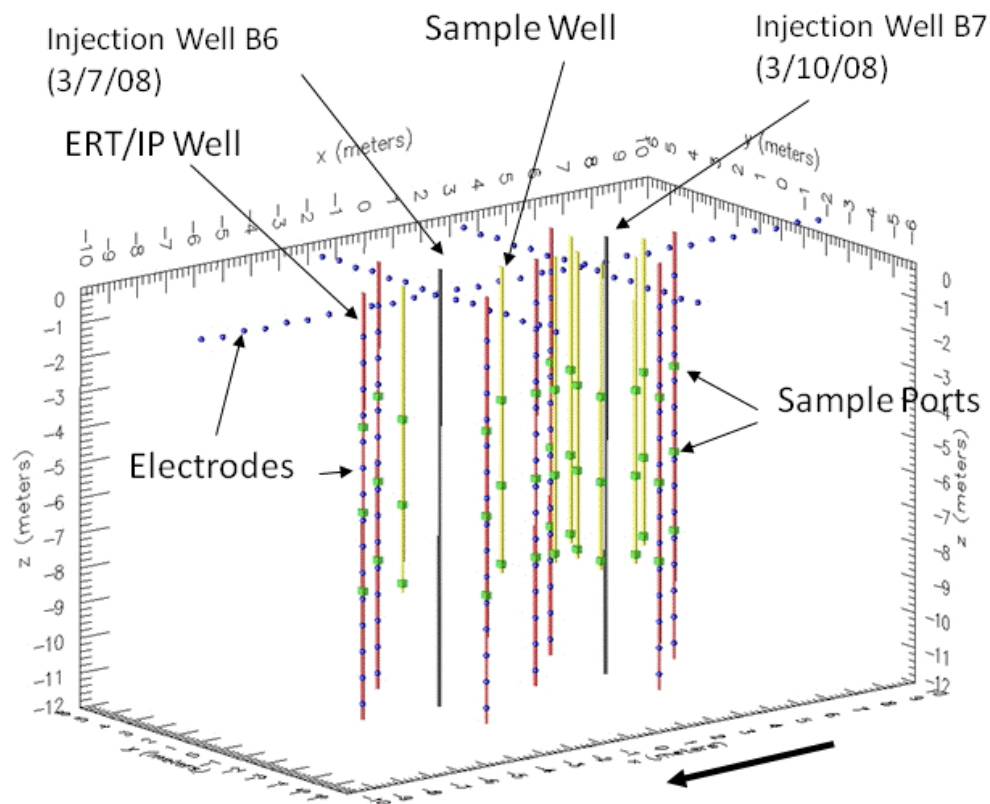


Figure 5-6 Site detail showing relationship between borehole wells and sample wells. Locations of two injections for long-term monitoring experiment are shown.



Figure 5-7 Shed housing the instrumentation



Figure 5-8 Resistivity hardware: left single channel system. Right multi channel system. Both systems use the same electrodes. The multichannel system was used to monitor the second injection

5.4.1 Injection points

Injections were performed using a one-person direct-push rig such that no permanent well was installed (Figures 5-9, 5-10). Injections of ABC were performed in March, 2008 and injections of molasses in August 2010. During these injections the amendment was prepared in a mixing tank. ABC was prepared according to the recipe: 250 gallons of ABC, 3200 gallons of water, 466 lbs NaHCO₃ for pH adjustment. Injections happened at well B6 on March 7, 2008, and in well B7 on March 10, 2008. The injection pipe was pushed to 34 feet bgs and then withdrawn one foot at a time to 8 ft bgs, releasing 36 gallons of amendment at each location, for a total of 950 gallons per injection. The resulting injectate for B6 had a conductivity of 15 mS/cm, and a pH of 8. At point B7, the injectate apparently was mixed differently by the contractor, as it shows a much higher conductivity increase in the geophysical results.

The molasses injections were performed in a manner similar to that of the ABC. The molasses was mixed with municipal tap water to achieve a 40% molasses mixture, which was injected at B6 and B7 with volumes of 900 and 950 gallons. A third injection was performed for surface-resistivity monitoring, with only 400 gallons released. The injection procedure was identical to that of the ABC, with the pipe pushed to 34 ft bgs and withdrawn to 8 ft bgs, injecting about 36 gallons per foot. The molasses was mixed in 8 batches with an average fluid conductivity of 14 mS/cm.



Figure 5-9 March 2008 injection

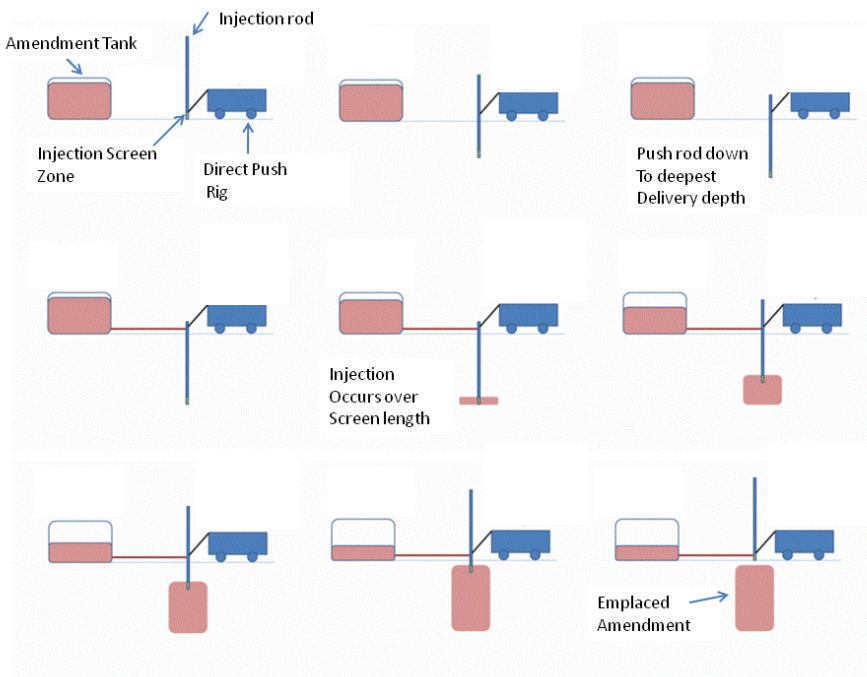


Figure 5-10 Schematic overview of amendment injection procedure. From top right to bottom left: direct push rig pushes down injection rod and insert amendments over injection screen depth, starting at the deepest point.

5.4.2 Electrode wells

Electrical resistivity tomography datasets were collected using seven borehole electrode wells ('E' wells). These electrode wells (Figure 5-11) were instrumented also for sampling, with three sampling ports of 15-cm stainless steel screen at depths of 11, 19 and 26 ft bgs. The stainless steel sampling ports are sold commercially by Geoprobe®, with barbed fittings to couple to 3/8-inch HDPE tubing. Electrodes consisted of 5-cm stainless-steel wire springs wrapped around and connected to multi-conductor cable with a polyethylene jacket. Electrode spacing was at 60-cm intervals along the electrode cables. Sampling tubing and electrodes were attached by cable ties to a PVC backbone, consisting of 1-inch schedule-40 PVC pipe with a 1-foot screen. The PVC screen was intended primarily to facilitate installation, as a means of allowing water into the pipe; however, it also provided a fourth sampling point, albeit one that required more purging because of the volume of the 1-inch pipe relative to that of the 3/8-inch tubing. Electrode wells extended deeper than the sampling ports to allow for good resolution by achieving a favorable ratio of horizontal well offset (2 – 4 m) to vertical electrode extent (~10 m).

Electrode installation construction (detail)

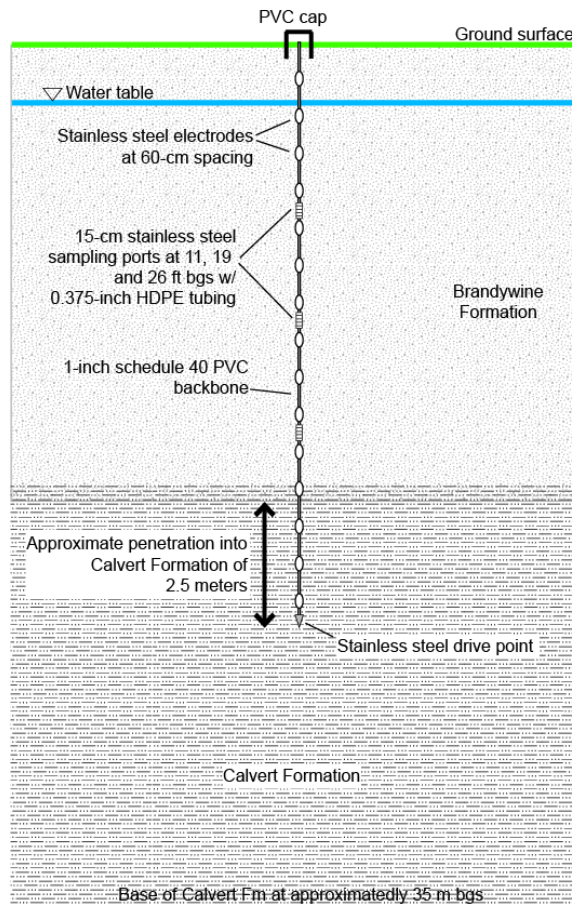


Figure 5-11 Schematic diagram showing construction of an electrode (E) well.

5.4.3 Sampling wells

Eight sampling wells without electrodes ('S' wells) were installed to collect multi-level samples to (1) develop calibrations for the geophysical interpretation and (2) provide validation datasets. The sampling wells (Figure 5-12) were instrumented with two ports of 15-cm stainless steel screen at depths of 11, and 19 ft bgs. Sampling tubing and electrodes were attached by cable ties to a PVC backbone, consisting of 1-inch schedule-40 PVC pipe with a 1-foot screen. The PVC screen provided a third sampling point at 26 ft bgs.

Sampling well construction (detail)

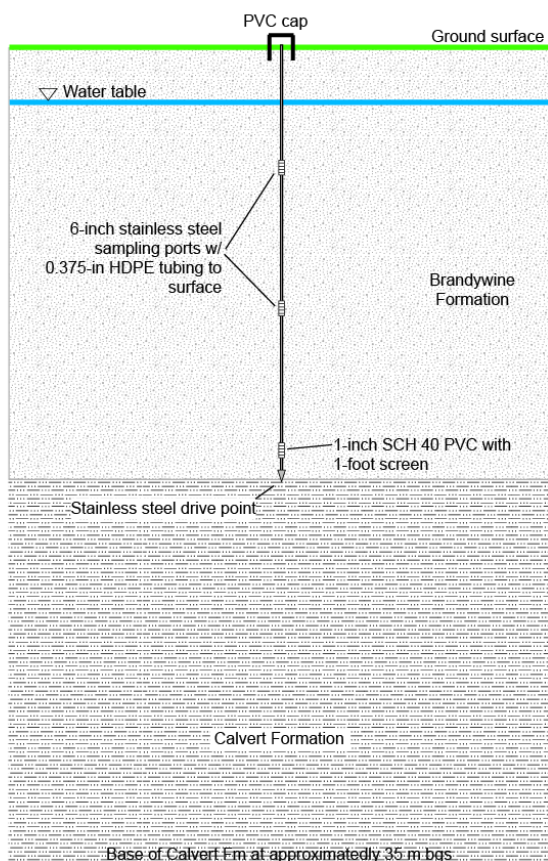


Figure 5-12 Schematic diagram showing construction of a sampling ('S') well.

5.4.4 Radar wells

Four ground-penetrating radar wells ('G' wells) were installed to allow for collection of crosshole GPR data and electromagnetic induction logs. Many geophysical logging tools require at least 2-inch or 3-inch wells. The four G wells (Figure 5-13) were installed using an 8-inch hollow-stem auger on a Geoprobe® rig. 3-inch PVC casing was set and holes were backfilled with native materials collected during the drilling process. To allow for good resolution, the G wells were installed to depths of 45 feet bgs, providing for favorable ratios of horizontal offset (~4-6 m) to vertical well extent (~10 m).

GPR well construction (detail)

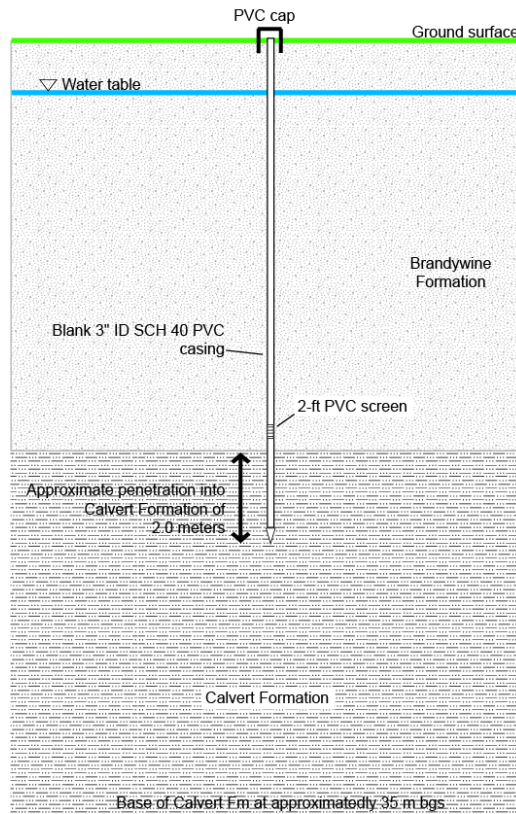


Figure 5-13 Schematic diagram showing construction of a GPR ('G') well.

5.4.5 Surface cables

Surface electrodes for the original injections were installed semi-permanently in trenches dug with a minitrencher machine to 18" (Figure 5-14). Electrodes were identical to the borehole electrodes, with stainless steel wire wrapped around multi-conductor cable, with electrodes at 60-cm spacing. A total of 4 15-electrode cables were installed, with two in-line with the injection points and two perpendicular, crossing through the injection points. Surface cables for monitoring the molasses injections were installed in July 2010 using copper grounding stakes. Two lines were installed with thirty electrodes each, one EW line of 134 feet long (6.5 feet/ 2 m spacing between electrodes), and one NW line of 328 feet long (16.4 feet/5 m spacing between electrodes). These lines are centered over the existing array. (Figure 5-15).



Figure 5-14 Installation of trenches for surface electrodes for the first injection experiment.



Figure 5-15 Surface array with temporarily installed electrodes for monitoring second injection experiment.

5.5 FIELD TESTING

The field testing and installation consisted of several phases

1. Phase 1: system planning. This occurred from October through November of 2007. In this phase we decided on the location and layout of our system
2. Phase 2: system installation. In this phase electrodes were installed using a USGS direct push rig, the shed was emplaced on site, and power was connected to the shed. This occurred in November 2007
3. Phase 3: system testing and background data collection (December 2007-March 2008). In this phase the system was tested and background data was collected
4. Phase 4: Amendment 1 monitoring (March 2008-May 2010). In this phase the first amendment injection was monitored
5. Phase 5: Amendment 2 preparation (June-July 2010). In this phase preparations were made for the second amendment injection, which was performed under an extension to the project duration and additional award
6. Phase 5: Amendment 2 monitoring (August-September 2010). In this phase two molasses injections were monitored, with the results being webcast live
7. Phase 6: System demobilization (October 2010-January 2011). In this phase the system was demobilized, i.e., wells were abandoned according to state regulations, and all instrumentation was removed from the site

During these phases waste consisted of drilling and sampling spoils. These were discharged by the project in accordance with the applicable regulations in a manner consistent with that employed by environmental contractors working on site.

5.6 SAMPLING METHODS

Sampling consisted of two types of sampling. The first was geophysical data collection. This was predominantly the collection of electrical geophysical data, but also included collection of cross-hole Ground Penetrating Radar and borehole-log (electromagnetic) data. The second was the collection and analysis of groundwater data from the sampling ports. The objective of this sampling was to provide confirmatory data. These sample were analyzed both in field using standard conductivity meters for conductivity and pH, as well as in the laboratory.

Groundwater sampling was done using the following protocol

- A pump was connected to a sampling port
- Water was pumped out of the sampling port at approximately 200 ml/minute
- Sampling lines were purged by pumping 1-2 gallons of water
- A sample was collected and immediately analyzed using a multi-parameter probe

- For samples undergoing subsequent chemical analysis, a two-step filtering process was used to remove particulates
- Sample bottles for organics analysis were prepared with nitric acid
- Samples were bottled appropriately depending on intended analytical procedure
- Samples for organics were placed in a dry-ice cooler

Multiparameter probes were calibrated each day using standards for pH and conductivity. Hazardous-waste operation procedures consistent with the site's Health and Safety Plan were followed, including use of nitrile gloves and eye protection during sampling. Decontamination procedures involved washing instruments and tubing with soapy water after each use, containerizing all purge and cleaning water in steel drums, and paying an environmental contractor to dispose of these materials.

5.7 Sampling Results

The results of our sampling—chemical and geophysical—are described in the context of the two injection efforts: ABC injections, and molasses injection. The ABC injection experiments included three components: (1) calibration, (2) validation, and (3) monitoring. The molasses injections, performed under a project extension and additional award, involved minimal chemical sampling; rather these injections were performed to demonstrate the detectability of other amendments. The three ABC component efforts and the molasses geophysical sampling each are discussed in sub section below. Baseline sampling, discussed above, provided background datasets against which geophysical and chemical samplings could be compared.

5.7.1 Initial sampling efforts: Investigation of correlation between geophysics and geochemistry

Field-scale relations between geophysical estimates and hydrologic or geochemical parameters are site-specific. The development and interpretation of such relations should proceed carefully, and take the effect of spatially variable geophysical resolution into account.

One of our primary objectives was to demonstrate that geophysics can provide information on relevant subsurface properties of interest for remedial efforts. One of the primary properties of interest is fluid geochemistry (fluid conductivity) and amendment concentration (Total Organic Acids).

5.7.1.1 Development of a correlation function between geochemistry and electrical geophysical properties

Our initial sampling efforts in 2008 focused on identifying and developing a field-scale and site-specific relation between fluid conductivity and ERT-estimated bulk conductivity. This relation was constructed empirically by calibration based on co-located chemical sampling and geophysical estimation (Figure 5-16).

The chemical sampling campaign for calibration occurred April 6, 2008 approximately 1 month after injection of ABC at the two injection points, B6 and B7. During this event fluid samples were taken from each of the 45 sampling ports and analyzed for fluid conductivity, total

organic acid, dissolved oxygen, Fe-I, Fe-II, sulfide, nitrite, pH and eH and other chemical indicators. In principle, each of these chemical indicators can be used to develop a petrophysical relation, but our sampling effort focused only on fluid conductivity. Background fluid conductivity measurements were subtracted from the corresponding April 6 measurements to reveal the change in fluid conductivity at 21 ports. To obtain the corresponding change in bulk conductivity at the same ports, we inverted the 3D ERT data collected just after the field sampling effort, and extracted the estimated bulk conductivity at the port locations. These were subtracted from the corresponding background bulk conductivity estimates to produce the estimated change in bulk conductivity at each port on April 6. Each point in Figure 5-16 corresponds to a measurement port at one of our wells. The best-fit line to our data can be used to construct a mapping function which allows us to predict the fluid conductivity from our inverted geophysical data.

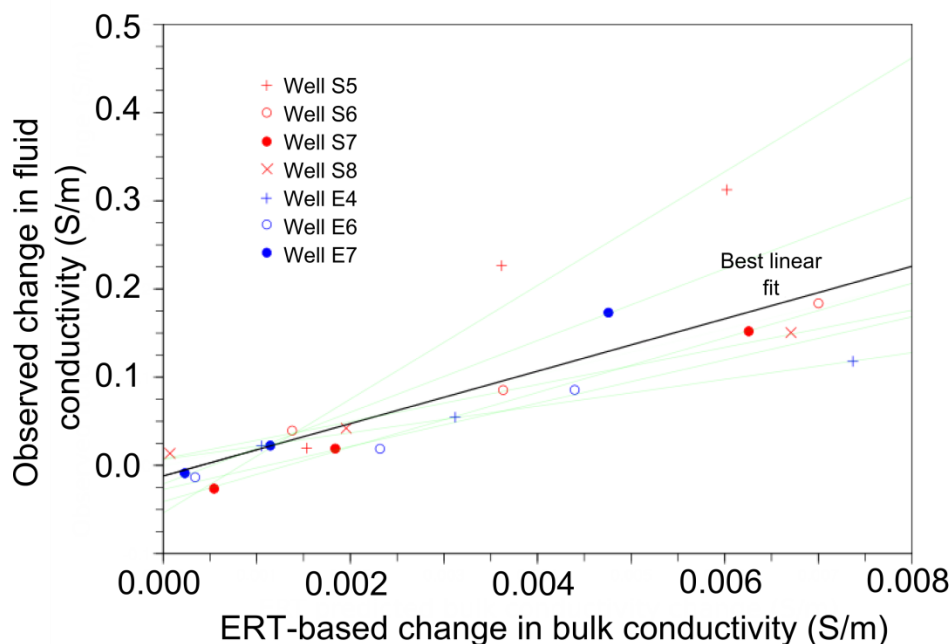


Figure 5-16 Calibration dataset used to develop field-scale petrophysical relation to predict fluid conductivity from ERT-estimated bulk conductivity

5.7.1.2 Use of correlation function: Prediction verification (Fall of 2008)

To test and validate the developed mapping function between geophysically derived electrical conductivity and fluid conductivity we staged a second chemical sampling campaign. ERT tomograms were used with the linear relation between estimated bulk conductivity and fluid conductivity (as described in Section 5.7.1) to predict fluid conductivities prior to the sampling event on August 9, 2008. This geophysical prediction was submitted to the management of the Environmental Security Technology Certification Program (ESTCP) and sequestered from the team responsible for sampling. Analyses of sampling results also were submitted to the program managers prior to sharing results within the research team. The comparison between predicted and sampled values is strong, with a coefficient of determination between predicted and sampled values of $R^2=0.87$ (Figure 5-17).

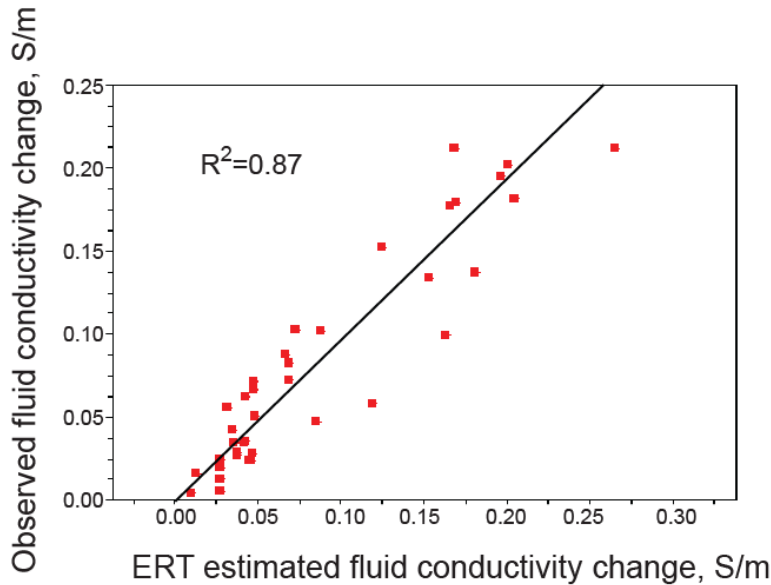


Figure 5-17. Validation sampling results, for which fluid conductivity was predicted based on ERT results.

This result provided an affirmative answer to one of the primary questions underlying the dem/val effort: Can geophysics provide information on geochemical parameters? Obviously, other parameters are also of interest, in this case specifically the total organic acid concentration (TOA). As part of the August sampling effort we investigated whether we could use geophysics to provide information on TOA based on the correlation between TOA and electrical conductivity. For this, 1/3 a randomized part of the August 2008 dataset was used to develop a correlation between TOA and fluid conductivity (Figure 5-18). This correlation was used to predict total organic acid concentration in the remaining samples. The results (Figure 5-19) show a good correlation. Obviously, this is dependent on a strong correlation between conductivity and TOA, which in this case holds true. Such a correlation needs to be ascertained for different amendment injection scenarios.

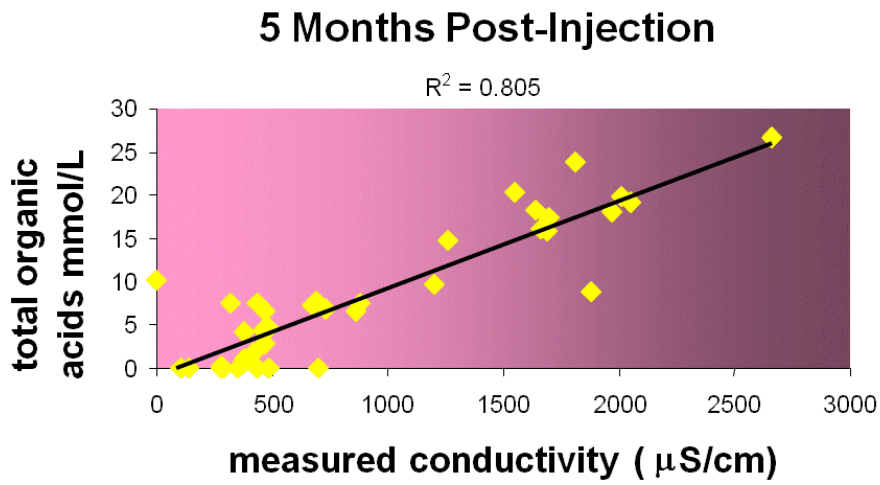


Figure 5-18 Correlation between total organic acids and fluid conductivity.

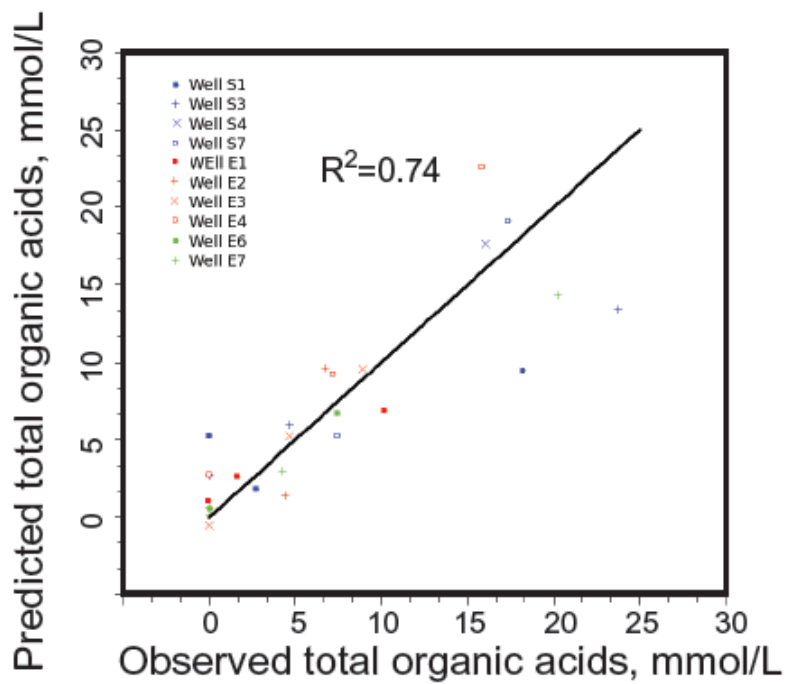


Figure 5-19 Predicted vs. observed TOA concentrations for August 2010 sampling event.

5.7.2 ABC amendment - long term monitoring results

Post-injection geophysical and chemical sampling continued through the summer of 2010. Geophysical sampling was continuous with the exceptions of power interruption, occasional system malfunctions, or connectivity issues. Chemical sampling occurred periodically (Table 5-5), with some sampling events focused on field parameters (fluid conductivity, pH) and others focused on laboratory analysis for ions and organics. In addition, site wide sampling results were obtained from HGL and Andrews AFB which provided site wide monitoring of subsurface conditions.

Table 5-5. Overview of sampling events performed by project team. The detailed results of the sampling events are provided in appendix 9.2

Groundwater sampling events

Injection of 7% ABC (ethyl lactate + fatty acids) + 200mM NaHCO₃



	March 2008 (pre-inject) subset	March (post-inject) Subset	April 2008 All wells	August 2008 All wells	July 2009 All wells	April 2010 All wells
pH	X	X	X	X	X	X
Fluid conductivity	X	X	X	X	X	X
Anions	X	X		X	X	
Cations	X	X		X	X	
Organic Acids	X	X		X	X	
VOC	X	X			X	
TOC	X	X		X	X	
Fe ²⁺	X	X			X	
Dissolved O ₂	X	X		X	X	
Sulfide	X	X		X	X	

The time-lapse ERT data were processed to provide 3D snapshots of the change in bulk conductivity from pre-injection conditions every other day. Figure 5-22 shows a small subset of the ERT results. During the first year the amendment slowly moved downward (likely from density-driven flow) to spread over the lower confining unit moving in the direction of groundwater flow. During this period, bulk conductivity decreased as the emplaced amendment plume underwent dilution and dispersion. Cross hole ground-penetrating radar provides a second line of evidence to support interpretation of the ERT results, providing validation to the extent possible using a second type of geophysical imaging. Figure 5-23 shows radar amplitudes for horizontal raypaths between well pairs collected in January 2008, April 2008, and August 2008

XHGPR events. The first data collection period was prior to ABC injections, and the second and third events subsequent to those injections. Amplitudes are seen to decrease following injections, with the largest decreases between 4.5 and 10 m depth below ground surface; these decreases in amplitude indicate increased electrical conductivity and thus total dissolved solids. The XHGPR results are qualitatively consistent with the results of the ERT, which also showed a high-conductivity anomaly in this region. Whereas the ERT results provide lateral resolution between wells, the XHGPR results do not provide such information, but rather horizontally averaged results. In comparison to ERT, XHGPR data require labor-intensive processing, and the processing and data acquisition are not amenable to automation.

During the second year a significant increase in bulk conductivity was observed in the ERT results, which corresponded to the onset of biological activity. At this time, our calibrated bulk-fluid conductivity relation began to break down (Figure 5-20, Figure 5-21).

An understanding of what happened was obtained from an interpretation of sampling results from both the project team and the onsite contractor. These sampling results are as follows

- April 2008: amendment injection. Increase in electrical resistivity from increase in fluid conductivity
- August 2008: ESTCP sampling shows large increase in sodium in lower ports, modest increase in iron, large increase in sulfate. There is a slight increase in pH and organic acids.
- October 2008: contractor sampling event, showing low methane, slight increase in iron and manganese and slow fermentation
- January 2009: contractor sampling event. Results similar to October 2008 sampling event
- April 2009: contractor sampling event. Significant development of reducing conditions since January. High Methane reduction. Low DO and ORP
- August 2009: HPMS sampling event. Decrease in sodium since August 2008. Large increase in iron and organic acids. Large decrease in sulfide and pH
- April 2010: HPMS sampling event (fluid conductivity only sampled). Decrease in fluid conductivity everywhere since August 2009

Our interpretation of this is the following (Figure 5-22)

- Between March 2008 and January 2009 there is little microbial activity. The rise and fall in bulk conductivity is due to changes in fluid conductivity, which are caused by groundwater flow driven migration of the amendment
- Between Jan 2009 to April 2010 the geochemical data suggest vigorous microbial activity. The coupled decrease in fluid conductivity decreases with increase in bulk conductivity suggests an increase in interfacial conductivity (possibly iron-sulfide precipitation). This is in agreement with the decreasing correlation between fluid conductivity and bulk conductivity. Most activity occurs just above confining unit (corresponding to amendment distribution)

We thus interpret the changing petrophysical relation as being caused by biologically mediated

precipitation of electrically conductive iron-sulfide on grain surfaces. Whereas initially the change of conductivity is caused by changes in the fluid phase, later it is a result of changes in the solid phase. This model corresponds with some recent findings by other groups, and is supported by sampling efforts and theory.

This finding has both negative and positive implications for geophysical monitoring of biostimulation. On the one hand, this finding indicates that calibrated bulk-fluid relations may evolve over time, as the geophysical response is dominated first by the amendment and later by precipitates. Re-calibration may prove necessary over the course of a multi-year monitoring effort. On the other hand, the finding points to strong the potential of ERT to serve as a means of confirming bioremediation, which goes far beyond the goal of our project, which is to monitor amendment emplacement. ***If ERT can be used to diagnose the onset of biological activity, the utility of our HPMS approach could be extended to other purposes post-emplacment.***

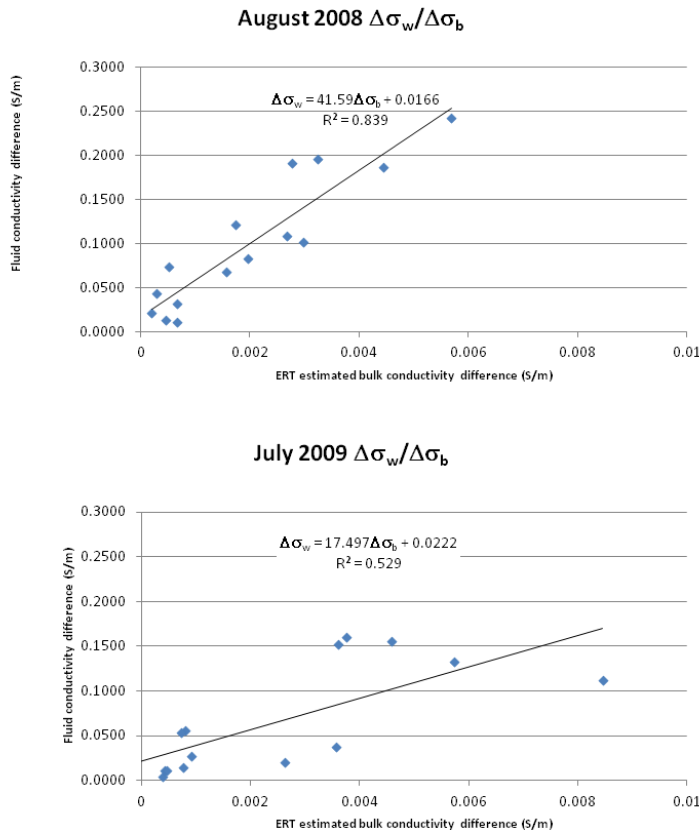


Figure 5-20 Comparison between correlation of fluid vs electrical geophysical conductivity in August 2008 (top) and July 2009 (bottom)

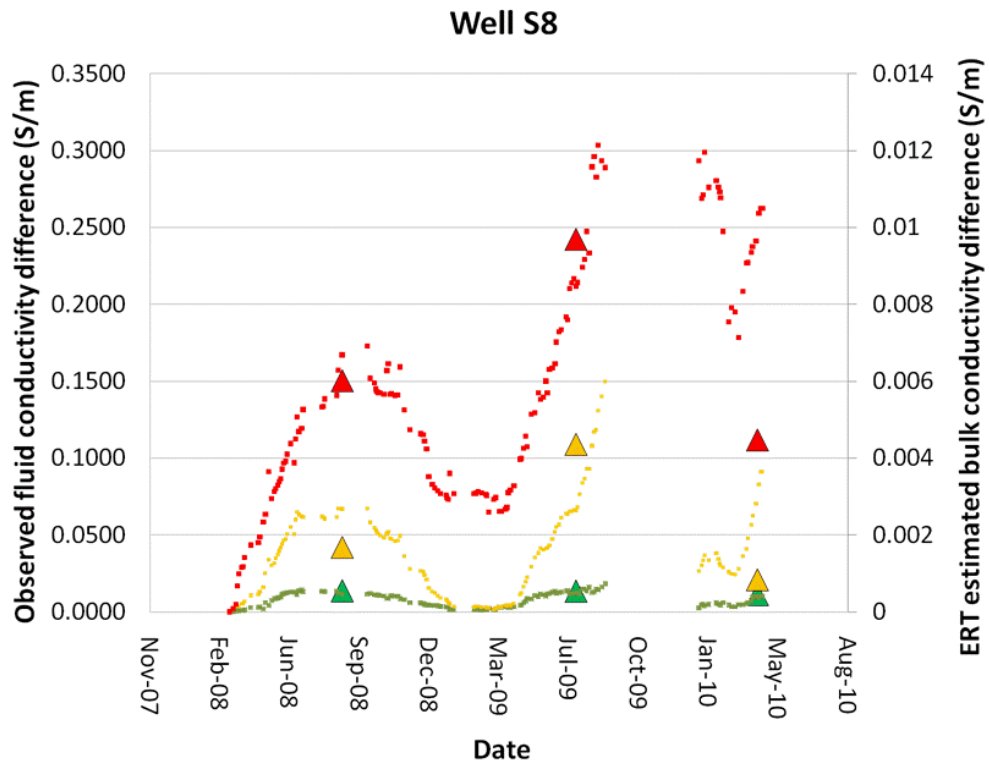


Figure 5-21 Comparison of ERT estimated conductivity against fluid measured conductivity. Dots are ERT inversion results. Triangles represent measurement at well ports. Green - 10 ft bgs, yellow - 18 ft bgs, red - 25 ft bgs. See text for discussion of interpretation

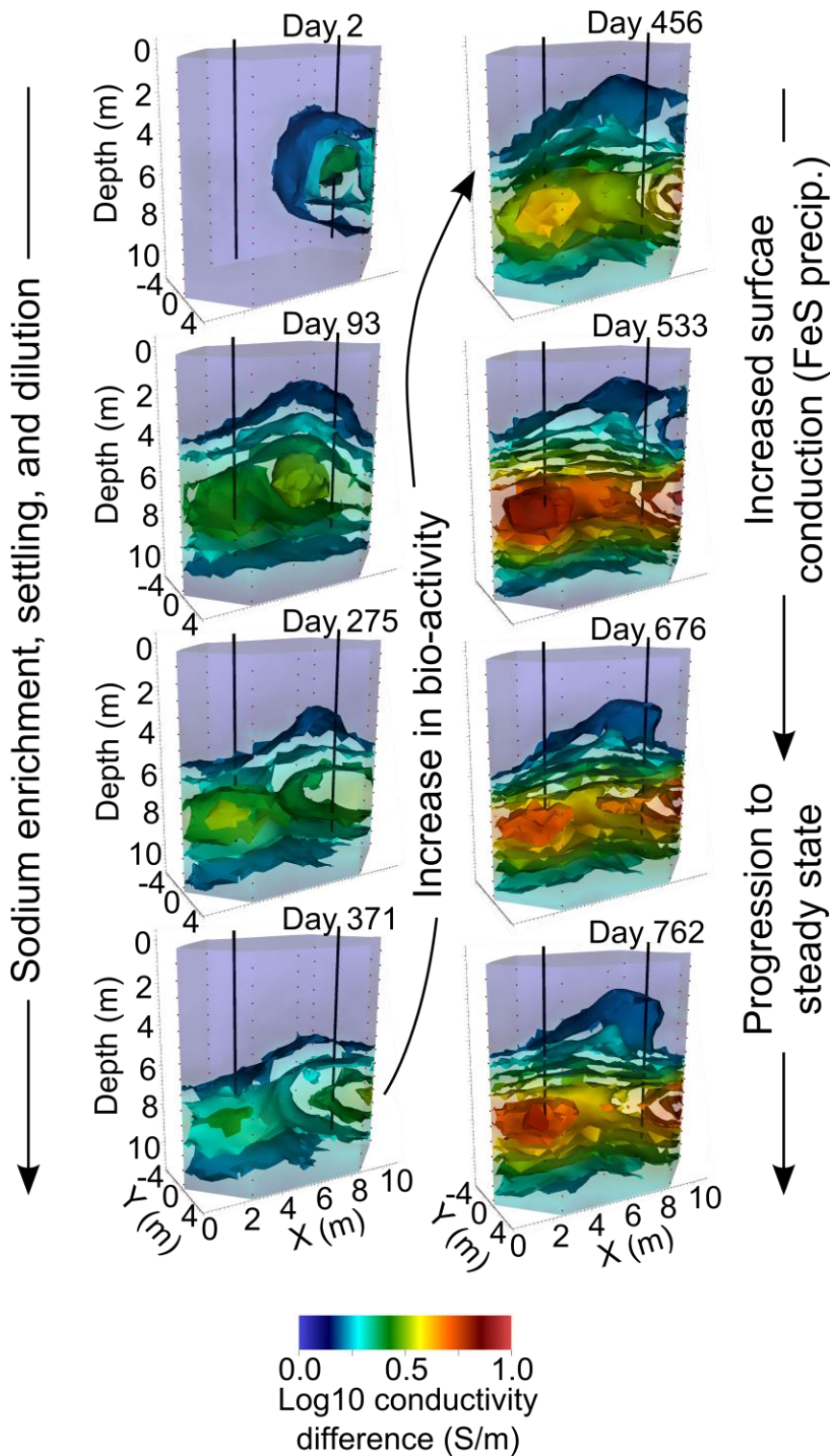


Figure 5-22. 3D time-lapse ERT monitoring results up to 762 days after the March 2008 injection. Injection intervals are shown as black vertical lines. Bulk electrical conductivity differences are shown as isosurfaces. The left column shows the amendment sinking, spreading, and diluting over the lower confining unit during the first year. In the second year, a significant increase in bulk conductivity corresponds to the onset of biological activity as confirmed through sampling efforts. Increase in bulk conductivity during this period are likely caused by iron sulfide precipitation

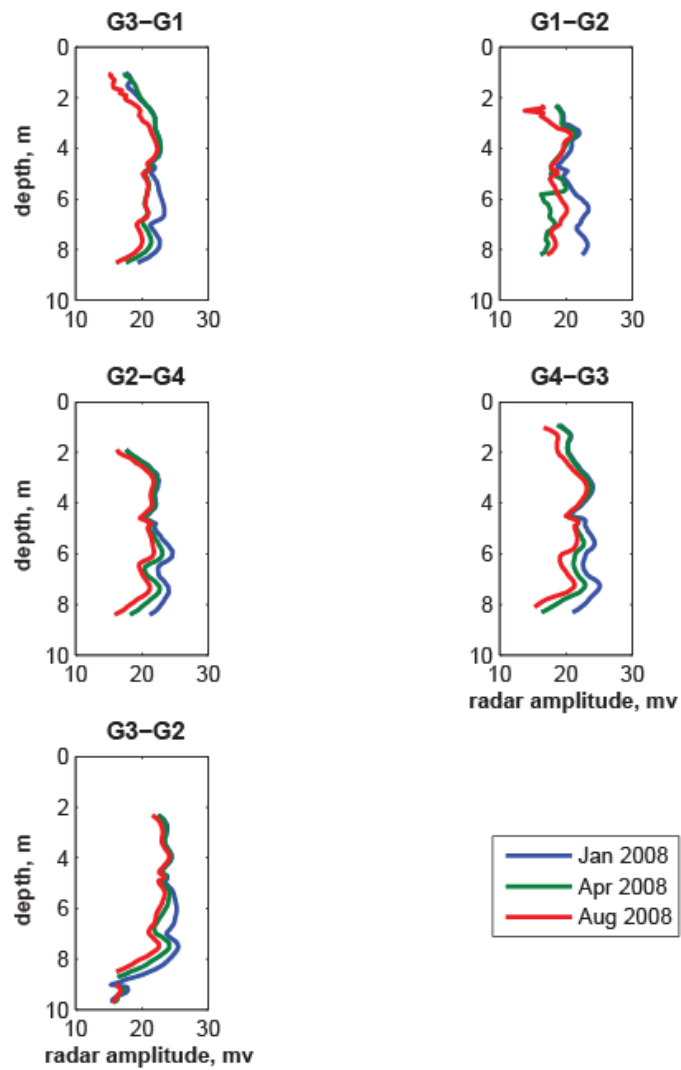


Figure 5-23. Cross-hole ground-penetrating radar amplitudes for five well pairs at three times, January, April, and August 2008. Decreases in radar amplitude indicate increased fluid conductivity and thus amendment presence.

Conceptual model of Biogeochemical Transformations and expected geophysical response

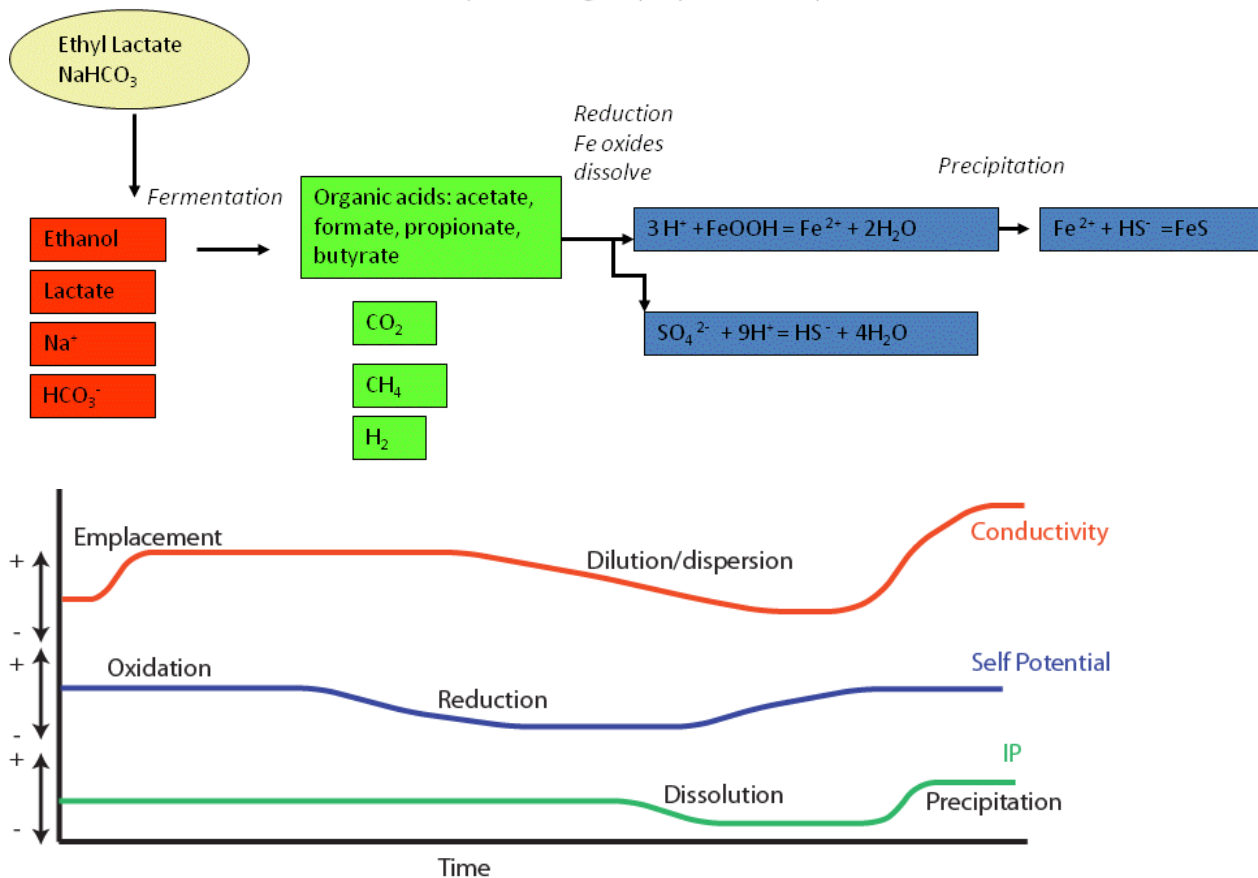


Figure 5-24. Conceptual model of amendment emplacement, expected biogeochemical changes and resulting geophysical signature

5.7.3 Sampling for molasses injections

Following the completion of the first injection the results were reported in an interim progress report (IPR) meeting. During that meeting the question arose to what extent the favorable results obtained from monitoring the ABC amendment could be generalized to other amendments. Based on this question the project team proposed to perform a second injection at the same site using the existing infrastructure, but with a different amendment. As resources would not allow a long term monitoring or chemical sampling the objective of this second experiment was narrowed down to three objectives

1. demonstrate that the HPMS system can monitor other amendments
2. demonstrate real time imaging ability
3. assess the performance of surface vs borehole electrodes in imaging the injection

Based on discussions with the program office, molasses was selected as an amendment. Two

injections of molasses were performed one on August 4th, and one on August 10th. Results from both injections were made available in real time on the web. For the second injection (on August 10th) members of the ESTCP program office, representatives from the Department of Energy, and site contractors attended the injection. For the two injections a total of 9300 lbs of molasses were used (Figure 5-25, Figure 5-26 Direct push rig used for 2nd injection). Molasses was diluted with water in a mixing tank, and injected in a similar manner as for the first injection (Figure 5-10)



Figure 5-25 Molasses tanks. Three tanks with 3100 lbs of molasses each were used for the injection



Figure 5-26 Direct push rig used for 2nd injection

Although the original HPMS array included some surface electrodes, the length of the surface array was confined to the footprint of our site and thus not sufficient to provide a comprehensive monitoring of the injection; consequently, the borehole array provided the bulk of the information for the ABC monitoring. Borehole electrodes commonly provide superior resolution compared to surface arrays, but at greater expense. The cost of using borehole electrodes is substantial both because of the drilling costs as well as because the borehole electrodes commonly cannot be reused. If, instead of using borehole electrodes one can use surface electrodes the system cost will go down substantially. For the second injection two long surface lines were deployed at the site which were used (together with the borehole array) to monitor the molasses injections (Figure 5-27)

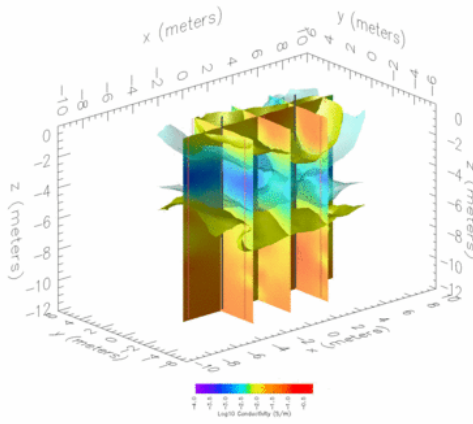
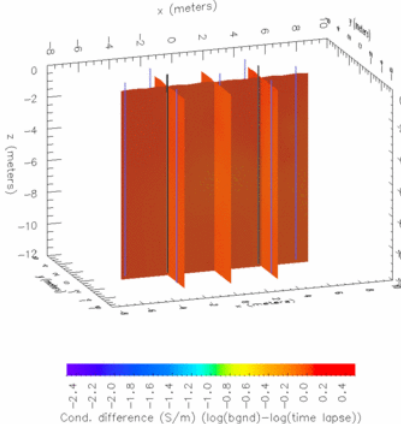


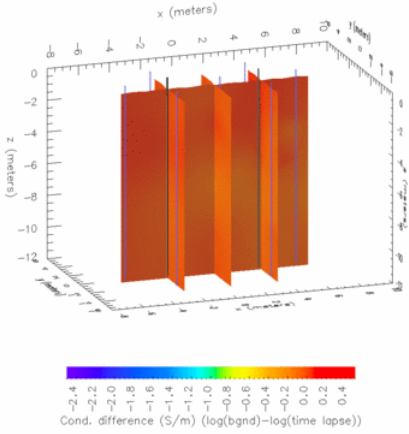
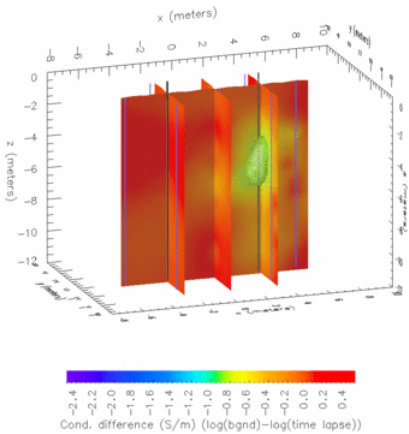
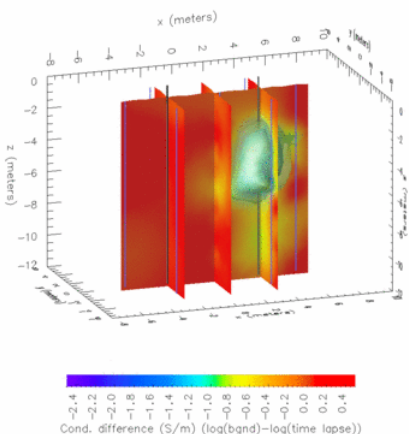
Figure 5-27 Surface array at site used in monitoring second injection

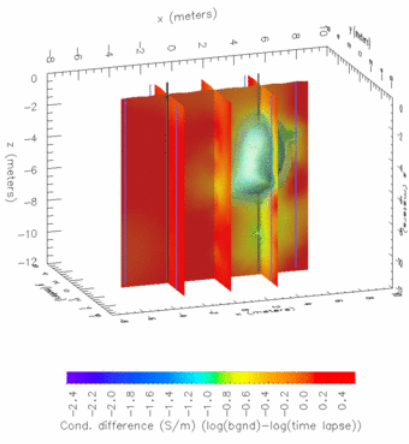
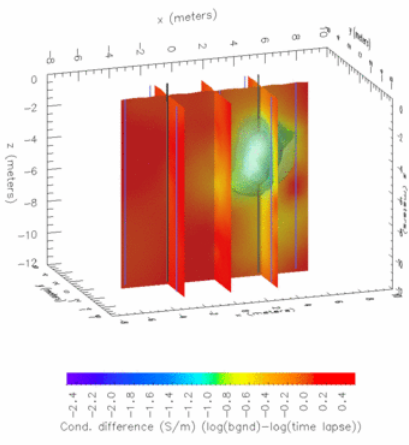
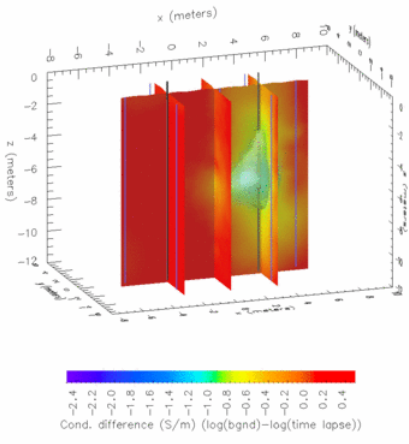
Table 5-6 below shows a sequential subset of ERT results for the molasses injections with accompanying interpretation. These results were broadcast (as images and as an animated movie) in near real time over the web as the injections proceeded. At the time of the experiment, this

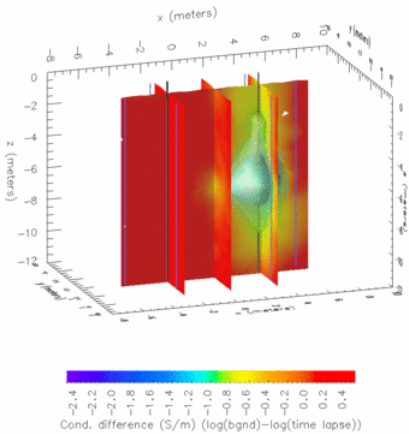
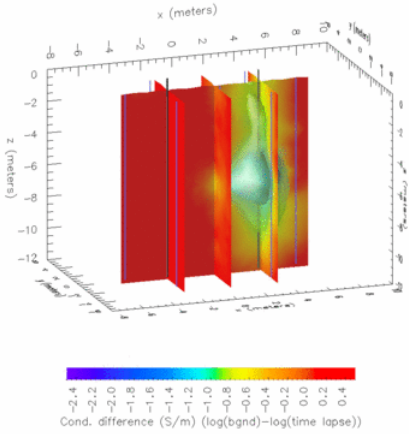
project website was maintained at a server housed at the Idaho National Laboratory (INL). Since then, the project website has been transferred to a Subsurface Insights server. The project website provides access to both the raw data as well as the results of the injections.

Table 5-6. Annotated results for the ERT monitoring of molasses amendment emplacement

Time	Data collected	Injection event	Inverted data	Comment
Tuesday August 3rd	Background conductivity	pre injection		The conductivity on August 3rd shows the structure resulting from the ABC injection and subsequent changes. This conductivity structure is changing very slowly at this time.
Wednesday August 4th 11:10 AM - 11:17 AM ET	Injection monitoring survey	Direct push probe is pushed down to 35 ft bgs (10.6 m).	No substantial change to background. This dataset is used as our reference dataset for change detection.	
Wednesday August 4th 1355 -1427 PM	Monitoring survey	First injection of 110 gallons occurred between 140 and 156 PM at depths 34-31 feet (10.3-9.4 m). Second injection of 110 gallons occurred between 201 and 219 PM at depths 31-28 feet (9.4-8.5 m). Partial injection of 60 gallons between 219 and	<p>08_04_2010-13:55</p> 	We do not see any substantial changes with regard to the background.

		223 PM at depths 28-25 feet. Injection stopped to mix new batches		
Wednesday August 4th 1458 - 1528 PM	Monitoring survey	Injection of 50 gallons between 310 and 316 PM at depths 28-25 feet (8.5-7.6 m). Injection of 110 gallons between 317 and 328 PM at depths 25-22 feet (7.6-6.7 m).	08_04_2010-14:58  <p>Cond. difference (S/m) (log(bgnd)-log(time lapse))</p>	Possible very modest changes, but nothing striking
Wednesday August 4th 1528 - 1558 PM	Monitoring survey	Injection of 110 gallons between 328 and 339 PM at depths 22-19 feet (6.7-5.8 m). Injection of 110 gallons between 340 and 400 PM at depths 19-16 feet (5.8-4.9 m)	08_04_2010-14:58  <p>Cond. difference (S/m) (log(bgnd)-log(time lapse))</p>	A conductivity anomaly shows up in the location of the injection. This clearly corresponds to the amendment.
Wednesday August 4th 1558-1628 PM	Monitoring survey	Injection of 110 gallons between 406 and 420 PM at depths 16-13 feet (4.9-4.0 m). Injection stopped at 420 to get new water.	08_04_2010-15:58  <p>Cond. difference (S/m) (log(bgnd)-log(time lapse))</p>	Anomaly increases in size and signature - in agreement with expectation of how amendment would behave (ie being pushed out from well)

<p>Wednesday August 4th 1658-1728 PM</p>	<p>Monitoring survey</p>	<p>Injection of 110 gallons between 500 and 513 PM at depths 13-10 feet (4.0-3.0 m). Injection of 20 gallons between 519 and 525 PM at depths 10-8 feet (3.0-2.4 m). Product surfacing around well - injection stopped.</p>	<p>08_04_2010-16:58</p> 	<p>Anomaly continues to increase.</p>
<p>Wednesday August 4th 1728 -1758 PM</p>	<p>Monitoring survey</p>	<p>Attempt to inject remaining product in 17-20 feet interval (5.2-6.1 m) between 538 and 545 pm. Could not establish flow. Injection stopped. Injection rod removed from well</p>	<p>08_04_2010-16:58</p> 	
<p>Wednesday August 4th 1758-1828 PM</p>	<p>Monitoring survey</p>	<p>Injection completed</p>	<p>08_04_2010-17:58</p> 	<p>Anomaly seems to sink down toward bottom of well</p>

<p>Thursday August 5th 1244-1550 PM</p>	<p>Monitoring survey w. reciprocals</p>	<p>About 18 hours after injection stopped</p>	<p>08_05_2010-12:44</p>  <p>A 3D plot showing the conductivity difference (S/m) over time. The x-axis is labeled 'x (meters)' and ranges from -10 to 10. The y-axis is labeled 'y (meters)' and ranges from -10 to 10. The z-axis is labeled '(easpeau) z' and ranges from 0 to -12. The plot shows a central region of high conductivity difference (red) that is slightly elongated and has a small dip in the center. A color bar below the plot indicates the conductivity difference values from -2.4 to 0.4 S/m.</p>	<p>Movement of anomaly downward has slowed down, but keeps on going.</p>
<p>Friday August 6th 1333 - 1640PM</p>	<p>Monitoring survey w. reciprocals</p>	<p>About 42 hours after injection stopped</p>	<p>08_06_2010-13:33</p>  <p>A 3D plot showing the conductivity difference (S/m) over time. The x-axis is labeled 'x (meters)' and ranges from -10 to 10. The y-axis is labeled 'y (meters)' and ranges from -10 to 10. The z-axis is labeled '(easpeau) z' and ranges from 0 to -12. The plot shows a central region of high conductivity difference (red) that is more elongated and has a deeper dip in the center compared to the previous plot. A color bar below the plot indicates the conductivity difference values from -2.4 to 0.4 S/m.</p>	<p>Continuation in decrease of changes, but similar trend (ie sinking downward).</p>

6 PERFORMANCE ASSESSMENT DISCUSSION

The performance objectives for our method as provided to the ESTCP office in the demonstration plan are provided in Table 6-1. All of these performance parameters were met. In the following sections we discuss the assessment of these performance parameters.

Table 6-1 Performance objectives for effort

Type of Objective	Primary Performance Criteria	Expected Performance (Metric)	Actual Performance Objective Met?
Quantitative	3D Spatial resolution of amendment maps	Better than 1.5 m	Yes
	Relative concentration gradients of amendments in 3D	Resolution in 15 % brackets	Yes
	Processing and delivery time of HPMS server	< 2 minutes	< 10 minutes ³
	Temporal resolution of amendment maps	Better than 2 hours	Yes
Qualitative	Effectiveness of HPMS system in delivering actionable information to RPMs	Utilization of system by RPMs demonstrating use and application	Yes
	Ability to map geochemical parameters of interest	Demonstrated correlation and between geochemistry and HPMS results	Yes

³ In our initial proposal we specified 2 minutes, but this period did not differentiate explicitly between the time when the raw data would be available (which is around 1 minute) and the time when the processed data are available (which depends on the size of the problem and the available computational resources, and was about 10 minutes in our case). Here, we make this distinction. We successfully collected and made data available in under the original 2-minute window, but we choose to report the time including processing, i.e., 10 minutes.

6.1 Quantitative performance criteria

6.1.1 3D Spatial resolution of amendment maps

The spatial resolution of electrical conductivity amendment maps is given in meters. It is defined as the extent to which our method can resolve the exact spatial position of the amendment. This resolution was calculated from independent knowledge of the position of the amendment, both in the initial long term ABC amendment injection and the molasses amendment injection. For both of these the emplacement location of the amendment was known and can be compared to the location of the amendment as provided by the electrical resistivity inversion. This comparison showed that the spatial resolution is better than 1.5 meters, and possibly as good as 0.5 meters. **This performance criteria was met.**

6.1.2 Relative concentration gradients of amendments in 3D

Our calibration demonstration (section 5.7) showed that we can correlate values of electrical conductivity to values of fluid conductivity and total organic acids for the first part of our amendment injection effort. This allows us to provide relative concentration gradients of amendments in 4D. **This performance criteria was met.**

6.1.3 Processing and delivery time of HPMS server

The processing and delivery time of the HPMS server is defined as the wall clock time expired between the arrival of data on the server and the associated posting of results on the web interface. During this time, the following steps happen automatically

1. Data arrival at the server triggers start of processing flow
2. Data is filtered using data qa/qc and common survey filters
3. Data is passed onto the inversion program
4. Parallel inverse code is executed
5. Result of inversion is included in output file for visualization
6. Results are visualized
7. Update is posted to website

The majority of the time in these steps (> 99 %) is spent in step 4, the execution of the parallel inverse code. Most of the other steps take 1-5 seconds to execute. The inversion step wall clock time depends both on the number of nodes that the inverse code can use, the size of the grid and the number of data points to invert, as well as on the initial model. The fastest execution time is achieved if the number of nodes is the same as the number of electrodes, and if the starting model is relatively close to the final model.

In the approach used here we started with a model which is the result of the inversion of the first (background) dataset. For the molasses experiment (where we formally timed the performance of our system) a typical inversion was performed in about 10 minutes. thus meeting our performance criteria. Note that improvements in the underlying code as well as improvements in computational hardware will further reduce this time. **This performance criteria was met.**

6.1.4 Temporal resolution of amendment maps

The temporal resolution is given as the time between each resistivity dataset. This temporal resolution is exactly the time it takes to collect each dataset (Figure 2-2). This time depends on the type of instrument use (single versus multi-channel), the total number of electrodes in the system, and the measurement schedule. The temporal resolution was on the order of 2 days for the ABC injection which was monitored for 1.5 years starting in March 2008. For the molasses injection the time for each data acquisition run was 28 minutes. Once data acquisition was completed data transfer, processing and visualization added another ten minutes such that data was available to the end user within 40 minutes of the start of data acquisition (again demonstrating the performance criterion under 6.3.1). **The temporal resolution performance criteria was met.**

6.2 Qualitative performance criteria

6.2.1 Effectiveness of HPMS system in delivering actionable information to RPMs

The effectiveness of the HPMS in delivering actionable information to RPMs was judged by (1) the form in which the HPMS provided information on amendment behavior, (2) on the ease of getting access to this information, and (3) on the time elapsed between when the amendment injection and when the information was available.

- **Form:** Our system provides information through an animation of spatial and temporal behavior of amendment behavior. This form makes it intuitively obvious to see where amendment is going;
- **Ease of access:** Our system provides information through a standard web browser. No special software needs to be installed, and the information is available to any authorized user on demand.
- **Time elapsed:** the time elapsed between data collection and information being available is in the range of tens of minutes to tens of hours (depending on several factors discussed previously). This is substantially faster than sampling based analysis results (which typically take weeks to months to become available).

A specific example of time the effectiveness of our system was provided during the August 2010 molasses injection. At that time our field team and guests to the site from DOE, DoD and industry, saw near-real time maps of amendment behavior as molasses were being injected. Actionable information was thus being delivered to operators and decision makers. **This performance criteria was judged to be met.**

6.2.2 Ability to map geochemical parameters of interest

The ability to map geochemical parameters of interest is based on relationships between the bulk electrical properties and those geochemical parameters. We demonstrated that our system is able to map and predict these parameters by providing a pre sampling estimate of anticipated sample results for our Fall 2008 sampling effort to the DoD program manager. We also demonstrated (as discussed in sections 5 and 6) that our results are highly correlated with known geochemical processes on site, thus meeting our performance criteria. **This performance criteria**

was judged to be met.

7 COST ASSESSMENT

7.1 Deployment, operational and analysis costs

The costs for installation and operation of the HPMS were tracked by the different project partners (DoD, USGS and INL) using the PI's respective account tracking systems. Costs for materials, labor, travel, and subcontracts were tracked relative to project milestones. The major costs associated with this effort are divided between:

- **Startup costs** covering initial system deployment, including purchase of a shed, purchase of electrode strings and control unit, well and electrode installation using a direct push rig, system set up and connection to power supplies.
- **Sampling costs** covering collection and analysis of groundwater samples and disposal of sampling spoils/purge water.
- **Operational costs** covering expenses associated with operating the system, including data processing and analysis, periodic site visits for trouble-shooting. For the experiment described here, it also includes the costs associated with the second injection effort (purchase of molasses, molasses injection).
- **Demobilization costs** including costs for site demobilization, well abandonment in accordance with Maryland regulations and USGS requirements, and appropriate disposal of materials from the site.

Based on these elements the life-cycle cost for the technology was estimated and a cost model was developed. Cost savings associated with deployment of a HPMS can derive from any or all of three mechanisms (Table 7-1):

Table 7-1 Cost Savings mechanisms

<i>Cost Savings Mechanisms:</i>
1. Accelerated time to remediation and site closure and (or) reduction of amendment injections resulting from improved delivery of amendments
2. Decreased frequency of sampling resulting from limited sampling events based on when changes are observed in geophysical monitoring results
3. Decreased number of samples collected resulting from use of geophysical results to fill in gaps spatially between sampling points

Although our demonstration shows that geophysical results provide insight into amendment delivery, our work did not entail collection of data to quantify accelerated cleanup (savings mechanism 1). Improvements in remediation procedures resulting from application of a HPMS will be highly site-dependent and thus difficult to generalize. Application of a HPMS might allow for reduction in the number of amendment injections or injection of less amendment through optimization of injection protocols; these cost savings cannot be predicted in a general way based

on data from our project. Our cost-benefit analysis thus focuses on savings strategies 2-3. We emphasize that any acceleration to site closure or reduction in amendment injections would result in further cost savings, and thus our cost detailed analysis is conservative with regard to the potential benefit of application of a HPMS. We discuss scenarios for additional savings achieved through mechanism 1, but we stress that these scenarios are speculative and underlying assumptions cannot be generalized easily. Additional long term demonstrations would be required to compare costs associated with HPMS-optimized remediation; these demonstrations would need to extend from the onset of biostimulation through site closure.

The costs for application of a HPMS at a remediation site will include startup, capital and installation costs and the subsequent monitoring costs related to system operation, sampling, and demobilization. Compared to long term, conventional sampling, the incremental costs for deployment of a HPMS are concentrated at the start of monitoring; thus, the return on investment is expected to increase over time.

7.1.1 Cost model

The cost model for the Brandywine demonstration/evaluation is provided in Table 7-2. This model reflects startup, sampling, operational, and demobilization costs associated with the HPMS and its demonstration/evaluation. The model, intended for use as a tool in costing adoption of a HPMS, does not reflect project expenditures related to development of software or research and development of components of the HPMS. Nor does the model reflect potential cost savings compared to the Brandywine project resulting from our ongoing development of installation procedures, as discussed in the next section.

Table 7-2 Cost model for a HPMS similar to the Brandywine dem/val

Cost Element	Data Tracked During the Demonstration	Costs (gross)	
Startup costs	<ul style="list-style-type: none"> • Drilling (19 wells) • Resistivity control-unit • Resistivity cables (7 wells, 4 surface cables) • Labor (total of 160 hours assumed, with travel and per diem) for two people – approximated • Labor (160 hours assumed) for survey geometry design and setup of database and server communications 	Drilling	\$40K
		Resistivity control unit	\$80K
		Resistivity cables	\$11K
		Labor and travel for fieldwork	\$22K
		Labor for design	\$16K
Operational costs	<ul style="list-style-type: none"> • 1-day site visit by one technician with salary, 1-day travel and per diem, once per quarter, for one year – approximated and site dependent • Electricity – not tracked • Labor for processing, inversion, interpretation – 80 hours per year, senior scientist 	Labor and travel for field visit	\$4K
		Electricity	\$360
		Labor for processing	\$9000
Sampling	<ul style="list-style-type: none"> • 4 sampling events, water-quality field parameters, major ions, contaminants with 2-day site visit by two scientists each time 	Labor and travel	\$24K
		Lab analysis	\$76K
Demobilization	<ul style="list-style-type: none"> • Well abandonment (19 wells) by certified driller • Disposal of materials • Two scientists, labor and travel, 3 days 	Driller	\$7.5K
		Waste disposal	\$4K
		Labor and travel	\$8K

7.2 COST DRIVERS

Important cost drivers affecting the application of the HPMS include the (1) scale of heterogeneity at the site, which dictates well offsets for the HPMS, (2) ease of drilling (e.g., suitability of direct-push, rock vs. unconsolidated material, etc.), and (3) on-site access to power and means of data transfer (e.g., availability of internet connection). Drivers 1-2 also are important for conventional monitoring efforts. For example, drilling costs affect conventional sampling even more than HPMS, which minimizes the need for boreholes. A short scale of heterogeneity would limit distance between observation wells even more than the distance between HPMS wells. Thus, the driver unique to the HPMS is the third, i.e., access to on-site power and means of data transfer. Without these, most applications of the HPMS would be cost-prohibitive, as frequent site visits would be required. Furthermore, the primary advantages of the HPMS—autonomous, automated and real-time monitoring—would not be realized.

7.3 COST ANALYSIS

We envision several different scenarios under which the HPMS would be useful; these range from monitoring at a single injection point for verifying general injection design to monitoring site-wide for verifying amendment extent spatially. We present three separate cost-analysis scenarios to quantify potential savings associated with deployment of a HPMS for different purposes and scales of remedial action:

- (1) A minimal HPMS system designed to monitor a single injection point (Cost Model 1, Table 7-3);
- (2) Site-scale HPMS system, designed to monitor 20 separate injection points spread across a large site (Cost Model 2, Table 7-4); and
- (3) Site-scale HPMS system, designed to monitor a 100-m by 100-m side, with spatial coverage site-wide (Cost Model 3, Table 7-5).

Whereas the Brandywine cost model (Table 7-2) reflects deployment costs of a HPMS based on our stage of research and development in 2007, the analyses presented here reflect potential deployment costs for a HPMS today, and thus reflect cost savings resulting from R&D under our ESTCP project and related ongoing grants. For example, co-PI's at the USGS have developed a low-cost alternative to the electrode/sampling setups installed in direct-push wells at Brandywine. These new setups do not rely on a PVC backbone or commercially fabricated resistivity cables; rather they use collapsible fiberglass backbones and stainless-steel adhesive-backed tape for electrodes; this design facilitates shipping and installation. The fiberglass setups decrease material costs associated with electrode/sampling setups from ~\$2000 to ~\$100. Furthermore, whereas the Brandywine setups were laboriously prepared in the field and required the presence of scientists on-site to assist drillers (thus impeding the drilling procedures and increasing drilling costs), the fiberglass setups are prepared beforehand and simply can be dropped into hollow direct-push rods by drillers. The new design has been used successfully by the USGS under two grants funded by the Dept. of Energy's Subsurface Biogeochemical Research program to study radionuclide-contaminated DOE sites in Naturita, CO, and Hanford, WA. In developing Tables 7-2, 7-3, and 7-

4, we assume use of the most cost-effective, state-of-the-art components.

7.3.1 Cost analysis scenario 1: Single-injection monitoring

The cost analysis presented in Table 7-3 is based on a project in which the objectives for the HPMS are focused on verification of general injection procedures by monitoring emplacement at a single injection point. A project of this scope would be appropriate for a geologically homogenous site, where verification of the general injection procedures is required and findings reasonably can be extrapolated across the site. The HPMS would be used for short-term (1-year) monitoring to image the extent of the amendment in the subsurface. In developing this analysis, we assume a site similar to Brandywine in terms of the depth of the target zone (~30 ft), and site of similar geologic materials, and hence similar drilling costs. We assume use of 4 electrode/sampling installations for the HPMS and quarterly sampling events for one year.

This cost analysis is scalable in that costs would increase linearly (perhaps with some savings for travel/mobilization) with the number of points to be monitored. Cost savings of this model are difficult to quantify fully, as most of the savings would likely derive from savings mechanism (1), i.e., acceleration to site closure. We can only fully assess savings associated with mechanisms (2) and (3), i.e., decreased frequency of sampling and decreased sampling points (Table 7-1). Thus we quantify the savings resulting from the HPMS as compared to conventional sampling performed at numerous locations and times.

Based on the calibration/validation from our demonstration/evaluation project, the HPMS technology is capable of providing information on amendment presence with a coefficient of determination on the order of 0.7; thus the HPMS results explain 70% of the variation in total organic acids (our surrogate for amendment presence) If we assume, therefore, that the HPMS is providing information of 70% quality compared to conventional sampling, we could reduce sampling by 70% and achieve the same information. We do not propose this, but more conservatively suggest reducing sampling events by 50% (relying on the geophysics between) and sampling locations by 50%. We emphasize that the HPMS does not replace conventional sampling. Indeed, conventional sampling is required for calibration/validation.

To estimate cost benefit for this scenario, we assume for reference, conventional sampling with 8 wells and 4 sampling events per year. With the HPMS, we assume 4 wells and 2 sampling events. As shown in Table 7-3, the HPMS for this scenario costs \$98K compared to \$116K for conventional sampling to provide similar information. Thus the HPMS achieves a ~15% cost savings, considering only savings resulting from the cost of equivalent information and neglecting potential savings associated with access to real-time information to improve decision making or optimize procedures in the field.

Table 7-3 Cost Analysis for HPMS - Scenario 1

HPMS Costs			
Cost Element	Sub elements	Costs (gross)	
Startup costs	<ul style="list-style-type: none"> • Drilling (4 ERT/sampling wells) • Resistivity control-unit • Resistivity setups (4 wells) • Labor (total of 40 hours assumed, with travel and per diem) for two people – approximated • Labor (40 hours assumed) for survey geometry design and setup of database and server communications 	Drilling	\$8K
		Resistivity control unit (reusable)	\$80K x 0.5 = \$40K
		Resistivity cables	\$800
		Labor and travel for fieldwork	\$10K
		Labor for design	\$4K
Operational costs	<ul style="list-style-type: none"> • 1-day site visit by one technician with salary, 1-day travel and per diem, twice – approximated and site dependent • Electricity – 1 year • Labor for processing, inversion, interpretation – 40 hours per year, senior scientist 	Labor and travel for field visit	\$2K
		Electricity	\$240
		Labor for processing	\$4K
Sampling	<ul style="list-style-type: none"> • 2 sampling events, 4 wells, water-quality field parameters, major ions, contaminants with 1-day site visit by two scientists each time 	Labor and travel	\$6K
		Lab analysis	\$18K
Demobilization	<ul style="list-style-type: none"> • Well abandonment (4 wells) by certified driller • Disposal of materials • Two scientists, labor and travel, 1 days 	Driller	\$1K
		Waste disposal	\$1K
		Labor and travel	\$3K
TOTAL (not including reusable hardware)			\$98K
Conventional Sampling Comparison			
Startup costs	• Drilling (8 sampling wells)	Drilling	\$16K
Sampling	<ul style="list-style-type: none"> • 4 sampling events, 8 wells, water-quality field parameters, major ions, contaminants with 2-day site visit by two scientists each time 	Labor and travel	\$24K
		Lab analysis	\$72K
Demobilization	<ul style="list-style-type: none"> • Well abandonment (8 wells) by certified driller • Disposal of materials 	Driller	\$2K
		Waste disposal	\$2K
TOTAL			\$116K

7.3.2 Cost analysis scenario 2: Site-scale monitoring at 10 locations

The cost analysis presented in Table 7-4 is based on a project in which the objectives for the HPMS are focused on verification of amendment emplacement at multiple injection points, as required at a site with substantial heterogeneity. Here, we assume the HPMS would be used for monitoring for 3 years of a longer remediation action, with sampling for calibration/validation (i.e., two sampling events) only in year 1 and subsequent use of that calibration for prediction in years 2 and 3. Our reference for comparison is based on 3 years of conventional sampling at quarterly frequency for two years and then one more event in year three (i.e., a switch to annual frequency). We again assume a site similar to Brandywine in terms of the depth of the target zone (~30 ft) with similar drilling costs. We assume use of 4 electrode/sampling installations at 10 locations for the HPMS. The reference costs are based on conventional sampling at 4 wells per injection location; hence the reference case for conventional sampling involves the same drilling costs, for the same number of sampling points. This scenario therefore aims at quantifying the cost-benefit of geophysical enhancing a conventional monitoring network. The HPMS provides more information, in space and time, than conventional sampling, although the quality of this information depends in years 2 and 3 on the strength of the relation between the geophysical results and amendment concentration, as identified in the calibration/validation step.

In this scenario, we do not discount the cost of the resistivity control unit, which would be fully dedicated to the site. 100% of its cost is included in the analysis.

As shown in Table 7-4, the HPMS for this 3-year scenario costs \$537K compared to \$1180K for conventional sampling to provide less information (in space and time) but using the same number of sampling points and drilling budget as the geophysically enhanced HPMS. Thus the HPMS achieves a ~55% cost savings while providing more information. As for Scenario 1, these savings do not include additional possible savings resulting from access to real-time information to improve decision making or optimize procedures in the field.

As stated previously, the incremental costs of the HMPS are concentrated in the first years of monitoring, in the capital costs for startup. The cost analysis presented in Table 7-4 would be more favorable toward the HPMS if a longer time horizon were considered. If we assume the calibration is re-established on a 5-yr interval and sampling for the conventional design is annually after year 2, our cost savings for a remediation monitoring effort would continue to increase for the life of the HPMS, reaching \$2.3M in 30 years (Figure 7-1). Note that this simple comparison does not account for inflation.

Table 7-4 Cost analysis for a HPMS - Scenario 2– Scenario 2 (30-year costs)

HPMS Costs			
Cost Element	Sub elements	Costs (gross)	
Startup costs	<ul style="list-style-type: none"> • Drilling (40 ERT/sampling wells) • Resistivity control-unit • Resistivity setups (40 wells) • Labor (total of 80 hours assumed, with travel and per diem) for two people – approximated to set up connections • Labor (40 hours assumed) for survey geometry design and setup of database and server communications 	Drilling	\$80K
		Resistivity control unit with additional multiplexers (dedicated)	\$120K
		Resistivity cables	\$8K
		Labor and travel for fieldwork	\$20K
		Labor for design	\$4K
Operational costs	<ul style="list-style-type: none"> • 2-day site visit by one technician with salary, 1-day travel and per diem, twice – approximated and site dependent • Electricity – 3 years • Labor for processing, inversion, interpretation – 80 hours per year, senior scientist 	Labor and travel for field visit	\$8K
		Electricity	\$720
		Labor for processing	\$24K
Sampling	<ul style="list-style-type: none"> • 2 sampling events in first year, 40 wells, water-quality field parameters, major ions, contaminants with 5-day site visit by 4 scientists each time 	Labor and travel	\$60K
		Lab analysis	\$180K
Demobilization	<ul style="list-style-type: none"> • Well abandonment (40 wells) by certified driller • Disposal of materials • Two scientists, labor and travel, 4 days 	Driller	\$10K
		Waste disposal	\$10K
		Labor and travel	\$12K
TOTAL (not including reusable hardware)			\$537K
Conventional Sampling Comparison			
Startup costs	• Drilling (40 sampling wells)	Drilling	\$80K
Sampling	<ul style="list-style-type: none"> • 9 sampling events over 3 years - water-quality field parameters, major ions, contaminants with 5-day site visit by four scientists each time 	Labor and travel	\$270K
		Lab analysis	\$810K
Demobilization	<ul style="list-style-type: none"> • Well abandonment (40 wells) by certified driller • Disposal of materials 	Driller	\$10K
		Waste disposal	\$10K
TOTAL			\$1180K

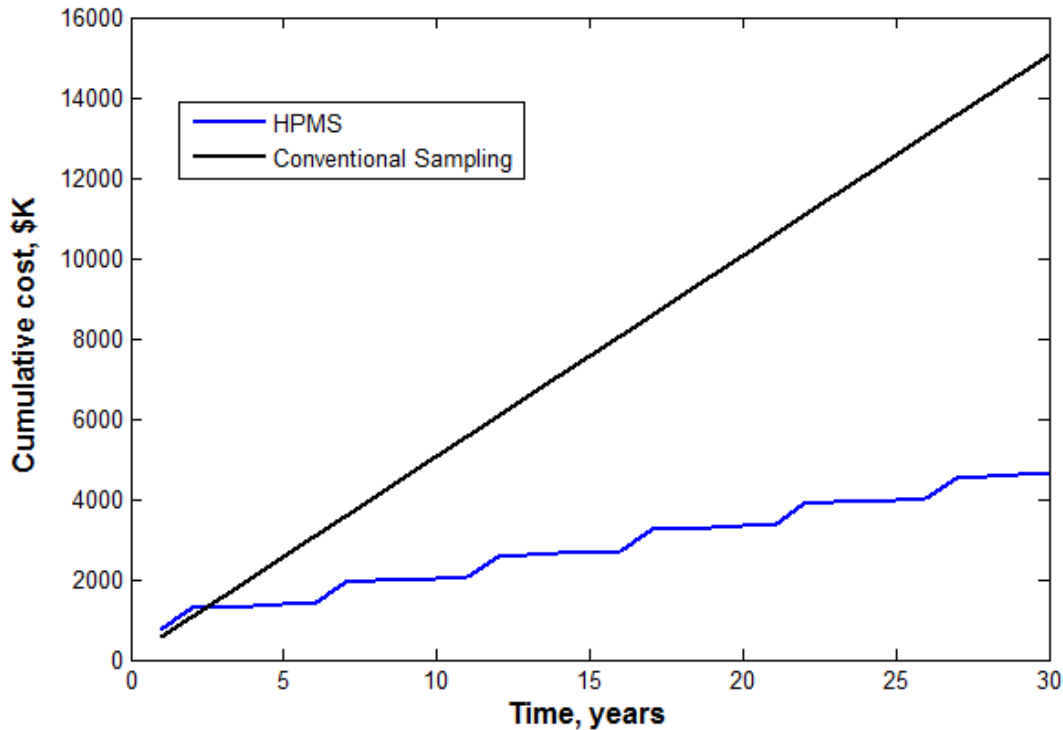


Figure 7-1 Cost-analysis comparison for HPMS and conventional sampling for Scenario 2, extended to a 30 year time frame (Table 7-4)

7.3.3 Cost analysis scenario 3: Site-scale, site-wide monitoring

The cost analysis presented in Table 7-5 is based on a scenario in which the objectives for the HPMS involve site-wide monitoring for 30 years. A 100-m by 100-m site is assumed, with geology and unit drilling costs similar to Brandywine. We consider HPMS operation with quarterly sampling for calibration in years 1-2 and then every 5 years thereafter. Our reference for comparison is based on 30 years of conventional sampling at quarterly frequency for two years and annual sampling thereafter, using 10 monitoring/HPMS wells. In contrast to Cost Analysis Scenarios 1-2, in this scenario we consider deployment of surface resistivity electrodes rather than borehole electrodes. Deployment of a surface system allows for coverage of much larger areas than possible with borehole installations at lower cost, as demonstrated in our project add-on which included surface-resistivity monitoring of molasses injections. Surface electrodes can be installed by trenching or hand-placement (hammering or simply pushing into soil) depending on site conditions, eliminating the need for costly drilling. We assume 11 surface electrode cables, 100-m long, with electrodes at 4-m spacing, deployed collinearly at 10-m spacing. The cable layout extends beyond the target area in order to achieve a depth of investigation of 30 ft, consistent with previous scenarios. We assume that the conventional sampling calibration/validation dataset would be collected from the 10 observation wells otherwise used in the reference scenario; these observation wells would be instrumented with electrodes, generating a small incremental cost for the HPMS.

As shown in Table 7-5, the HPMS for this 30-year scenario costs \$1149K compared to \$1735K for conventional sampling; thus the HPMS achieves a ~34% cost savings. As for Scenario 1, these savings do not include additional possible savings resulting from access to real-time information to improve decision making or optimize procedures in the field; nor are savings considered for possible reduction in the number of wells, which also are employed here in the HPMS. Cost savings are achieved in this scenario only through savings mechanism 2, reduction in the frequency of sampling, using geophysical results to replace sampling only in time, not space.

Table 7-5 Cost for site scale, site-wide monitoring

HPMS Costs			
Cost Element	Sub elements	Costs (gross)	
Startup costs	<ul style="list-style-type: none"> • Drilling (10 sampling wells) • Resistivity control-unit • Resistivity cables (11) • Labor (80 hours assumed,) for two people – approximated to set up connections • Labor (40 hours assumed) for survey geometry design and setup of database and server communications 	Drilling	\$20K
		Resistivity control unit with additional multiplexers (dedicated)	\$180K
		Resistivity cables	\$33K
		Labor and travel for fieldwork	\$40K
		Labor for design	\$4K
Operational costs	<ul style="list-style-type: none"> • 2-day site visit by one technician with salary, 1-day travel and per diem, twice – approximated and site dependent • Electricity – 30 years • Labor for processing, inversion, interpretation – 40 hours per year, senior scientist 	Labor and travel for field visit	\$8K
		Electricity	\$7K
		Labor for processing	\$120K
Sampling	<ul style="list-style-type: none"> • 2 sampling events in first year and every 5 years thereafter (total 12) - water-quality field parameters, major ions, contaminants with 5-day site visit by 4 scientists each time 	Labor and travel	\$180K
		Lab analysis	\$540K
Demobilization	<ul style="list-style-type: none"> • Well abandonment (10 wells) by certified driller • Disposal of materials • Two scientists, labor and travel, 4 days 	Driller	\$2.5K
		Waste disposal	\$2.5K
		Labor and travel	\$12K
TOTAL			\$1149K
Conventional Sampling Comparison			
Startup costs	<ul style="list-style-type: none"> • Drilling (10 sampling wells) 	Drilling	\$20K
Sampling	<ul style="list-style-type: none"> • 4 sampling events in first two years, 1 per year thereafter over 30 years (total of 36) - water-quality field parameters, major ions, contaminants with 2-day site visit by two scientists each time • GO TO ONCE PER YEAR AFTER 5 YRS 	Labor and travel	\$540K
		Lab analysis	\$1170K
Demobilization	<ul style="list-style-type: none"> • Well abandonment (10 wells) by certified driller • Disposal of materials 	Driller	\$2.5K
		Waste disposal	\$2.5K
TOTAL			\$1735K

8 IMPLEMENTATION ISSUES

8.1 Deployment

The HPMS system requires the installation of vertical arrays of electrodes and/or surface electrodes, as well as the deployment of electrical geophysical data acquisition hardware and supporting infrastructure (power infrastructure, wireless data transmission capabilities, hardware enclosures). An example of deployment cost for system data acquisition hardware, electrodes, electrode geometry, and typical mix of surface and borehole electrodes is provided in Section 7.3 Cost Analysis. This configuration can be scaled to fit site-specific requirements.

The most variable cost is that of electrode installation, especially if that is done in boreholes. Whereas surface electrode installation is fairly straightforward and low cost (for example, the installation of the two surface cables for the molasses monitoring were done in 1 day by one person), installation of borehole electrodes can be very costly.

Until recently, the installation of borehole resistivity arrays was done by the installation of electrodes either in fully screened PVC boreholes or connected to the side of pvc or fiberglass rods. This method is time consuming and costly. To address this problem, several of our project PI's have leveraged experience from Brandywine Dem/Val to design much lower-cost, smaller diameter electrode/sampling setups that do not require setting casings and which can be fabricated off-site; these fold up, facilitating shipping to remote sites. With these modifications, we estimate that the hardware cost for each electrode string is reduced by 90%, and direct-push installation can be performed with smaller diameter drill rod and thus performed more rapidly.

Surface electrodes and cables can be repurposed, whereas borehole electrode arrays are commonly abandoned or destroyed during removal. If borehole electrodes were emplaced in heavily contaminated soil, removal and decontamination costs may exceed replacement costs.

8.2 Operational Environment Issues

Operation of the HPMS system typically requires some kind of enclosed and protected space to house the resistivity instrument, power supplies for the resistivity instrument and a field computer. A field trailer or small shed will generally suffice. A standard 15 Amp, 120 V power circuit will typically be sufficient to operate the system. A standard problem which is encountered in the field is that small enclosures tend to experience large temperature fluctuations during the year. While both the resistivity equipment and computers typically can deal with low temperatures found in winter, extreme heat has led to equipment failures. Thus, some kind of basic climate control (heat in the winter, air conditioning in the summer) is often recommended. In the dem/val effort we encountered several issues with reliable power at the site. Power interruptions shut down the system, and current resistivity hardware requires a manual reboot of the control computer for resumption of data acquisition. Reliable power is a requirement for system operation.

8.3 Regulatory Issues

In general, if installed correctly the geophysical wells will not provide contaminant conduits. The material involved in the electrode arrays is generally relatively benign (stainless steel for the electrodes and PVC jacketed copper cable for the cabling) and not expected to be a contaminant source. Thus, the only permits/regulations would be those which would normally apply to environmental restoration site well installations.

The only requirement for accessing the results of the HPMS system is a web browser. However, as the information generated by HPMS is potentially sensitive, controls will be put in place whereby access to information and data is tied to user/passwords and different levels of access to data. Such a control would generally implement standard Official-Use Only restrictions.

9 APPENDICES

9.1 Appendix A: Points of Contact

Table 9-1 Points of contact for ESTCP DEM/VAL effort

POINT OF CONTACT Name	ORGANIZATION Name Address	Phone/Fax/email	Role in Project
Arun Gavaskar	Naval Facilities Engineering and Expeditionary Warfare Center	Phone: 805-982-1661 Email: arun.gavaskar@navy.mil	NAVFAC point of contact. Note that Bill Major was the project PI, but Bill retired in early 2014
Frederick Day- Lewis	United States Geological Survey	Phone: 860-487-7402 x 21 Email: daylewis@usgs.gov	System installation lead and GPR characterization
Roelof Versteeg	Subsurface Insights 62 Lebanon Street Hanover, NH 03755	Phone: 603-443-2202 email: roelof.versteeg@subsurfaceinsights.com	Project lead on electrical geophysical monitoring, sampling
Tim Johnson	Pacific Northwest National Laboratory	Phone: 509-372-4715 Email: tj@pnnl.gov	Electrical geophysical inversion and data processing
John W. Lane, Jr.	United States Geological Survey	Phone: 860-487-7402 x13 Email: jwlane@usgs.gov	Operations management, demobilization lead

Useful links

https://e4d.pnnl.gov/Pages/Home.aspx	Home page of open source electrical resistivity code E4D maintained by Dr. Tim Johnson. A precursor of this code was used in this project
http://www.subsurfaceinsights.com/brandywine	Webpage describing Brandywine results. Includes animations
http://water.usgs.gov/ogw/bgaw/	Home page of the USGS Office of Groundwater, Branch of Geophysics

10 References

- Aal, G. Z. A., E. A. Atekwana, et al. (2004). Effect Of Different Phases Of Diesel Biodegradation On Low Frequency Electrical Properties Of Unconsolidated Sediments. Symposium on the Application of Geophysics to Engineering and Environmental Problems, Colorado Springs, Environmental and Engineering Geophysical Society.
- Archie, G. E. (1942). "The electrical resistivity log as an aid to determining some reservoir characteristics." Transactions of the American Inst. Min. Metall. Petr. Eng. **146**: 54-62.
- Arts, R. J., R. A. Chadwick, et al. (2007). Synthetic versus real time-lapse seismic data at the Sleipner CO2 injection site. SEG Annual Meeting San Antonio, Texas, SEG.
- Atekwana, E., E. Atekwana, et al. (2004). Relationship Between Biodegradation And Bulk Electrical Conductivity. Symposium on the Application of Geophysics to Engineering and Environmental Problems, Colorado Springs, Environmental and Engineering Geophysical Society.
- Atekwana, E. A., D. D. Werkema, et al. (2004). "Insitu apparent conductivity measurements and microbial population distribution at a hydrocarbon contaminated site." Geophysics **69**(1): 56-63.
- Bevc, D. and H. F. Morrison (1991). "Borehole-to-surface electrical resistivity monitoring of a salt water injection experiment." Geophysics **56**(6): 769-777.
- Burkhart, T. R., A. R. Hoover, et al. (2000). "Time-lapse (4D) seismic monitoring of primary production of turbidite reservoirs at South Timbalier Block 295, offshore Louisiana, Gulf of Mexico." Geophysics **65**(2): 351-367.
- Chen, K.-F., C.-M. Kao, et al. (2010). "Control of petroleum-hydrocarbon contaminated groundwater by intrinsic and enhanced bioremediation." Journal of Environmental Sciences **22**(6): 864-871.
- Cunningham, J. A., H. Rahme, et al. (2001). "Enhanced In Situ Bioremediation of BTEX-Contaminated Groundwater by Combined Injection of Nitrate and Sulfate." Environmental Science and Technology **35**(8): 1663-1670.
- Daily, W. (1984). "Underground oil-shale monitoring using geotomography." Geophysics **49**(10): 1701-1707.
- Daily, W. and E. Owen (1991). "Cross-borehole resistivity tomography." Geophysics **56**(8): 1228-1235.
- Daily, W., A. Ramirez, et al. (1992). "Electrical Resistivity Tomography of Vadose Water Movement." Water Resources Research **28**(5): 1429-1442.
- Davis, C. A., E. Atekwana, et al. (2006). Laboratory-scale investigation of the effect of microbial growth on the geoelectrical properties of porous media. 19th Annual SAGEEP Meeting, Seattle, Washington, EEGS.

- Day-Lewis, F., K. Singha, et al. (2005). "Applying petrophysical models to radar travel time and electrical resistivity tomograms: Resolution-dependent limitations. ." Journal of Geophysical Research **110(B8)**.
- Day-Lewis, F. D., J. M. Harris, et al. (2002). "Time-lapse Inversion of Crosswell Radar Data." Geophysics **67(6)**: 1740-1752.
- Day-Lewis, F. D., J. W. J. Lane, et al. (2004). "Combined Interpretation of Radar, Hydraulic and Tracer Data from a Fractured-Rock Aquifer." Hydrogeology Journal. **14(1-2)**: 1-14.
- Day-Lewis, F. D., J. W. J. Lane, et al. (2003). "Time-Lapse Imaging of Saline Tracer Tests Using Cross-Borehole Radar Tomography." Water Resources Research **39(10)**: 1290-1304.
- Dey, A. and H. F. Morrison (1979). "Resistivity modeling for arbitrarily shaped three-dimensional structures." Geophysics **44(4)**: 753-780.
- Dodds, K. (2005). Time-lapse EM and Seismic Imaging of a CO2 Plume. Fourth annual conference on carbon capture & sequestration, Virginia.
- EPA (2006). EPA Superfund Record of Decision: BRANDYWINE DRMO.
- EPA (2006). EPA Superfund record of decision: Brandywine DRMO EPA ID: MD 9570024803 OU 01 Brandywine MD.
- EPA. (2012). "Resistivity methods." from http://www.epa.gov/esd/cmb/GeophysicsWebsite/pages/reference/methods/Surface_Geophysical_Methods/Electrical_Methods/Resistivity_Methods.htm.
- Fanchi, J. R. (2001). "Time-lapse seismic monitoring in reservoir management." The Leading Edge **20**: 1140-1147.
- Frangos, W. (1997). "Electrical detection of leaks in lined disposal ponds." Geophysics **62(6)**: 1737-1744.
- GAO (2005). Groundwater contamination - DoD Uses and develops a range of remediation technologies to clean up military sites - reports to congressional committees.
- Gasperikova, E., G. M. Hoversten, et al. (2004). A feasibility study of geophysical methods for monitoring geologic CO2 sequestration. SEG 2004 Annual Meeting.
- Gropp, W., E. Lusk, et al. (1996). "A high performance, portable implementation of the MPI message passing interface standard." Parallel Computing **22**: 789-828.
- Johnson, T., R. Versteeg, et al. (2010). Electrical Geophysical and Geochemical Monitoring of in situ Enhanced Bioremediation. Goldschmidt 2010, Knoxville, Tennessee.
- Johnson, T., R. Versteeg, et al. (2010). "Improved hydrogeophysical characterization and monitoring through parallel modeling and inversion of time-domain resistivity and induced polarization data." Geophysics **75**: 27-41.
- Kearey, P., M. Brooks, et al. (2002). An introduction to geophysical exploration, Blackwell Science Ltd.
- LaBrecque, D. J., G. Heath, et al. (2004). "Autonomous Monitoring of Fluid Movement Using Electrical Resistivity Tomography." Journal of Engineering and Environmental Geophysics **9(3)**: 167-176.
- LaBrecque, D. J., M. Miletto, et al. (1996). "The effects of noise on Occam's inversion of resistivity tomography data." Geophysics **61**: 538-548.
- Laine, E. F. (1987). "Remote monitoring of the steam-flood enhanced oil recovery proces." Geophysics **52(11)**: 1457-1465.
- Lane, J. W., F. Day-Lewis, et al. (2006). "Geophysical monitoring of field-scale vegetable oil injections for biostimulation." Ground Water: 14.
- Lane, J. W., F. D. Day-Lewis, et al. (2004). "Object-Based Inversion of Crosswell Radar

- Tomography Data to Monitor Vegetable Oil Injection Experiments." Journal of Environmental and Engineering Geophysics **9**(2): 63-77.
- Lane, J. W., F. D. Day-Lewis, et al. (2004). Application Of Cross-Borehole Radar To Monitor Fieldscale Vegetable Oil Injection Experiments For Biostimulation. Symposium on the Application of Geophysics to Engineering and Environmental Problems, Colorado Springs, Environmental and Engineering Geophysical Society.
- Lane, J. W., Jr., F. D. Day-Lewis, et al. (2007). "Monitoring Engineered Remediation with Borehole Radar." The Leading Edge **26**(8): 1032-1035.
- Lesmes, D. P. and K. M. Frye (2001). "Influence of pore fluid chemistry on the complex conductivity and induced polarization responses of Berea sandstone." Journal of Geophysical Research **106**(B3): 4079-4090.
- Li, G. (2003). "4D seismic monitoring of CO₂ flood in a thin fractured carbonate reservoir." The Leading Edge **22**.
- Loke, M. H. and R. D. Barker (1996). "Rapid least-squares inversion of apparent resistivity pseudosections using a quasi-Newton method." Geophysical Prospecting **44**: 131-152.
- Naudet, V., A. Revil, et al. (2003). "Relationship between self-potential (SP) signals and redox conditions in contaminated groundwater." Geophysical Research Letters **30**(21).
- Naudet, V., A. Revil, et al. (2004). "Groundwater redox conditions and conductivity in a contaminant plume from geoelectrical investigations." Hydrology and Earth System Sciences **8**: 8-22.
- Ogilvy, R. D., P. I. Meldrum, et al. (2009). "Automated monitoring of coastal aquifers with electrical resistivity tomography." Near Surface Geophysics **7**(5-6): 367-375.
- Orange, A., S. Constable, et al. (2007). The feasibility of reservoir monitoring using marine 4D-CSEM. 2007 SEG Annual meeting, San Antonio, TX, SEG.
- Park, J. H., D. Lamb, et al. (2011). "Role of organic amendments on enhanced bioremediation of heavy metal(loid) contaminated soils." Journal of Hazardous Materials **185**(2-3): 549-574.
- Parra, J. O. (1988). "Electrical response of a leak in a geomembrane liner." Geophysics **53**(11): 1445-1452.
- Parra, J. O. and T. E. Owen (1988). "Model studies of electrical leak detection surveys in geomembrane-lined impoundments." Geophysics **53**(11): 1453-1458.
- Parsons (2004). Principles and practices of enhanced anaerobic bioremediation of chlorinated solvents.
- Peale, J. G. D., J. Mueller, et al. (2010). "Successful ISCR-enhanced bioremediation of a TCE DNAPL source utilizing EHC and KB-1." Remediation Journal **20**(3): 63-81.
- Pidlisecky, A., E. Haber, et al. (2007). "RESINVM3D: A MATLAB 3-D Resistivity Inversion Package." Geophysics.
- Pope, K. (2009). Zend Framework 1.8 Web application Development, Packt Publishing.
- Ramirez, A., W. Daily, et al. (1996). "Detection of leaks in underground storage tanks using electrical resistance methods." Journal of Environmental and Engineering Geophysics **1**: 189-203.
- Ramirez, A., W. Daily, et al. (1995). "Electrical resistance tomography for steam injection and process control." Journal of Environmental and Engineering Geophysics **0**: 39-51.
- Revil, A. and V. Naudet (2004). Geoelectrical Effects Associated With the Presence of Bacteria in Contaminated Groundwater. EOS Trans. AGU, 85(47), Fall Meet. Suppl, Abstract B51F-02.
- Reynolds, J. M. (1997). An introduction to applied and environmental geophysics, John Wiley

- and Sons.
- Rodriguez, R. and H. Rodriguez (1999). "Real-time monitoring of rock-pile volumes by electrical resistivity." The Leading Edge: 1398-1401.
- Sauck, W. A., E. A. Atekwana, et al. (1998). "High Conductivities Associated with an LNAPL Plume Imaged by Integrated Geophysical Techniques." Journal of Engineering and Environmental Geophysics **2**(3): 203-212.
- Shima, H. (1992). "2-D and 3-D resistivity image reconstruction using crosshole data." Geophysics **57**(10): 1270-1281.
- Slater, L. and A. Binley (2003). "Evaluation of permeable reactive barrier (PRB) integrity using electrical imaging methods." Geophysics **68**(3): 911-921.
- Slater, L., A. Binley, et al. (2002). "A 3D ERT study of solute transport in a large experimental tank." Journal of Applied Geophysics **49**(4): 211-229.
- Slater, L. and D. Glaser (2003). "Controls on induced polarization in sandy unconsolidated sediments and application to aquifer characterization." Geophysics **68**(5): 1547-1558.
- Slater, L. and D. P. Lesmes (2002). "Electrical-hydraulic relationships observed for unconsolidated sediments." Water Resources Research **38**(10): 31-31 - 31-10.
- Slater, L. and S. Sandberg (2000). "Resistivity and induced polarization monitoring of salt transport under natural hydraulic gradients." Geophysics **65**(2): 408-420.
- Suzuki, K. and S. Higashi (2001). "Groundwater flow after heavy rain in landslide-slope area from 2-D inversion of resistivity monitoring data." Geophysics **66**(3): 733-743.
- URS (2005). Final Remedial Investigation Report, Site SS-01 – Brandywine DRMO, Andrews Air Force Base, Maryland.
- URS (2006). Final Focused Feasibility Study, Site SS-01, Former Brandywine DRMO, Andrews Air Force Base, Maryland. .
- Van, G. P., S. K. Park, et al. (1991). "Monitoring leaks from storage ponds using resistivity methods." Geophysics **56**(8): 1267-1270.
- Versteeg, R. (2004). Time-lapse geophysics for mapping fluid flow in near real time: results from a controlled mesoscale experiment. Aquifer Characterization - SEPM Special Publication No.80, SEPM: 93-106.
- Versteeg, R., M. Ankeny, et al. (2004). "A structured approach to the use of near surface geophysics in long term monitoring." The Leading Edge **23**(7): 700-703.
- Versteeg, R. and R. Birken (2001). An automated facility to study processes using 4D GPR. SAGEEP 2001, Denver, Colorado, Society of Environmental and Engineering Geophysics.
- Versteeg, R., R. Birken, et al. (2000). Controlled imaging of fluid flow and a saline tracer using time lapse GPR and electrical resistivity tomography. SAGEEP 2000, Washington, Society of Environmental and Engineering Geophysics.
- Versteeg, R., B. Blackwelder, et al. (2004). Experimental investigation of the link between geophysical signatures and biogeochemical properties and processes: experimental design, data collection and interpretation. EOS Trans. AGU, 85(47), Fall Meet. Suppl, Abstract B51F-03.
- Versteeg, R. and T. Johnson (2008). "Using time-lapse electrical geophysics to monitor subsurface processes." The Leading Edge **27**(11): 1448-1497.
- Versteeg, R. and T. Johnson (2009). Electrical Geophysical Performance Monitoring of Amendment Enhanced Bioremediation. Proceedings of the 2009 SAGEEP meeting, Fort Worth, TX.
- Versteeg, R., A. Richardson, et al. (2005). Automated multisensor monitoring of environmental

- sites: results from the Ruby Gulch Waste Rock Repository. SEG 2005 Annual Meeting, Houston.
- Versteeg, R., A. Richardson, et al. (2006). "Web accessible scientific workflow system for performance monitoring." Environmental Science and Technology **10.1021/es0517421S0013-936X(05)01742-6**.
- Versteeg, R., K. Wangerud, et al. (2005). Web Based Autonomous Geophysical/Hydrological Monitoring of the Gilt Edge Mine Site: Implementation and Results. Eos Trans. AGU, 86(18), Jt. Assem. Suppl., Abstract H43C-01.
- White, P. A. (1994). "Electrode arrays for measuring groundwater flow direction and velocity." Geophysics **59**(2): 192-201.
- Williams, K. H., D. Ntarlagiannis, et al. (2005). "Geophysical imaging of stimulated microbial biomineralization." Environmental Science & Technology **39**(19): 7592-7600.
- Zach, J. J., M. A. Frenkel, et al. (2009). Marine CSEM time-lapse repeatability for hydrocarbon field monitoring. SEG 2009 International Exposition and Annual Meeting, Houston, TX, SEG.
- Zhang, J., R. L. Mackie, et al. (1995). "3-D resistivity forward modeling and inversion using conjugate gradients." Geophysics **60**: 1313-1325.